A Review of the *Eliurus tanala* Complex (Rodentia: Muroidea: Nesomyidae), with Description of a New Species from Dry Forests of Western Madagascar

Sharon A. Jansa, Michael D. Carleton, Voahangy Soarimalala, Zafimahery Rakotomalala, and Steven M. Goodman

Bulletin of the American Museum of Natural History

A REVIEW OF THE *ELIURUS TANALA* COMPLEX (RODENTIA: MUROIDEA: NESOMYIDAE), WITH DESCRIPTION OF A NEW SPECIES FROM DRY FORESTS OF WESTERN MADAGASCAR

SHARON A. JANSA
Department of Ecology, Evolution, and Behavior
Bell Museum of Natural History, University of Minnesota

MICHAEL D. CARLETON
Department of Vertebrate Zoology
National Museum of Natural History, Smithsonian Institution

VOAHANGY SOARIMALALA
Association Vahatra, Antananarivo

ZAFIMAHERY RAKOTOMALALA
Mention Zoologie et Biodiversité Animale,
Faculté des Sciences, Université d'Antananarivo

STEVEN M. GOODMAN
The Field Museum of Natural History, Chicago
Association Vahatra, Antananarivo;

BULLETIN OF THE AMERICAN MUSEUM OF NATURAL HISTORY
Number 430, 67 pp., 20 figures, 9 tables
Issued May 8, 2019

ISSN 0003-0090

CONTENTS

Abstract....3
Introduction....3
Materials and Methods....6
Results....10
Molecular Phylogenetic Analyses....10
Patterns of Morphometric Differentiation....15
Taxonomy....24
Eliurus tanala Species Group....25
Eliurus antsingy Group vis-à-vis *E. tanala* Group....28
Species of the *E. tanala* Group....31
Eliurus tsingimbato, New Species....31
Eliurus tanala Major, 1896....43
Eliurus ellermani Carleton, 1994....48
Discussion....51
Taxonomic Issues and Species Delimitation....51
Biogeography....54
Acknowledgments....56
References....57
Appendix 1. Gazetteer of Collecting Localities....61
Appendix 2. Primers Used to Amplify the Six Genetic Loci Sequenced in This Study....66
Appendix 3. Comparative Specimens Examined....67

ABSTRACT

Based on 372 specimens examined, we integrated information from two mitochondrial and four nuclear gene sequences, morphological comparisons and morphometric analyses, as well as distributional patterns and ecological occurrences to revise the *Eliurus tanala* species group (Nesomyinae), a rodent complex endemic to Madagascar's forests. These evidentiary sources generally proved concordant, supporting description of a new species, *E. tsingimbato*, indigenous to western dry deciduous forest, mostly associated with limestone karst (*tsingy*); the two other members of this species group, *E. ellermani* and *E. tanala*, are restricted to eastern montane humid forest. Phylogenetic relationships among the three species were poorly resolved, suggesting that their speciation was both recent and rapid. We encountered one instance of conflict between mitochondrial DNA and all other data sources, which we interpret as incomplete lineage sorting involving a population of the new western species. Attention was focused on molecular and morphometric discrimination of the *E. tanala* and *E. antsingy* groups where their species distributions overlap in limestone-associated forests of western and northern Madagascar. Phyletic divisions demonstrated within the *E. tanala* species group are discussed apropos of current models of speciation identified for Malagasy forest-dwelling organisms.

INTRODUCTION

Over the past 20 years, considerable field inventory and museum-based research have focused upon Madagascar's native small mammals, including rodents of the endemic subfamily Nesomyinae (Muroidea: Nesomyidae sensu Musser and Carleton, 2005). As exemplified by the nesomyine genus *Eliurus*, specimen documentation has increased sevenfold compared with the early descriptive era and resulted in a doubling of recognized species, now totaling 12 (fig. 1). Coincidentally, or perhaps inevitably, the dramatic increase in specimen and geographic documentation of *Eliurus* populations has generated questions about species limits, their distributions, and interspecific relationships. Resolution of these fundamental systematic questions is critical for addressing broader questions of species diversification and biogeography on Madagascar.

Such knotty taxonomic issues surround the *Eliurus tanala* complex, a rodent group distributed in western and eastern Madagascar, occurring in both dry-deciduous and humid-evergreen forests and ranging in elevation from nearly sea level to above 1500 m. One particular western forest formation inhabited by members of this species group covers heavily sculpted karst limestone, a rugged landscape characterized by ragged pinnacles and walled palisades known as *tsingy* (e.g., as mapped by Bésairie, 1964). Application of the senior name *E. tanala* Major (1896a) to populations found in montane settings of the Central and Southern highlands is unproblematic (e.g., Soarimalala and Goodman, 2011; Goodman et al., 2013a); however, the status and affinity of *tanala*-like forms known from western biomes and from the Northern Highlands remain unresolved.

When Carleton et al. (2001) described *E. antsingy*, the first *Eliurus* associated with *tsingy* formations, they also reported the presence of another large form that exhibits "traits suggestive of *E. tanala* or *E. ellermani* from eastern Madagascar" (Carleton et al., 2001: 980). Later, Carleton and Goodman (2007) assigned similar specimens from the Bemaraha region to the *Eliurus* aff. *E. tanala* group. Renewed fieldwork in western Madagascar, including the Bemaraha and Namoroka limestone formations (fig. 2), has uncovered additional examples of this same large-bodied, *tanala*-like *Eliurus* whose taxonomy needs clarification.

Populations in the Northern Highlands have been variously associated with *E. tanala*, whether allocated provisionally to *E. tanala* (Carleton and Goodman, 1998), or to *Eliurus* sp. B (Jansa et al.,

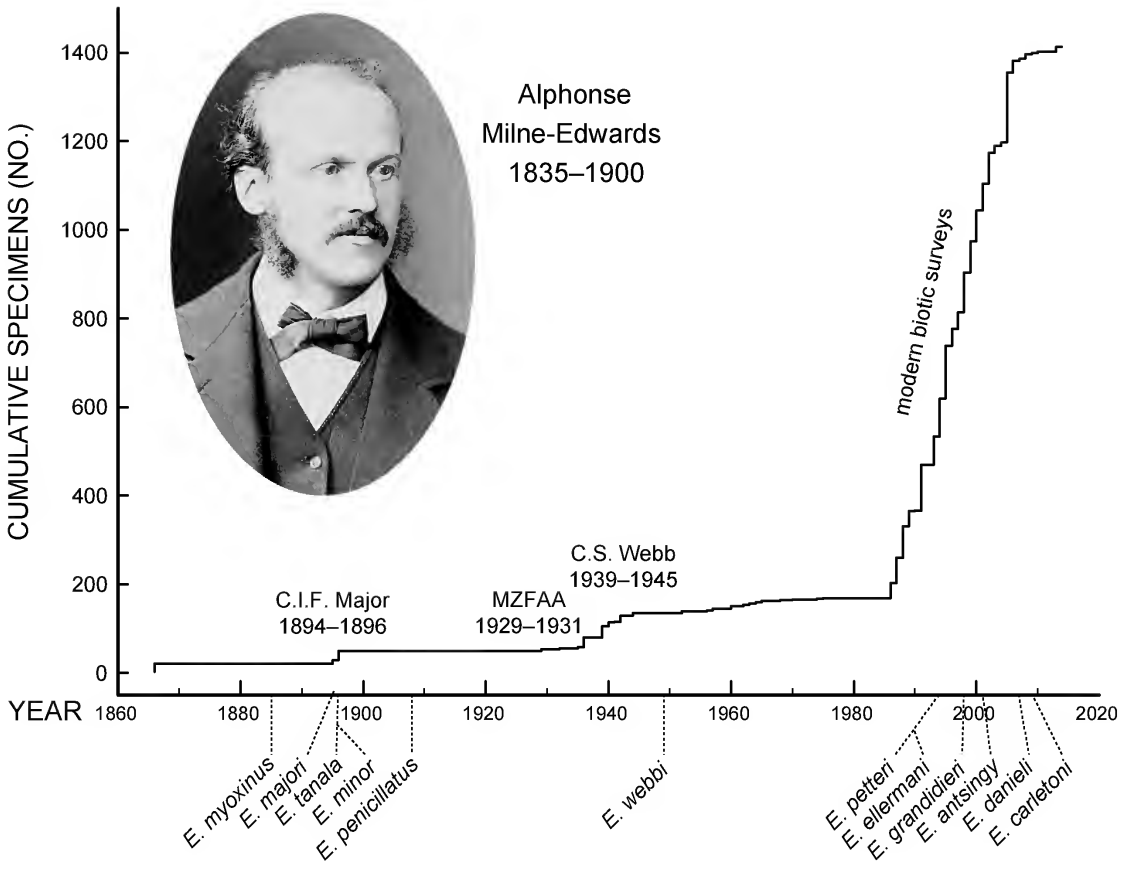

FIG. 1. Growth in systematic knowledge of tufted-tailed rats, genus *Eliurus*, concurrent with growth in vouchered material maintained in the World's natural history collections. While the earlier, historically important expeditions conducted by C.I. Forsyth Major, the Mission Zoologique Franco-Anglo-américaine (MZFAA), and Cecil S. Webb yielded modest increases in preserved specimens, museum-based documentation of *Eliurus* diversity has increased sevenfold during the past 25 years and substantiated the doubling of recognized species (dotted lines along the abscissa link new species to their year of description). Inset: Alphonse Milne-Edwards, former Director of the Muséum national d'Histoire naturelle and describer (1885) of *Eliurus myoxinus*, new genus and species.

1999), or to the *Eliurus* aff. *E. tanala* Group (Carleton and Goodman, 2007), or to *E. tanala* proper (Rakotoarisoa et al., 2013). Two of the aforementioned studies disclosed strong genetic divergence, based on cytochrome-*b* sequences, between their samples from the Northern Highlands and those of *E. tanala* sensu stricto from the Central and Southern Highlands (Jansa et al., 1999; Rakotoarisoa et al., 2013); two of the studies discussed the possible application of the name *E. ellermani* Carleton (1994), described from a mountain range on the Masoala Peninsula (fig. 2), to the large *tanala*-like *Eliurus* in the Northern Highlands (Carleton and Goodman, 1998, 2007). Such taxonomic indecision invites resolution.

We herein integrate mitochondrial and nuclear DNA sequences, morphometric and morphological data in order to review the systematics of the *Eliurus tanala* species group. Specifically, we (1) diagnose a new species from dry forests of western Madagascar; and (2) demonstrate the applicability of *E. ellermani* Carleton (1994) to

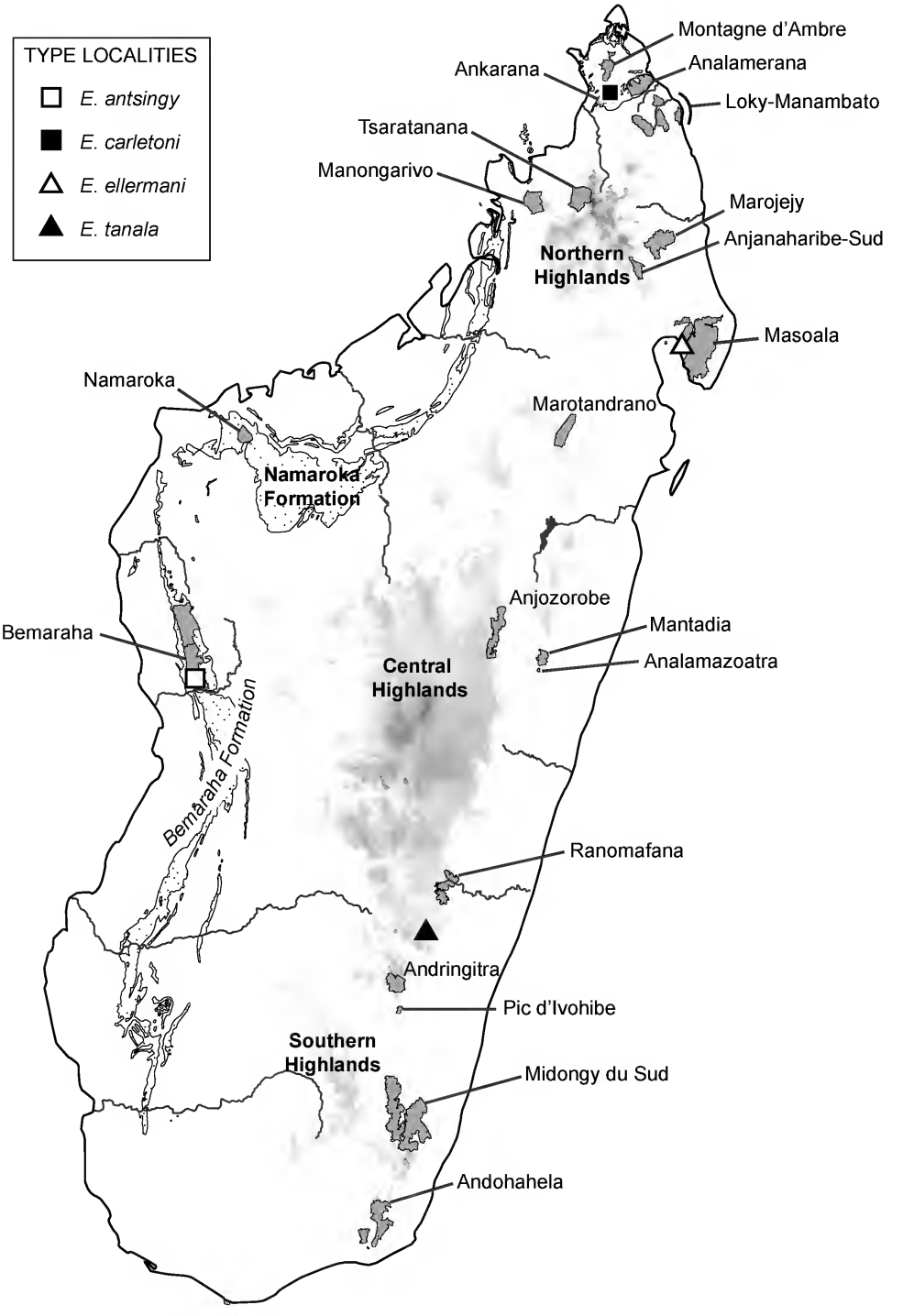

FIG. 2. Map of Madagascar showing regions of Mesozoic limestone (stippled) and elevations over 800 m (grayscale, with darker shades corresponding to higher elevations). Also illustrated are type localities of the four taxa considered herein and selected protected areas (dark gray) where most specimens examined have been collected.

populations in the Northern Highlands and accordingly amend the taxon's definition and distribution. In order to address these central goals, we necessarily amplify the means for discriminating species of the *E. antsingy* group (*E. antsingy* Carleton et al., 2001, and *E. carletoni* Goodman et al., 2009) from members of the *E. tanala* group, especially in those regions of western Madagascar and the Northern Highlands where the two assemblages geographically overlap.

MATERIALS AND METHODS

Specimens, Museums, and Abbreviations: Our investigation is based on 372 museum specimens, whether used in morphometric or molecular analyses or in both. These traditional and molecular preparations are housed in the following museums, identified by their institutional abbreviations as used throughout the text and in tables and figures: the Natural History Museum, London (BMNH, formerly British Museum of Natural History); Field Museum of Natural History, Chicago (FMNH); Museum of Comparative Zoology, Harvard University (MCZ); Muséum national d'Histoire naturelle, Paris (MNHN); Mention Zoologie et Biodiversité Animale, Université d'Antananarivo, Antananarivo (UADBA, formerly Département de Biologie Animale); and National Museum of Natural History, Smithsonian Institution, Washington, DC (USNM, formerly U.S. National Museum). The 372 vouchered specimens represent 83 principal collecting localities whose coordinates and supplementary geographic description are given in appendices 1 and 3. These numbered localities were used to define composite analytical samples and to compose the distributional map (fig. 16).

Taxonomic and distributional conclusions are founded on complementary genetic and traditional morphological data for many localities. Of the 372 vouchered specimens reported herein, 43% were gene sequenced, as indicated by museum catalog numbers for the terminal branches of molecular trees, and 82% possessed measurable skulls for morphometric analyses, as are visually contrasted to gene-sequenced specimens in multivariate graphs; 31% of the total specimens examined were used in both molecular and morphometric analyses. Half (43) of the 83 georeferenced localities are represented by one or more specimens with processed tissues, along with those consisting of conventional museum preparations; many localities (32) were taxonomically allocated based only on morphological evidence, and a few (8) based only on molecular evidence. Past molecular studies—Jansa et al. (1999); Goodman et al. (2009); Rakotoarisoa et al. (2010, 2012, 2013)—were consulted to assign the genetic identity of many specimens (mostly *E. carletoni* from the Loky-Manambato region) used in morphometric analyses, although such specimens were not necessarily sequenced again for the present study.

Holotypes of *Eliurus* taxa relevant to the taxonomic questions at issue have been studied by the authors, namely those of *antsingy*, *carletoni*, *ellermani*, and *tanala*. Skulls of all four types were measured and included where appropriate in our morphometric analyses. Molecular samples were directly available for the holotypes of *E. carletoni* (FMNH 173105) and *E. ellermani* (MNHN 1981.871), the former from fresh tissues preserved with the recently collected type and the latter based on DNA extracted from the MNHN round skin. Although sequences were not obtained from the holotypes of *E. antsingy* and *E. tanala*, newly collected material of these species was obtained from essentially topotypic locations and leaves no doubt about the identity of the taxon in question (see comments for localities 40 and 64, appendix 1).

We employed Carleton (1994) for morphological terms to describe *Eliurus* anatomy. The upper- and lowercase abbreviations M1–3 or m1–3 are used to individually reference the upper (maxillary) and lower (dentary) molars, respectively. Throughout the text, figures, and Specimens Examined sections, abbreviations are used for the different classes of protected areas in Madagascar: PHP, Paysage Harmonieux Protégé; PN, Parc National; RF, Réserve For-

estière; RNI, Réserve Naturelle Intégrale; RS, Réserve Spéciale. Mount (Mt) and Mountains (Mts) are similarly contracted where they form part of the proper placename.

Measurements, Analytical Samples, and Morphometric Analyses: For each specimen, we recorded a maximum of seven external and 18 craniodental measurements, all taken in millimeters (mm) with the exception of weight in grams (g). External measurements are those made in the field by collectors and were transcribed from skin tags or field books: total length of body and tail (TOTL); head and body length (HBL); length of tail vertebrae (TL); hindfoot length (HFL, excluding claw length except as noted); ear length (EL); and weight (WT). Most external measurements were obtained by collectors using the same measurement protocol. Because external measurements are unavailable for most old specimens or uncertainty exists whether the HFL datum reflects with or without the claw (con unguis, c.u., versus sin unguis, s.u.), Carleton also measured a dry hindfoot length, with claw (DHFL), on museum skins whose metatarsal and phalangeal bones dried in more or less straight alignment. Shrinkage of the hindfoot on a dried skin of a large *Eliurus* species averages about 1.0–1.5 mm.

Sixteen cranial and two dental variables were measured by Carleton to 0.01 mm, using handheld digital calipers, accuracy rated as ±0.02 mm, while viewing crania under a stereomicroscope. These measurements, following the anatomical landmarks defined in Carleton (1994), and their abbreviations as used in text and tables, are as follows: breadth of the braincase (BBC); breadth across both incisive foramina (BIF); breadth of the bony palate across the first upper molars (BM1s); breadth across the occipital condyles (BOC); breadth of the rostrum (BR); breadth of zygomatic plate (BZP); depth of auditory bulla (DAB); interorbital breadth (IOB); length of bony palate (LBP); length of diastema (LD); length of incisive foramen (LIF); coronal length of maxillary toothrow (LM1–3); length of rostrum (LR); occipitonasal length (ONL); posterior breadth of the bony palate (PPB); postpalatal length (PPL); width of the first upper molar (WM1); and zygomatic breadth (ZB).

Specimens were sorted into four age classes based on a combination of pelage and tooth wear: juvenile or subadult (J)—soft gray or dusky gray pelage, M3 not erupted or if erupted wholly unworn; young adult (Y)—adult pelage acquired or in transitional molt to adult pelage, M3 completely erupted but essentially unworn; full adult (A)—adult pelage fully acquired, molars moderately worn, dentinal basins about as wide as reentrant folds; old adult (O) molars heavily worn, dentinal basins wider than reentrant folds.

Our study faced the usual impediments in assembling sample sizes suitable for informative morphometric analyses, drawing upon natural history collections accumulated over some 130 years and these reflecting the sampling biases inherent in short field sessions and localized collecting, differing collector interests and abilities, and changing inventory equipment and survey protocols. Of the 83 georeferenced localities (appendix 1, fig. 16), approximately 70% consist of one to five specimens; just 8% consist of 10 or more. The removal of juvenile animals and damaged crania further reduced the number of wholly intact, measurable skulls suitable for multivariate analysis. The lack of large samples from a single locality in particular hindered rigorous evaluation of nongeographic variation (e.g., age-related size variation and sexual dimorphism). In this instance, we relied upon a large cluster of localities of *E. carletoni* ($N = 58$) collected in forests around Daraina, mostly within the PHP de Loky-Manambato (appendix 1: localities 7–15, 17; see Goodman and Wilmé, 2006), whose genetic identity is well understood (Rakotoarisoa et al., 2010, 2012). We employed a principal component analysis to assess nongeographic variation in cranial measurements for this population, as well as one-way ANOVAs with either sex or age class as categorical variables. Small sample sizes also affected our analytical approach to investigating geographic variation in the *E. tanala* species group; as a result of the small size,

we employed a discriminant function analysis, which requires predefined groups of suitable size. Because most collecting localities comprise 5 or fewer specimens, we clustered geographically nearby localities into seven operational taxonomic units (OTUs) of *E. tanala*, labeled t1–t7 from north to south, corresponding to the principal geographic sources of specimens used in our molecular analyses. These OTUs form the units for a discriminant function analysis designed to test diagnosability of geographic units in the *E. tanala* species group.

For the purpose of labeling trees and graphs, the name of a Malagasy protected area (see fig. 2) is employed to indicate the general geographic origin of a sequenced specimen or to broadly designate an OTU. Use of the modifier "and vicinity" acknowledges that some included specimens may be drawn from localities outside the boundaries of a protected area or that specimens may have been collected before the site was officially named. We adopt nominal tags to identify *tanala*-like specimens from *tsingy* landscapes of western Madagascar ("*E. tanala*-A") and those from wet montane forests of the Northern Highlands ("*E. tanala*-B"). Our analytical units are defined below with reference to geographic locality numbers given in the gazetteer (appendix 1).

E. antsingy: Namoroka formation (localities 31, 33, 34) and Bemaraha formation (localities 40, 42), (N = 12).

E. carletoni: RS d'Ankarana and vicinity (localities 2–5) and PHP de Loky-Manambato (localities 7–15, 17), (N = 72).

E. tanala-A: Namoroka formation (localities 32, 33, 36), Forêt d'Analamavo (locality 35) and Bemaraha formation (localities 37–42) for principal component analysis (N = 30); all western Madagascar samples (localities 32, 33, 35–42) as a single OTU for discriminant function analysis (N = 26).

E. tanala-B: all Northern Highland samples (localities 16–18, 22–29) for principal component analysis (N = 33); RS d'Anjanaharibe-Sud and vicinity (localities 22–29) for discriminant function analysis (N = 18).

E. tanala: t1–PN d'Analamazaotra and vicinity (localities 47–54; N = 21); t2–PN de Ranomafana and vicinity (localities 56–59; N = 27); t3–Forêt de Vinanitelo and vicinity (localities 63–66; N = 11); t4–PN d'Andringitra and vicinity (localities 67–71; N = 25); t5–RS du Pic d'Ivohibe and vicinity (localities 72–75; N = 17); t6–PN de Befotaka-Midongy du Sud (localities 77, 78; N = 12); t7–PN d'Andohahela and vicinity (localities 79–82; N = 16).

Individuals representing all three adult cohorts were used to derive conventional descriptive statistics (sample mean, observed range, and standard deviation) and to conduct morphometric analyses of the 18 craniodental variables. Means and ranges of external variables are tabulated as guidance to identification or indicators of general size, but were not input into morphometric analyses. One-way analysis of variance, discriminant function classification, and principal component scores were computed using only the 18 craniodental variables, all of which were first transformed to natural logarithms. Principal components were extracted from the variance-covariance matrix, and variable loadings are expressed as Pearson product-moment correlation coefficients of the derived principal components or canonical variates with the log-transformed original cranial measurements. In the PCAs, we employed an oblique factor rotation method (Oblimin) to assist interpretation of variable loadings. Oblique factor rotation is preferred over orthogonal methods (e.g., Equamax, Varimax) when there is reasonable a priori expectation that the extracted factors are correlated (e.g., Brown, 2009). The variance-covariance matrices of interest here, generated from linear measurements of the rodent skull, aptly meet this criterion, the mammalian cranium being a complex, three-dimensional structure composed of integrated growth fields and functionally correlated parts. Hierarchical clustering of analytical samples was based

on Mahalanobis distances between OTU centroids and generated by the unweighted pair-group method using arithmetic averages (UPGMA). Analytical procedures were implemented using statistical packages contained in SYSTAT (Systat Software, 2004, version 11.0) or PAST (Hammer et al., 2001, version 3.12).

DNA Extraction, Amplification and Analysis: For most specimens of the *E. tanala* and *E. antsingy* complexes, DNA was extracted from tissue samples that were preserved in 0.5% EDTA buffer using a DNAeasy extraction kit (Qiagen Inc., Valencia, CA). Extractions from dried museum specimens were conducted in a separate laboratory that did not contain polymerase chain reaction (PCR) products from mammals. Sequences from other species of *Eliurus*—*E. myoxinus* Milne Edwards (1885), *E. majori* Thomas (1895), *E. minor* Major (1896a), *E. webbi* Ellerman (1949), and *E. grandidieri* Carleton and Goodman (1998)—were included, bringing our generic representation to nine of the 12 currently recognized species. Prior phylogenetic work on nesomyines (Jansa et al., 1999), using cytochrome-*b* data, has suggested that the genus *Voalavo* Carleton and Goodman (1998) is nested within *Eliurus*; therefore, our phylogenetic analysis assumes an ingroup comprising the nine *Eliurus* species plus *V. gymnocaudus*, and trees were rooted by specifying *Gymnuromys roberti* Major (1896b) as the outgroup.

We PCR-amplified the mitochondrial cytochrome-*b* gene (*Cytb*) from broad geographic samples of individuals representing *E. tanala* (Central and Southern Highlands), *E. tanala*-A (western Madagascar), *E. tanala*-B (Northern Highlands), *E. antsingy* (Bemaraha and Namoroka formations) and *E. carletoni* (RS d'Ankarana and PHP de Loky-Manambato). For most samples, the entire mitochondrial *Cytb* gene was amplified, but only two, noncontiguous 150–175 base-pair fragments were recovered from the dried skin of *E. ellermani* (MNHN 1981.871). Our full data matrix of *Cytb* sequences included 162 terminal specimens. We also sequenced the mitochondrial gene NADH dehydrogenase 2 (*Nd2*) and four nuclear genes from 31 specimens selected to represent the same broad geographic areas and nominal taxa. Nuclear loci included two autosomal exons (retinol binding protein 3—*Rbp3*—and von Willebrand factor—*Vwf*), one autosomal intron (fibrinogen beta chain, intron 7—*Fgb*) and one X-linked intron (opsin 1, medium-wave sensitive, intron 3—*Opn1mw*). Primers used for amplifying and sequencing the nuclear loci are given in appendix 2. All PCR reactions were performed using reaction conditions described in Jansa and Weksler (2004), with annealing temperatures modified as necessary. PCR products were Sanger-sequenced in both directions, and resulting chromatograms were inspected and edited in Geneious ver. 7.05 (available from http://www.geneious.com; Kearse et al., 2012). The resulting DNA sequences were aligned using MUSCLE (Edgar, 2004) in Geneious ver. 7.0.5. Sequences have been deposited in GenBank (accession numbers MK806697–MK807006).

Phylogenetic analysis of the 162-specimen *Cytb* matrix was performed using maximum likelihood inference (ML) under the GTRGAMMA model as implemented in RAxML (Stamatakis, 2006). For the 31-specimen concatenated mitochondrial-gene matrix, we first determined the best partitioning scheme for the six gene-by-codon sets using ParitionFinder (Lanfear et al., 2012) and then specified that scheme in RAxML with likelihoods evaluated under the GTRGAMMA model. Nodal support for both analyses was assessed using 1000 replicates of standard bootstrap searches, specifying the GTRGAMMA model in RAxML. For each nuclear-gene matrix, we phased heterozygotes using PHASE ver. 2.1 (Stephens et al., 2001; Stephens and Donnelly, 2003) and determined the best model of nucleotide substitution using the Bayesian information criterion (BIC) as implemented in jModelTest (Posada, 2008). We performed gene-tree and species-tree inference for the four nuclear loci in *BEAST, ver. 1.7.4 (Drummond and Rambaut, 2007; Heled and Drummond,

2009) with these substitution models and a strict clock specified as part of the prior set. For species-tree analysis, we specified a constant-population-size demographic model for the multispecies coalescent, along with the appropriate ploidy level for each locus. Species-tree analysis requires prior assignment of individuals to species; we assigned each individual to a species based on its haplogroup membership in the *Cytb* phylogeny. We assigned the individuals from Forêt d'Analamavo to an ersatz "species" because mitochondrial DNA and nuclear DNA differed in whether these specimens allied with *E. tanala* (mtDNA), *E. tanala*-A (*Opn1mw*), or did not coalesce into a single species (the three autosomal loci; see results below). We ran the MCMC chain for 3×10^7 generations, sampling trees and parameters every 3000 generations. We removed the first 10% of these as burn-in and assessed estimated sample size (ESS) values and convergence using Tracer ver. 1.5 (Rambaut et al., 2014).

Finally, we used the species-delimitation program Bayesian Phylogenetics and Phylogeography (BPP), ver 3.2 (Yang and Rannala, 2010; Rannala and Yang, 2013), to test whether the four nuclear genes supported the species limits suggested by the mitochondrial phylogenies. Because the Forêt d'Analamavo sample showed potential evidence of incomplete lineage sorting (see below), we performed two sets of BPP analyses: one that omitted the six individuals from the Forêt d'Analamavo from the analysis and another that included them as a separate population. We used the A11 analysis option of BPP, which performs species delimitation and species-tree inference simultaneously. The BPP algorithm requires prior values specified for effective population size (θ) and divergence time (τ). Because analytical results can be sensitive to the specified values, we tested four prior schemes, comprising combinations of effective population size and divergence depth. Priors on θ and τ were specified through the α and β parameters of the gamma distribution, $\Gamma(\alpha,\beta)$, where the prior mean = α/β and its variance = α/β^2. For τ, we used $\Gamma(2,200)$ and $\Gamma(2,20000)$ for deep and shallow divergence time priors; assuming a mutation rate of 10^{-9} substitutions per site per year (generation), these correspond to 10 million years and 100,000 years before present, respectively. For effective population size, large and small values of θ were specified with $\Gamma(2,1000)$ and $\Gamma(2,100)$, which correspond to $\theta \approx 0.02$ and $\theta \approx 0.002$, respectively. We specified a heredity scalar to account for the different effective population sizes of X-linked and autosomal loci and performed the analysis with algorithm 0 for the rjMCMC algorithm (Rannala and Yang, 2013). We assigned sequenced individuals to either nine or 10 populations (depending on whether individuals from the Forêt d'Analamavo sample were included); these populations correspond to all the named haplogroups recovered in analyses of mitochondrial genes, except *Voalavo gymnocaudus* and *Eliurus grandidieri*, which were excluded from the species-delimitation analysis. We specified a guide tree for these populations based on the mitochondrial phylogeny and assumed a species-model prior of 1 (equal probabilities for all rooted trees). The analysis was run for 10,000 generations, sampling every two generations, with a burn-in of 4000 generations.

RESULTS

Molecular Phylogenetic Analyses

Mitochondrial and Nuclear Gene Trees: Phylogenetic analysis of the 162-specimen matrix of *Cytb* sequences recovered a large, well-supported clade (bootstrap = 98%) that circumscribes *tanala*-like specimens representing the nominal taxa *E. tanala*, *E. tanala*-A and *E. tanala*-B, to the exclusion of other species of *Eliurus* (fig. 3). The concatenated analysis of mitochondrial genes *Cytb* and *Nd2* (fig. 4) recovered this same clade with equally strong support (bootstrap = 100%), as did each of the individual nuclear-gene trees (fig. 5), and the species tree based on all four nuclear genes (fig. 6). Three haplotype groups within this large

clade are identifiable from the mitochondrial trees (figs. 3, 4). The largest includes specimens from the humid montane forests of the Central and Southern highlands (*E. tanala*; bootstrap = 98%); individuals collected near the type locality of *E. tanala*, Forêt de Vinanitelo (appendix 1: locality 65), are interspersed among the branches of this haplogroup (fig. 3). A second subclade (*E. tanala*-B; bootstrap = 97%) encompasses individuals from humid forests of northern Madagascar; the partial DNA sequence from the type specimen of *E. ellermani* (MNHN 1981.871) is associated with this haplogroup. The third haplogroup (*E. tanala* A; bootstrap = 100%) comprises specimens collected from *tsingy* regions around Namoroka and Bemaraha (*E. tanala*-A); no species name is presently available for this subclade.

Unexpectedly, six individuals collected in the Forêt d'Analamavo, a *tsingy*-associated, dry forest in on the Namaroka Formation of western Madagascar (fig 2; see also fig. 16: locality 35), have a mitochondrial haplotype that aligns them with typical *E. tanala*, a montane species from eastern humid forest in the Central and Southern highlands (figs. 3, 4). Based on geographic proximity alone, we had expected that the Forêt d'Analamavo sample would be allied with the western dry-forest form *E. tanala*-A, which it otherwise resembles morphologically (see next section). Analyses of the nuclear loci provide additional insight into this apparent conflict. When analyzed independently, the three diploid loci (*Rbp3*, *Vwf*, *Fgb*) do not show a clear pattern of coalescence along meaningful geographic or taxonomic lines; however, the X-linked locus, *Opn1mw*, clearly allies the populations from Forêt d'Analamavo with the western, dry-forest form *E. tanala*-A (fig. 5). Moreover, a species-tree analysis of the four nuclear loci, which treated the Forêt d'Analamavo sample as a distinct entity, places this population as the sister-group to *E. tanala*-A with high posterior probability, not to *E. tanala* sensu stricto (fig. 6). This result is not driven solely by the X-linked locus: a species-tree analysis based on only the three diploid loci recovers the same relationship, albeit with lower posterior probability (PP = 0.77 vs. 1.0). The increased support for this relationship from the X-linked locus reflects expectations of the coalescent process, whereby genes on the X chromosome, which have a relatively lower effective population size than do those on autosomes should coalesce relatively more recently.

Multilocus Species Delimitation: When the Forêt d'Analamavo sample is treated as an equivalent species-level taxon in the nuclear-gene BPP analysis, it either forms a unit independent from all other *Eliurus* species or forms a unit with *E. tanala*-A; no evidence supports the combination of the Forêt d'Analamavo sample with any other *Eliurus*, including *E. tanala* proper, to form a species-level unit (table 1). This result bolsters the allocation of the Forêt d'Analamavo sample to *E. tanala*-A, notwithstanding the population's retention of a mitochondrial haplotype that relates it more closely to *E. tanala*. When samples from the Forêt d'Analamavo are excluded from analysis, the model with the highest posterior probability includes nine independent species-level units; this model receives high posterior probabilities in analyses that assume a small effective population size, regardless of assumptions about divergence time (PP = 0.989 or 0.964; table 1). For analyses that assume a larger effective population size, there is no clear evidence for this nine-species model over one that combines *antsingy* and *carletoni* into a single species-level unit (table 1). All nine species-level groupings are recovered with high posterior probability (PP >0.95) across most combinations of prior values for population size and divergence time (table 2). Even under the difficult scenario of large effective population size and shallow divergence times, BPP analyses uniformly provided strong evidence for recognition of *E. tanala*, the *tanala*-like population from the Northern Highlands (*E. tanala*-B), and an undescribed species from western landscapes (*E. tanala*-A) as separate entities.

FIG. 3. The maximum-likelihood (lnL = -6820.4) tree of *Eliurus* resulting from a codon-partitioned analysis of 162 *Cytb* sequences (rooted with *Gymnuromys roberti,* not shown). Numbers at nodes are bootstrap support, support values <50% not shown; the dashed line indicates the phylogeny has been broken across two columns, the actual branch length is shown with a solid line (branch length units in substitutions/site as indicated by scale bar below). The arrow indicates the type specimen of *E. ellermani* (MNHN 1981.871). Terminal branches are labeled with locality name, locality number in parenthesis (appendix 1, fig. 16) and museum voucher number.

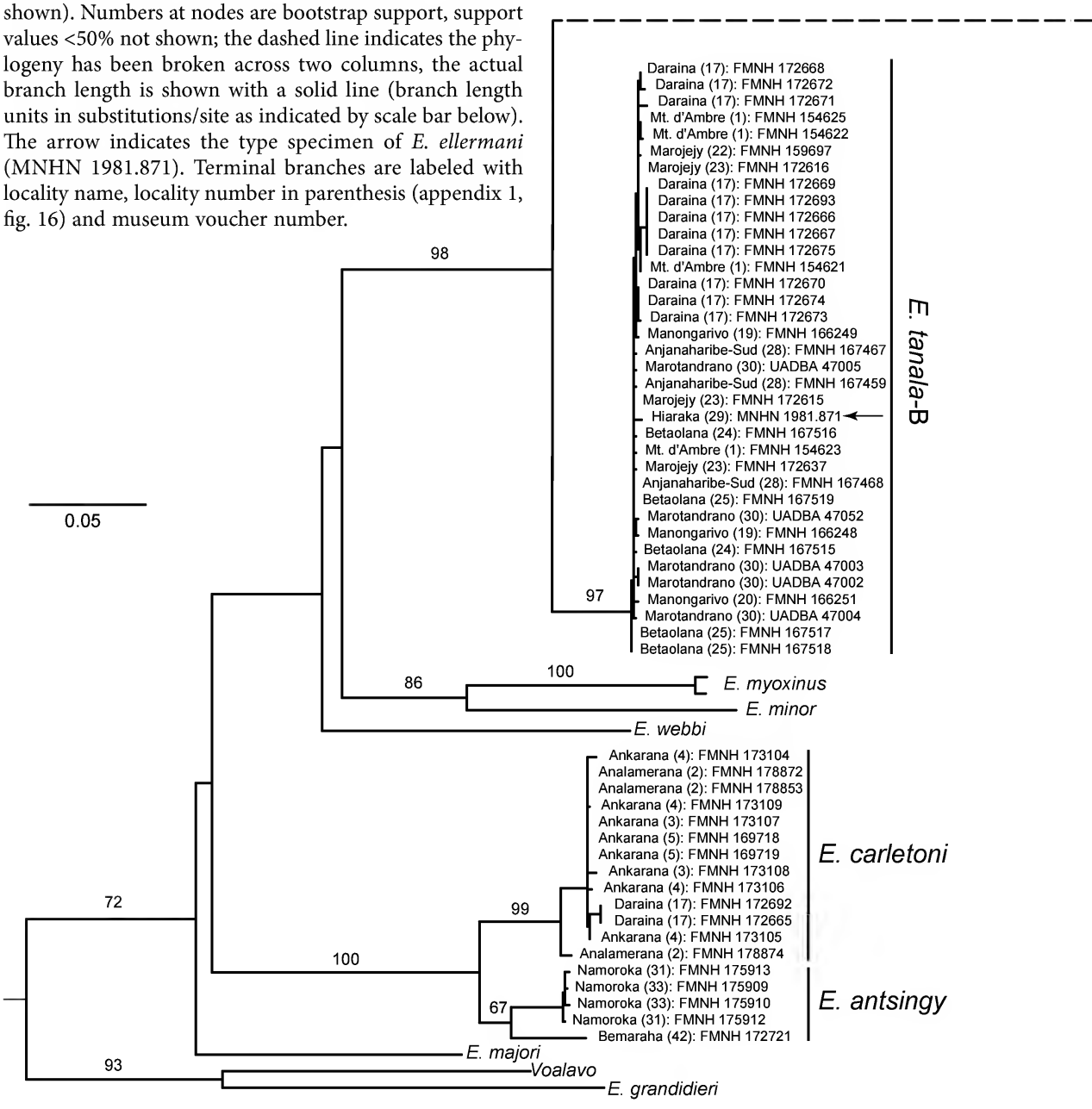

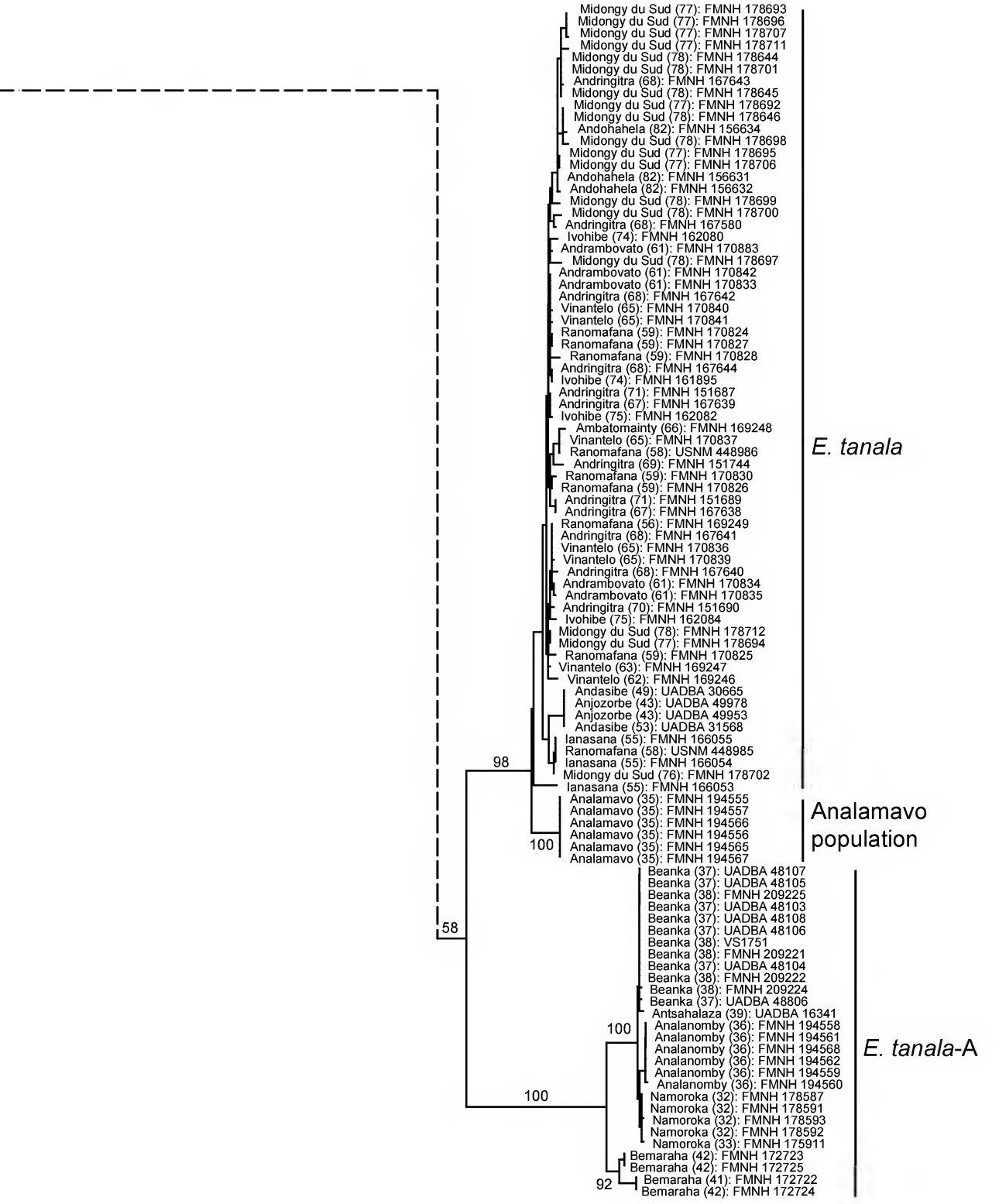
Midongy du Sud (77): FMNH 178693
Midongy du Sud (77): FMNH 178696
Midongy du Sud (77): FMNH 178707
Midongy du Sud (77): FMNH 178711
Midongy du Sud (78): FMNH 178644
Midongy du Sud (78): FMNH 178701
Andringitra (68): FMNH 167643
Midongy du Sud (78): FMNH 178645
Midongy du Sud (77): FMNH 178692
Midongy du Sud (78): FMNH 178646
Andohahela (82): FMNH 156634
Midongy du Sud (78): FMNH 178698
Midongy du Sud (77): FMNH 178695
Midongy du Sud (77): FMNH 178706
Andohahela (82): FMNH 156631
Andohahela (82): FMNH 156632
Midongy du Sud (78): FMNH 178699
Midongy du Sud (78): FMNH 178700
Andringitra (68): FMNH 167580
Ivohibe (74): FMNH 162080
Andrambovato (61): FMNH 170883
Midongy du Sud (78): FMNH 178697
Andrambovato (61): FMNH 170842
Andrambovato (61): FMNH 170833
Andringitra (68): FMNH 167642
Vinantelo (65): FMNH 170840
Vinantelo (65): FMNH 170841
Ranomafana (59): FMNH 170824
Ranomafana (59): FMNH 170827
Ranomafana (59): FMNH 170828
Andringitra (68): FMNH 167644
Ivohibe (74): FMNH 161895
Andringitra (71): FMNH 151687
Andringitra (67): FMNH 167639
Ivohibe (75): FMNH 162082
Ambatomainty (66): FMNH 169248
Vinantelo (65): FMNH 170837
Ranomafana (58): USNM 448986
Andringitra (69): FMNH 151744
Ranomafana (59): FMNH 170830
Ranomafana (59): FMNH 170826
Andringitra (71): FMNH 151689
Andringitra (67): FMNH 167638
Ranomafana (56): FMNH 169249
Andringitra (68): FMNH 167641
Vinantelo (65): FMNH 170836
Vinantelo (65): FMNH 170839
Andringitra (68): FMNH 167640
Andrambovato (61): FMNH 170834
Andrambovato (61): FMNH 170835
Andringitra (70): FMNH 151690
Ivohibe (75): FMNH 162084
Midongy du Sud (78): FMNH 178712
Midongy du Sud (77): FMNH 178694
Ranomafana (59): FMNH 170825
Vinantelo (63): FMNH 169247
Vinantelo (62): FMNH 169246
Andasibe (49): UADBA 30665
Anjozorbe (43): UADBA 49978
Anjozorbe (43): UADBA 49953
Andasibe (53): UADBA 31568
Ianasana (55): FMNH 166055
Ranomafana (58): USNM 448985
Ianasana (55): FMNH 166054
Midongy du Sud (76): FMNH 178702
Ianasana (55): FMNH 166053
Analamavo (35): FMNH 194555
Analamavo (35): FMNH 194557
Analamavo (35): FMNH 194566
Analamavo (35): FMNH 194556
Analamavo (35): FMNH 194565
Analamavo (35): FMNH 194567
Beanka (37): UADBA 48107
Beanka (37): UADBA 48105
Beanka (38): FMNH 209225
Beanka (37): UADBA 48103
Beanka (37): UADBA 48108
Beanka (37): UADBA 48106
Beanka (38): VS1751
Beanka (38): FMNH 209221
Beanka (37): UADBA 48104
Beanka (38): FMNH 209222
Beanka (38): FMNH 209224
Beanka (37): UADBA 48806
Antsahalaza (39): UADBA 16341
Analanomby (36): FMNH 194558
Analanomby (36): FMNH 194561
Analanomby (36): FMNH 194568
Analanomby (36): FMNH 194562
Analanomby (36): FMNH 194559
Analanomby (36): FMNH 194560
Namoroka (32): FMNH 178587
Namoroka (32): FMNH 178591
Namoroka (32): FMNH 178593
Namoroka (32): FMNH 178592
Namoroka (33): FMNH 175911
Bemaraha (42): FMNH 172723
Bemaraha (42): FMNH 172725
Bemaraha (41): FMNH 172722
Bemaraha (42): FMNH 172724
98
100
58
100
100
92
E. tanala
Analamavo population
E. tanala-A

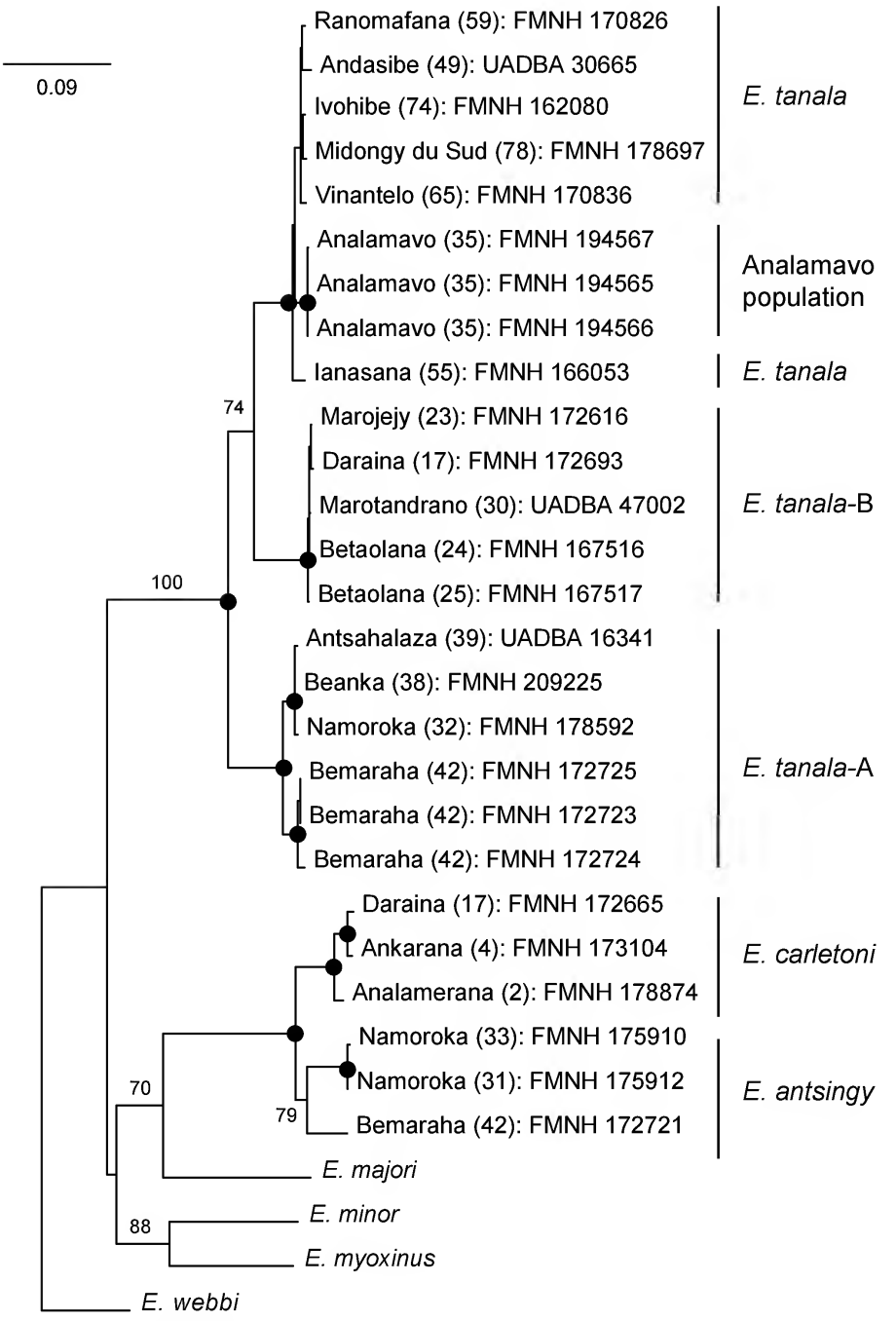

FIG. 4. The maximum-likelihood (lnL = -9767.1) tree of *Eliurus* resulting from a partitioned analysis of concatenated *Cytb* and *Nd2* sequences (rooted with *Gymnuromys roberti*, not shown). The best partitioning scheme included four partitions: one each for first codon positions of *Cytb* and *Nd2*, one for all second codon positions, and one for all third codon positions. Numbers at nodes indicate bootstrap support; support values <50% not shown, 100% shown with solid circles. Terminal branches are labeled with locality name, locality number in parenthesis (appendix 1, fig. 16), and museum voucher number.

Patterns of Morphometric Differentiation

In the following sections, we first explore sexual dimorphism and age-related size differences, the two sources of nongeographic variation typically accessible with museum material. Subsequently, we use principal component analysis (PCA) to illuminate patterns of variation in two regions where populations of the *E. antsingy* and *E. tanala* complexes occur in sympatry or close allopatry. Finally, we apply discriminant function analysis (DFA) to assay differentiation among geographically defined OTUs of the *E. tanala* complex that covers its entire distribution.

Nongeographic Variation: According to one-way ANOVAs that designated sex as a categorical effect, males and females do not differ in cranial size within the large sample of *Eliurus carletoni* from the PHP de Loky-Manambato (table 3). The nearly identical skull size of males and females is remarkably fine: most continuous variables are equal, the remainder differing by only 0.1–0.3 mm.

In contrast, a majority of cranial dimensions of *E. carletoni* disclosed moderate to highly significant differences with age class as categorical effect in one-way ANOVAs (table 3). These variables are characterized by regular, incremental increases in mean size across the three adult age cohorts we defined, producing age-correlated differences that measurably affect variation within our sample. In general, F values and attained significance levels are greatest for the three largest variables (ONL, PPL, ZB) and those measured on the facial region (BIF, LR, WR, WZP); dimensions of the neurocranium (BBC, BOC, IOB) generally yielded lower F values. Measurements of the maxillary toothrow (LM1–3, WM1) constitute a notable exception to the pattern of age-correlated size increase; once erupted, the rooted molars of *Eliurus* may decrease in crown height during trituration, but do not grow in length and width (table 3). Some postweaning ontogenetic variation is usually captured by the first principal component, often characterized as a size factor, in craniometric studies of closely related (congeneric) muroid species. This relationship explains the elongated constellations of specimen scores commonly observed in plots of the first two principal components extracted, the major axis of each taxon ellipse typically oriented obliquely to the PC eigenvectors (e.g., Voss et al., 1990; Voss and Marcus, 1992; Carleton et al., 1999; Carleton and Stanley, 2012).

Given these results, we combined measurements of all adult males and females in computing descriptive statistics and conducting morphometric comparisons. We also united measurements of the three adult age classes (Y, A, and O), notwithstanding the potential variation introduced by postweaning cranial growth, rather than restrict ordination to a single age class and further diminish sample sizes. Although some age-related size increase may contribute to within-sample variation of *Eliurus*, it consistently emerged as negligible relative to those extracted factors that proved to be taxonomically informative.

Principal Component Analysis of *Eliurus antsingy* and *E. tanala*-A: Carleton et al. (2001) characterized the first individual (MNHN 1966.2221) provisionally identified as a western *tanala*-like form (herein as *E. tanala*-A) as large in cranial size, resembling the newly described *E. antsingy*. This cranial similarity is borne out by certain dimensions of the skull (ONL) and molars (LM1–3), a bivariate scatterplot that randomly intermixed specimens of *E. tanala*-A, including the series from the Forêt d'Analamavo, with those of *E. antsingy* (fig. 7A). Other cranial dimensions, however, offer sharp distinction between examples of *E. tanala*-A and *E. antsingy*, especially those involving the size of the incisive foramina (LIF) relative to the bony palate (LBP), as plotted in fig. 7B. The latter variables figured prominently in multivariate discrimination of the two western forms.

A PCA of all 18 craniodental variables produced nonoverlapping, unambiguous segregation of examples of *E. antsingy* from those of *E.*

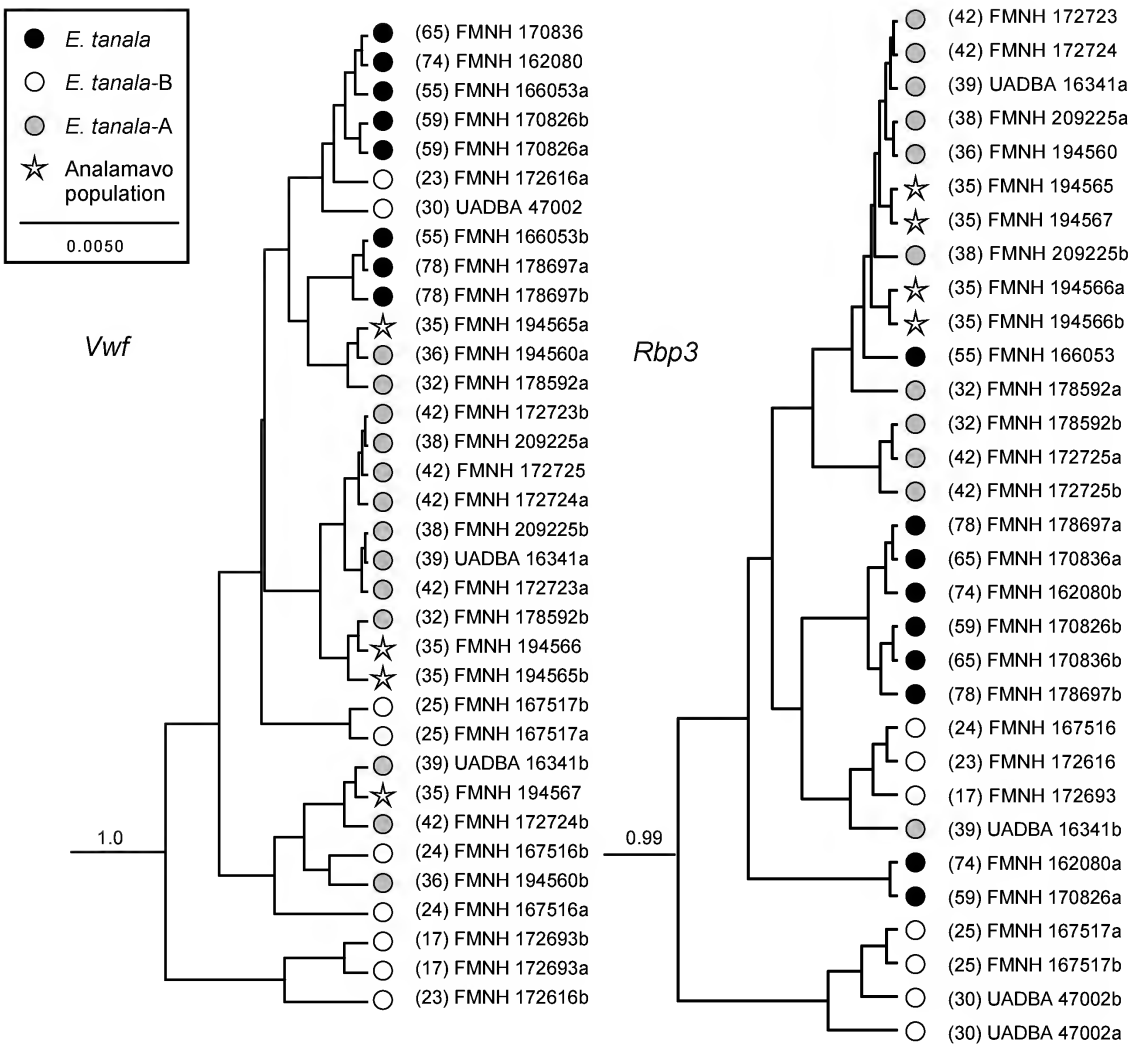

FIG. 5. Individual nuclear-gene trees (*above and opposite page*) inferred during a species-tree analysis using *BEAST. In each case, trees are maximum-clade-credibility trees showing relationships among members of the *Eliurus tanala*-like clade (other species were included in the analysis but are omitted from the figure for clarity). Terminal branches are labeled with locality number in parenthesis (appendix 1, fig. 16) followed by museum voucher number; for heterozygous individuals, alleles are labeled "a" or "b" after the specimen number. Specimens were assigned species identity (shown by symbols) according to haplogroup membership in the *Cytb* phylogeny (fig. 3). Numbers at nodes are posterior probability values ≥0.99.

tanala-A (fig. 7C). Phenetic cohesion of both gene-sequenced specimens and nonsequenced specimens is apparent within each elliptical spread; the series from the Forêt d'Analamavo broadly intersects the constellation representing *E. tanala*-A, a placement consistent with analyses of nuclear-gene sequences (figs. 5, 6). Each constellation also encloses scores from localities where *E. antsingy* and *E. tanala*-A occur in sympatry; such specimens are appropriately grouped consistent with their genetic affinity (specimens not flagged in fig. 7C, but see appendix 1: localities 33, 40, 42). The nonsequenced holotype of *E. antsingy* (MNHN 1966.2220) is obviously associ-

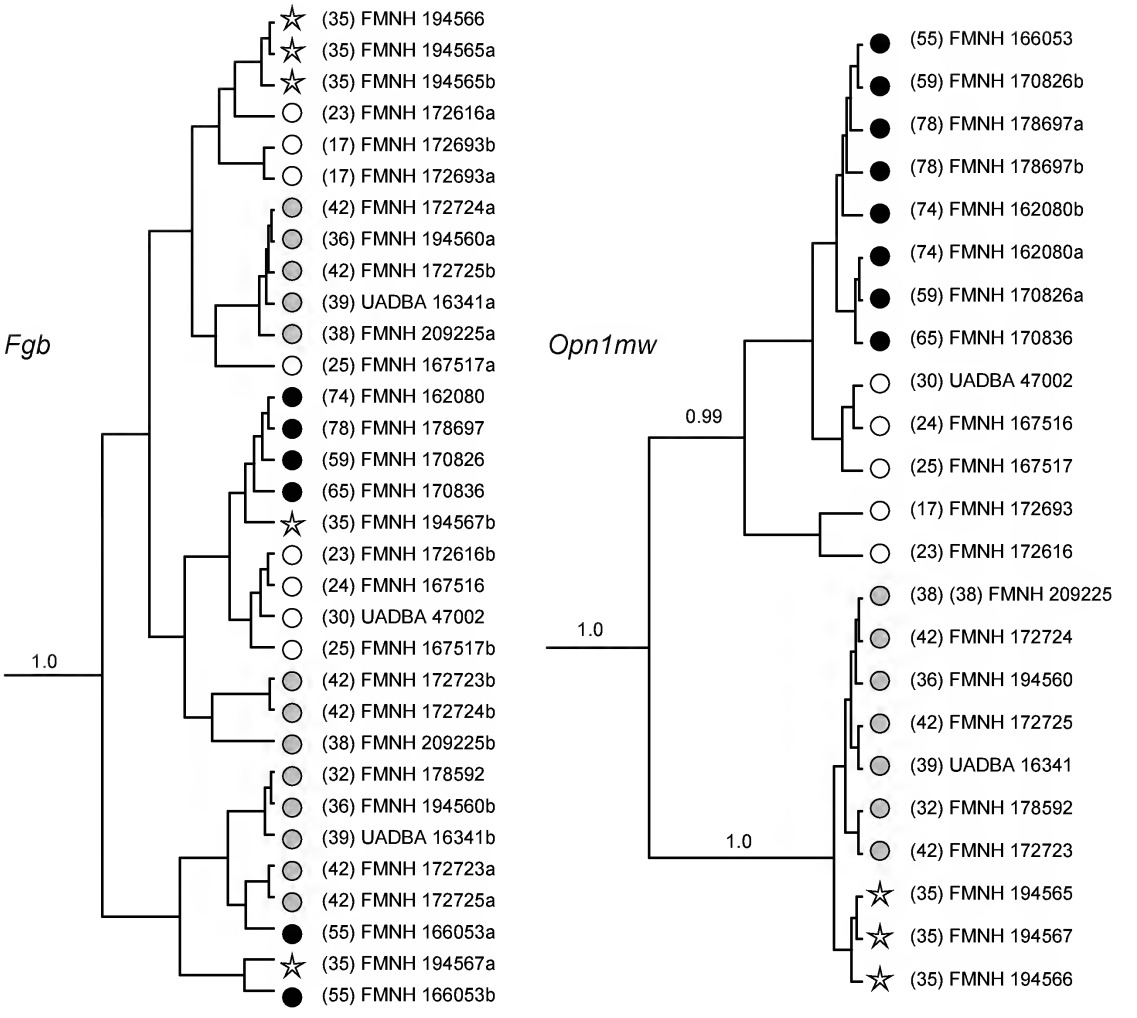

ated with sequenced and nonsequenced specimens that have a similar cranial morphology, confirming application of that name to the clade recovered in our molecular trees (fig. 3) and in past investigations (Goodman et al., 2009; Rakotoarisoa et al., 2010). The nonsequenced specimen (MNHN 1966.2221) first reported as a western *tanala*-like form clustered with others later collected on the Bemaraha and Namoroka Massifs for which molecular data are available, but for which no name is currently applicable.

Subsequent Oblimin rotation of the variable loadings comprehensibly decomposed age effects (RPC I) and taxon effects (RPC II). A majority of measurements loaded positively and highly significantly on RPC I (r = 0.6–0.9), except those taken on the molars (table 4A). Variation along this axis captured substantial within-sample age variation, as reflected by a post hoc one-way ANOVA with age class as effect (df = 2, 36; F = 26.6; $P \leq 0.001$); on the other hand, taxon (sample) as categorical variable yielded insignificant results in a one-way ANOVA of RPC I scores (df = 2, 37; F = 2.4; P = 0.101). Discrimination between samples is clearly appreciated by those variables that strongly correlate with the rotated second component, which is oriented perpendicular to the major axes of the sample ellipses (fig. 7C); logically, a one-way ANOVA of RPC II scores with taxon as effect is highly significant

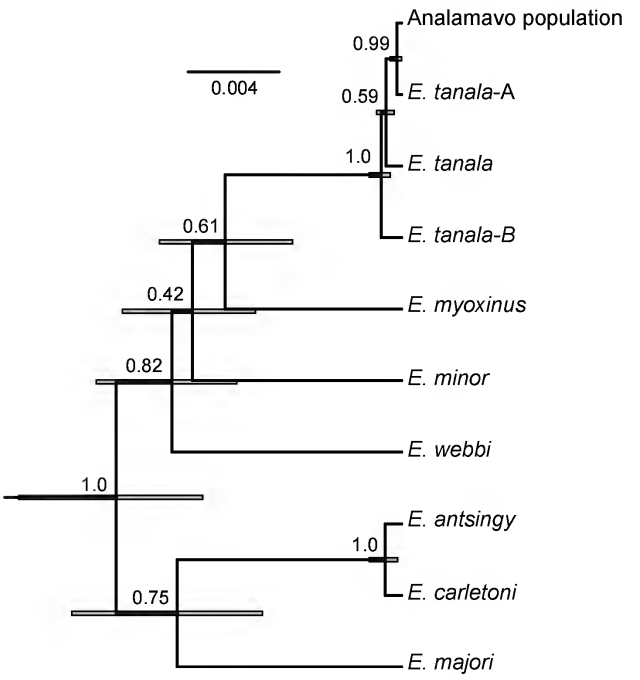

FIG. 6. The maximum-clade-credibility species tree resulting from species-tree analysis of four nuclear genes in *BEAST. Numbers at nodes represent posterior probabilities, error bars are 95% credibility intervals on node height.

(df = 2, 37; F = 118.0; $P \leq 0.0001$). Compared with specimens of *E. antsingy*, the sign and magnitude of loading coefficients on RPC II (table 4A) describe the *E. tanala*-A skull as having a smaller neurocranium (BBC, BOC, IOB), shorter and narrower incisive foramina (BIF, LIF), but longer hard palate (LBP), and less inflated auditory bulla (DAB).

The sample from the Forêt d'Analamavo warrants additional comment in view of the contradictory relationships apparent in analyses of the mitochondrial genes (figs. 3, 4) and nuclear genes (fig. 5). Visually, the major axes of the three sample ellipses appear more or less parallel to one another, and the scatters of *E. tanala*-A and the Forêt d'Analamavo animals overlap appreciably based on their factor scores (fig. 7C). Statistically, the slopes of the major axes of all three samples were inseparable (df = 2, 37; F = 0.2; P = 0.849). The Y-intercept of *E. antsingy* contrasted substantially with both *E. tanala*-A (df = 1, 30; F = 157.1; $P \leq 0.001$) and Forêt d'Analamavo (df = 1, 17; F = 149.2; $P \leq 0.001$); whereas, the Y-intercept of the latter two samples failed to attain a significant difference (df = 1, 27; F = 2.0; P = 0.169). Based on the 18 cranial variables we measured and on the PCA performed, the Forêt d'Analamavo animals are quantitatively inseparable from other *tanala*-like specimens obtained from western dry forests. In the DFA reported below, we treat the series from Forêt d'Analamavo as part of the *E. tanala*-A OTU.

Principal Component Analysis of *Eliurus carletoni* and *E. tanala*-B: In the first taxonomically broad molecular study of Nesomyinae, Jansa et al. (1999) identified three specimens from the Northern Highlands (appendix 1: localities 1, 22) as *Eliurus* sp. B because of their substantial genetic divergence, revealed by *Cytb* sequences, from vouchers of *E. tanala* collected in the Central (appendix 1: localities 58, 69–71) and Southern highlands (appendix 1: locality

TABLE 1

Results from eight different species-delimitation analyses in BPP

Analyses either include or exclude the Forêt d'Analamavo sample, and assume one of four combinations of priors[1] for divergence time (τ, shallow or deep) and effective population size (θ, large or small). Numbers indicate posterior probabilities for the species-delimitation model shown in the first column; results are shown for only the top-scoring models.

	Prior Scheme [1]			
	Small, shallow	Small, deep	Large, shallow	Large, deep
Analamavo included				
(ant+car tanB maj min myo tan tanA+ana web)[2]	0.005	0.007	0.214	0.523
(ant car tanB maj min myo tan tanA+ana web)[2]	0.270	0.666	0.410	0.363
(ant+car tanB maj min myo tan tanA web ana)[2]	0.008	0.003	0.101	0.071
(ant car tanB maj min myo tan tanA web ana)[2]	0.712	0.325	0.170	0.037
Analamavo excluded				
(ant car tanB maj min myo tan tanA web)[2]	0.989	0.964	0.515	0.414
(ant+car tanB maj min myo tan tanA web)[2]	0.009	0.032	0.345	0.575

[1] Prior specification for population size: large $\theta \approx \Gamma(2,100)$; small $\theta \approx \Gamma(2,1000)$; prior specification for divergence time: deep $\tau \approx \Gamma(2,200)$; shallow $\tau \approx \Gamma(2,20000)$.

[2] Abbreviations correspond to haplogroups recovered from phylogenetic analysis of *Cytb* sequences (fig. 3): ant = *E. antsingy*, car = *E. carletoni*, tanB = *E. tanala*-B, maj = *E. majori*, myo = *E. myoxinus*, tan = *E. tanala*, tanA = *E. tanala*-A, ana = Forêt d'Analamavo, web = *E. webbi*.

82). The much denser geographic sampling used herein reveals that this genetically distinctive, *tanala*-like form (*E. tanala*-B) is widely distributed in the Northern Highlands (fig. 3). As in western Madagascar, the northern *tanala*-like form may occur in sympatry or contiguous allopatry with a morphologically similar member of the *E. antsingy* group, *E. carletoni*, described by Goodman et al. (2009) from the Ankarana formation and distributed broadly within the Loky-Manambato region (Rakotoarisoa et al., 2010, 2012, 2013). Below we expand the morphological discrimination of *E. tanala*-B from *E. carletoni* based on a PCA of log-transformed, craniodental measurements, including most specimens used in our molecular analyses (figs. 3–5) along with the gene-sequenced holotypes of *E. carletoni* and *E. ellermani*.

Two discrete clouds of specimen scores are evident in a scatterplot of the first two principal components extracted from ordination of all intact adult skulls representing *E. carletoni* and *E. tanala*-B (fig. 8). Whether based on sequenced or nonsequenced specimens, the separate groups are readily evident in morphometric space, and their membership conforms to the distinctive species-level clades recovered in the molecular trees (figs. 3, 4). Slopes of the major axis within each constellation are statistically equivalent (df = 1, 101; $F = 0.2$; $P = 0.628$), but their Y-intercepts differ markedly (df = 1, 101; $F = 482.7$; $P \leq 0.0001$). The holotype of *E. carletoni* (FMNH 173105) is nestled predictably near the center of the *E. carletoni* ellipse; the holotype of *E. ellermani* (MNHN 1981.871) is associated with specimens of *E. tanala*-B, concordant with its affinity based on the partial *Cytb* sequence recovered from the MNHN prepared skin (see fig. 3).

Oblique rotation of PC correlations usefully enhanced interpretation of the extracted eigen-

TABLE 2

Results from species-delimitation analysis in BPP

The Forêt d'Analamavo sample was not included in this analysis, and four combinations of priors[1] were assumed for divergence time (τ, shallow or deep) and effective population size (θ, large or small). Numbers indicate posterior probabilities for recognizing the mitochondrial haplogroup in the first column as a species-level unit. Posterior probabilities >0.95 are in bold.

	Prior Scheme			
	Small, shallow	Small, deep	Large, shallow	Large, deep
E. tanala-A	**1.0**	**1.0**	**1.0**	**1.0**
E. tanala-B	**1.0**	**1.0**	**1.0**	**1.0**
E. tanala	**1.0**	**1.0**	**1.0**	**1.0**
E. minor	**1.0**	**1.0**	**0.97**	**1.0**
E. webbi	**1.0**	**1.0**	0.93	**1.0**
E. myoxinus	**1.0**	**1.0**	0.93	**1.0**
E. majori	**1.0**	**1.0**	0.89	**0.99**
E. antsingy	**0.99**	**0.96**	0.60	0.42
E. carletoni	**0.99**	**0.96**	0.60	0.42
E. antsingy + *E. carletoni*	0.01	0.04	0.40	0.58

[1] Prior specification for population size: large $\theta \approx \Gamma$ (2,100); small $\theta \approx \Gamma$ (2,1000); prior specification for divergence time: deep $\tau \approx \Gamma$ (2,200); shallow $\tau \approx \Gamma$ (2,20000).

vectors. As in the morphometric comparison of *E. antsingy* and *E. tanala*-A, nearly all variable correlations (loadings) with RPC I are large and positive (table 4B). Age class as a categorical effect explains much of the spread in a one-way ANOVA of RPC I scores (df = 2, 102; $F = 27.3$; $P \leq 0.001$), but not taxon as a categorical variable (df = 1, 103; $F = 0.3$; $P = 0.587$). Conversely, age class contributed trivially to separation of specimens along RPC II (df = 2, 102; $F = 0.3$; $P = 0.775$), whereas taxon as group effect was singularly explanatory (df = 1, 103; $F = 482.7$; $P \leq 0.0001$). According to the sign and magnitude of RPC II loadings (table 4B), the skull of *E. tanala*-B possesses relatively short and narrow incisive foramina (BIF, LIF) but a longer bony palate (LBP) compared with *E. carletoni*, a proportional relationship that mirrors results of the *E. tanala*-A vis-à-vis *E. antsingy* morphometric comparison. Nevertheless, the skull of *E. tanala*-B is overall stoutly constructed compared with that of *E. carletoni*, a size difference conveyed by the large, positive correlations of the largest cranial dimensions (ONL, ZB), the longer rostrum (BR, LD, LR), and broader hard palate (BM1s) and zygomatic plate (BZP).

Discriminant Function Analysis of the *Eliurus tanala* Group: DFAs conducted in earlier studies, using smaller sample sizes, were inconclusive in resolving the status of *E. ellermani* compared with *E. tanala* (Carleton, 1994; Carleton and Goodman, 1998). The locality samples now available substantially expand our geographic perspective for addressing differentiation among *tanala*-like populations broadly distributed in eastern humid forests, from the Southern to the Northern highlands, and for assessing that differentiation in view of the well-defined mitochondrial haplogroups evident across this same region (figs. 3, 4). Too few specimens of *tanala*-like animals from western *tsingy*-associated forests, *E. tanala*-A, were heretofore available to

TABLE 3

Sex and age variation in *Eliurus carletoni*

Arithmetic means (in mm) of 18 craniodental variables and results of one-way ANOVAs for sex and age cohorts in adult *Eliurus carletoni* collected within the PHP de Loky-Manambato region (N = 58, localities 7–15, 17; F and M = female and male, respectively; Y, A, and O = young, full, and old adult age classes, respectively; F (sex) and F (age) = univariate F values; see Materials and Methods for variable abbreviations)

	Sex			Age			
Variable	F (N = 33)	M (N = 24)	F (sex)	Y (N = 19)	A (N = 28)	O (N = 11)	F (age)
ONL	40.0	39.9	0.7	38.5	40.5	41.3	42.1***
ZB	19.5	19.2	0.5	18.5	19.7	20.1	41.3***
BBC	15.1	15.0	0.3	14.8	15.2	15.2	7.1**
IOB	5.7	5.7	0.3	5.6	5.7	5.7	1.3
BOC	8.9	8.9	0.4	8.7	8.9	9.1	4.1*
LR	13.2	13.4	2.0	12.9	13.5	13.6	7.4**
BR	7.1	7.0	0.3	6.7	7.2	7.3	19.5***
LD	11.1	11.1	1.2	10.6	11.3	11.8	32.7***
LIF	5.7	6.0	3.0	5.7	5.9	6.0	2.4
BIF	2.7	2.6	0.9	2.6	2.7	2.7	5.5**
PPL	14.5	14.3	0.8	13.7	14.7	15.0	56.1***
LBP	7.6	7.6	0.3	7.4	7.7	7.9	5.9**
BM1s	7.5	7.5	0.7	7.3	7.5	7.7	13.1***
PPB	5.6	5.6	1.6	5.5	5.6	5.6	0.3
DAB	5.4	5.4	0.0	5.4	5.4	5.5	1.5
BZP	3.7	3.8	0.5	3.5	3.8	3.9	18.9***
LM1–3	5.58	5.63	0.8	5.57	5.62	5.67	0.9
WM1	1.51	1.53	0.2	1.51	1.53	1.52	0.4

* = $P \leq 0.05$; ** = $P \leq 0.01$; *** = $P \leq 0.001$.

apply multivariate analyses; we included the series from the Forêt d'Analamavo within the *E. tanala*-A OTU because the BPP and PCA results, as reported above, demonstrated their genetic and morphometric inclusion.

The first two canonical variates extracted from the nine-group DFA summarized 72.7% of among-group craniodental variation (table 5), and a scatterplot of the two conveyed informative taxonomic and geographic structure (fig. 9). Eigenvalues of CVs 1 and 2 are ≥1, and multivariate means among the nine predefined groups differ significantly (Wilks' Lambda = 0.043; df = 8, 149; F = 3.6; $P \leq 0.0001$). One-way ANOVAs on CV scores uncovered no significant age-class effect that influenced the dispersion of specimens along CV 1 (df = 2, 157; F = 2.9; P = 0.060) or CV 2 (df = 2, 157; F = 0.1; P = 0.944); the same one-way ANOVAs did disclose highly significant taxon (OTU) effects for both CV 1 (df = 8, 151; F = 40.6, $P \leq 0.001$) and CV 2 (df = 8, 151; F = 24.2; $P \leq 0.001$).

In general, CV 1 partitions the western moiety of the *E. tanala* group (*E. tanala*-A) from the eight OTUs distributed along the island's eastern side (*E. tanala*-B and *E. tanala*); whereas, CV 2

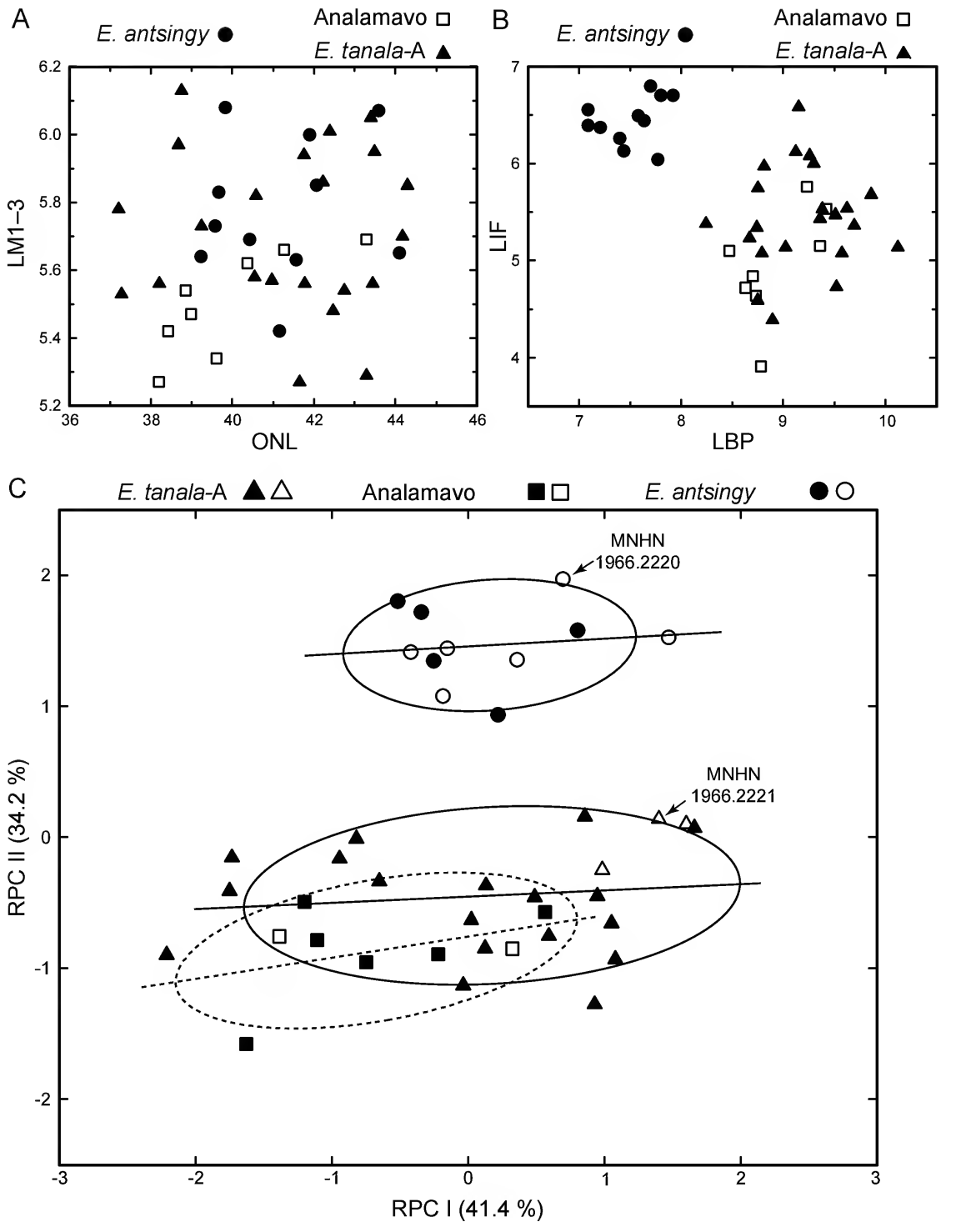
A
E. antsingy
Analamavo
E. tanala-A
LM1–3
ONL
B
E. antsingy
Analamavo
E. tanala-A
LIF
LBP
C
E. tanala-A
Analamavo
E. antsingy
MNHN
1966.2220
MNHN
1966.2221
RPC II (34.2 %)
RPC I (41.4 %)

captures size trends among the eastern population samples (fig. 9). Two dimensions, interorbital width (IOB) and bullar size (DAB), load prominently on CV 1 ($r \geq 0.6$), the former negatively and the latter positively (table 5), and primarily account for the isolation of *E. tanala*-A on that factor. The predominant influence of these two variables was unexpected in view of their nearly imperceptible difference when comparing skulls side by side; these same two variables logically generated the largest *F* values in univariate ANOVAs conducted across all nine OTUs. In a previous DFA iteration (not illustrated), we had treated the Forêt d'Analamavo sample as a separate OTU; this 10-group DFA affirmed the congruence of the Forêt d'Analamavo OTU with that of *E. tanala*-A, both set apart from the eight eastern OTUs along CV1.

In contrast to CV 1 loadings, a majority of variables correlate moderately and positively (r = 0.4–0.6) with CV 2, in effect grading OTUs by size, from smaller in the Southern Highlands (t6–PN de Befotaka-Midongy du Sud, t7–PN d'Andohahela) to larger toward the north (t1–PN d'Analamazaotra, *E. tanala*-B). The same geographic groupings are suggested by the pair-group associations portrayed in the phenogram generated from Mahalanobis' distances between OTU centroids (fig. 9C). The OTU *E. tanala*-B, represented by specimens from the RS d'Anjanaharibe-Sud and vicinity, is superimposed in morphometric space with OTU t1 (PN d'Analamazaotra) from the northern area of the Central Highlands (fig. 9A, B); their strong phenetic linkage is repeated in the cluster analysis (fig. 9C). Although our DFA involved more OTUs and larger sample sizes, these results reprise those of Carleton and Goodman (1998) regarding the lack of clear phenetic separation of population samples from the Northern Highlands. The indistinguishable morphometric footprint of our two northernmost OTUs, *E. tanala*-B and t1 (PN d'Analamazaotra), contradicts their unambiguous genetic separation, using *Cytb* and *Nd2* sequences (figs. 3, 4), between examples broadly drawn from the Northern Highlands and those of *E. tanala* proper, the latter including specimens from the PN d'Analamazaotra and vicinity (OTU t1).

The disposition of certain specimens employed in the DFA deserves mention based on a posteriori calculations of their group membership. The CV score for the holotype of *E. ellermani* (MNHN 1981.871) is positioned approximately equidistant to the centroids of *E. tanala*-B and OTU t1–PN d'Analamazaotra (fig. 9B); consequently, its post hoc classification is statistically inconclusive, although the predicted membership is actually greater for t1–PN d'Analamazaotra (P = 0.76) than *E. tanala*-B (P = 0.23). The post hoc assignment of the holotype of *E. tanala* (BMNH 97.9.1.154) is most strongly affiliated with the OTU embracing its geographic origin, t3–Forêt de Vinanitelo; nonetheless, the probability of its membership, although high (P = 0.83), falls below a comfortable level of statistical certainty (i.e., $P \geq 0.95$). The series from the Forêt d'Ianasana (Itremo), an isolated site at the western margin of the Central Highlands (see appendix 1: locality 55), was not defined as an OTU because of the

FIG. 7. Scatterplots of select raw cranial dimensions (A and B) and of extracted principal components (C) for examples of *Eliurus antsingy* (N = 11), *E. tanala*-A (N = 21), and the genetically enigmatic sample from Forêt d'Analamavo (N = 8). **A,** Bivariate plot of molar size (LM1–3) by occipitonasal length (ONL). **B,** Bivariate plot of palatal dimensions, LIF × LBP. **C,** Projection of specimen scores, based on all 18 log-transformed cranial variables, onto the first two principal components (RPC) extracted from ordination of all specimens representing the three samples, followed by oblique factor rotation (Oblimin). Confidence ellipses (1 SD) around sample centroids and the major axis of sample constellations were computed post hoc; highlighted specimen scores include the holotype of *E. antsingy* (MNHN 1966.2220) and the individual compared with *E. tanala* (MNHN 1966.2221) by Carleton et al. (2001). Closed symbols denote specimens used in gene-sequence analyses; open symbols represent nonsequenced individuals. See table 4A for variable correlations (loadings) and variance explained by the latent principal components.

TABLE 4

Results of two principal components analyses that compare regional samples of the *Eliurus antsingy* and *E. tanala* groups

A, *E. antsingy* and *E. tanala*-A in western Madagascar; **B,** *E. carletoni* and *E. tanala*-B in northern Madagascar. See figures 7 and 8 for plots of rotated principal component (RPC) scores and Materials and Methods for variable abbreviations.

	A *E. antsingy* & *E. tanala*-A		**B** *E. carletoni* & *E. tanala*-B	
	Rotated correlations		Rotated correlations	
Variable	RPC I	RPC II	RPC I	RPC II
ONL	0.96***	0.13	0.89***	0.43***
ZB	0.92***	0.15	0.89***	0.25**
BBC	0.83***	0.43**	0.78***	-0.08
IOB	0.36*	0.55***	0.45***	0.21*
BOC	0.51***	0.53***	0.59***	-0.03
LR	0.89***	-0.09	0.64***	0.67***
BR	0.85***	0.10	0.80***	0.38***
LD	0.86***	-0.28	0.71***	0.70***
LIF	0.63***	0.83***	0.48***	-0.62***
BIF	0.39*	0.90***	0.33***	-0.80***
LBP	0.24	-0.84***	0.43***	0.91***
PPL	0.89***	0.27	0.83***	0.12
BM1s	0.78***	0.14	0.72***	0.48***
PPB	0.17	0.36*	0.29**	-0.28**
DAB	0.58***	0.40**	0.40***	-0.25*
BZP	0.79***	0.04	0.75***	0.34***
LM1–3	0.20	0.43**	0.53***	0.10
WM1	0.27	0.17	0.54***	0.16
Eigenvalue	0.037	0.030	0.029	0.033
% Variation	41.4	34.2	33.4	37.6

* = $P \leq 0.05$; ** = $P \leq 0.01$; *** = $P \leq 0.001$.

small sample (N = 3), but all three individuals were entered as unknowns in the computation. Concordant with their relationship as divulged by *Cytb* (fig. 3), the specimens from Forêt d'Ianasana were classified among various OTUs of *E. tanala*, albeit none with a $P \geq 0.5$ (FMNH 166053 with t7–PN d'Andohahela; 166054 with t6–PN de Befotaka-Midongy du Sud; 166055 with t5–RS du Pic d'Ivohibe); moreover, all three displayed negligible affinity with the OTUs *E. tanala*-B or t1–PN d'Analamazaotra.

TAXONOMY

As an informal taxonomic category, the species group historically emerged within speciose muroid genera following the early phase of biological discovery and description, and accommodated tendencies of character variation among morphologically similar taxa and allopatric populations of indeterminate status. In the early through middle 1900s, the species group served as a conceptual stepping-stone to the artenkreis,

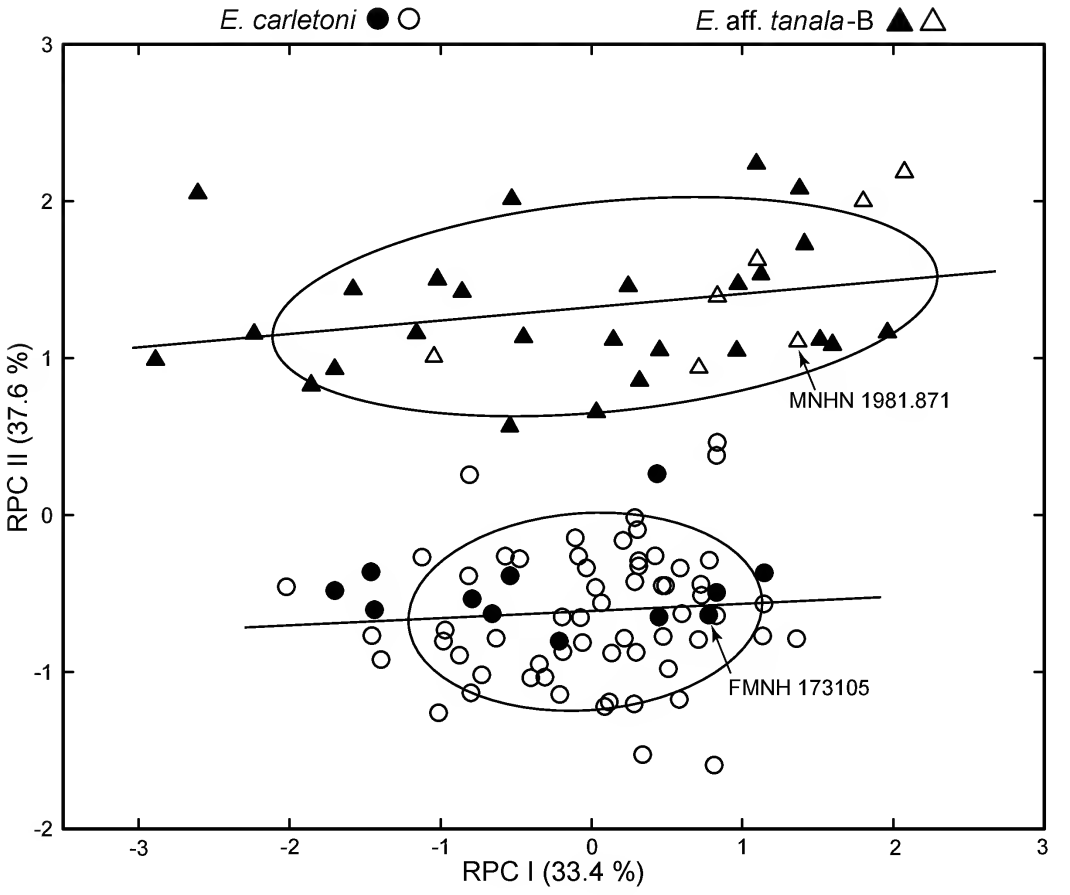

FIG. 8. Projection of specimen scores, based on 18 log-transformed cranial variables, onto the first two principal components (RPC) extracted from ordination of *Eliurus carletoni* ($N = 72$) and *E. tanala*-B ($N = 33$) from the Northern Highlands, followed by oblique factor rotation (Oblimin). Confidence ellipses (1 SD) around sample centroids and the major axis of sample constellations were computed post hoc; highlighted specimen scores include the holotypes of *E. carletoni* (FMNH 173105) and *E. ellermani* (MNHN 1981.871). Closed symbols denote specimens used in gene-sequence analyses; open symbols represent nonsequenced individuals. See table 4B for variable correlations (loadings) and variance explained by the latent principal components.

allospecies, and superspecies of the New Systematics (see Zachos, 2016). Our continued employment of the species group within *Eliurus* is intended to convey community of evolutionary descent among closely related, valid species.

Eliurus tanala Species Group

The genetic and morphometric results collectively support recognition of three species within the *Eliurus tanala* group, i.e., that node that defines the common ancestor of *E. tanala*-A, *E. tanala*-B, and *E. tanala* in the several molecular trees (figs. 3, 4, 6). Applicable names are available for two of those, *E. tanala* Major, 1896, for populations in the Central and Southern highlands, and *E. ellermani* Carleton, 1994, for those in the Northern Highlands (*Eliurus tanala*-B). The third well-defined clade, *Eliurus tanala*-A, represents several localities in dry forest associated with *tsingy* formations of western Madagascar and lacks a scientific name; we describe it below as a new species.

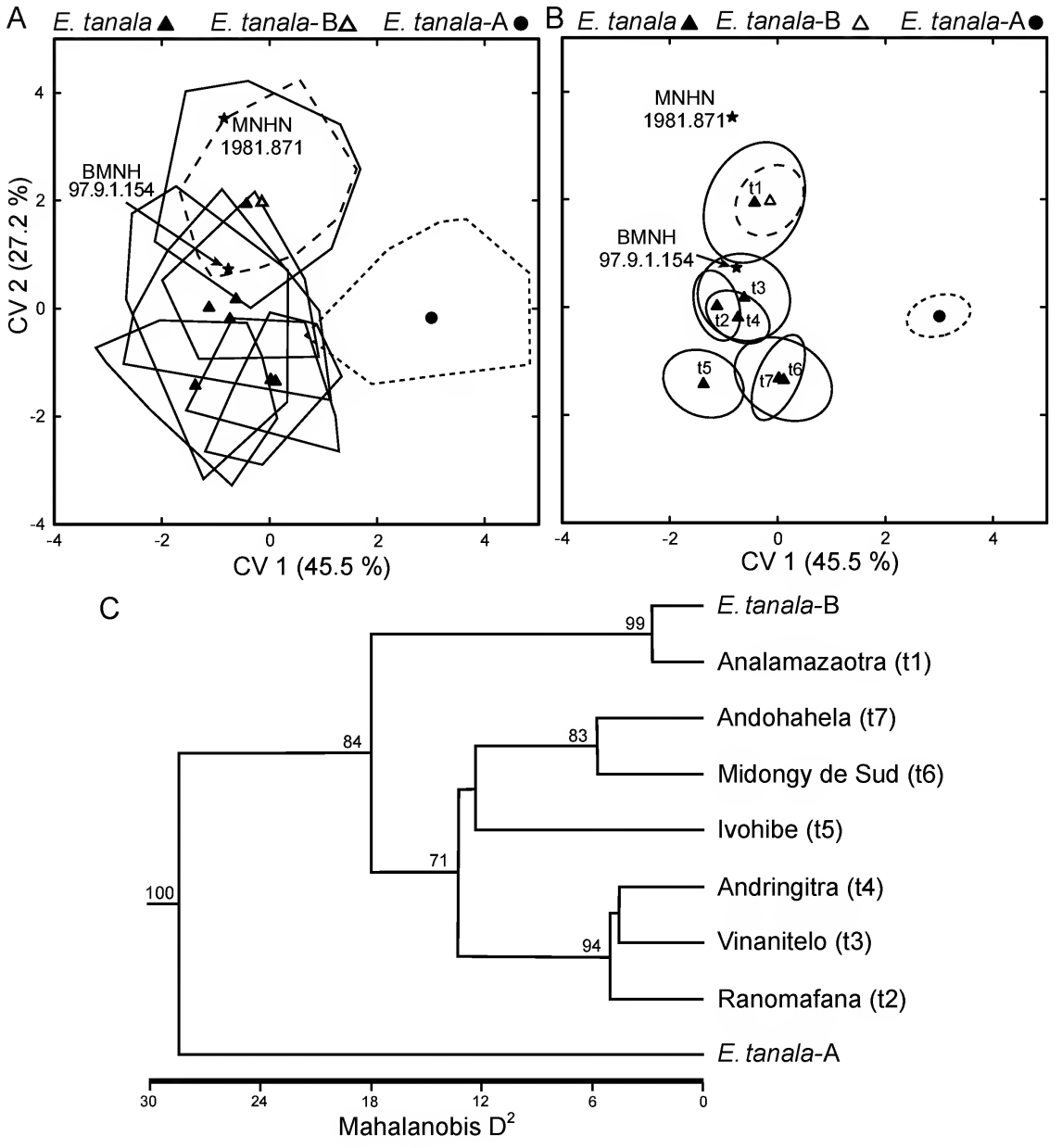

FIG. 9. Three graphic depictions of discriminant function analysis performed on nine OTUs of the *Eliurus tanala* group, based on 18 log-transformed cranial variables as measured on 161 intact adult specimens. **A.** Projection of OTU centroids, each enclosed by maximally inclusive polygons of specimen scores, onto the first two canonical variates (CV) extracted. **B.** Projection of OTU centroids, each surrounded by 95% confidence envelopes of the *n*-dimensional mean, onto the first two canonical variates extracted. Highlighted scores in A and B represent the holotypes of *E. ellermani* (MNHN 1981.871) and *E. tanala* (BMNH 97.9.1.154), both represented by stars; figure B indicates the centroid placement of the seven OTUs (t1–t7) of *E. tanala*; see table 5 for variable correlations (loadings) and percent variance explained by the latent canonical variates. **C.** Cluster diagram (UPGMA) based on Mahalanobis distances between the nine OTU centroids (coefficient of cophenetic correlation = 0.959). Bootstrap values are indicated for nodes that were consistently recovered (≥ 70%, 10,000 iterations).

TABLE 5

Results of discriminant function analysis and univariate one-way ANOVAs based on nine OTUs representing populations of the *Eliurus tanala* group (*N* = 161)

See figure 9 for plot of first two canonical variates and Materials and Methods for variable abbreviations; F (OTU) = univariate F values.

	Correlations		
Variable	CV 1	CV 2	F (OTU)
ONL	0.13	0.44***	3.9***
ZB	0.08	0.35***	3.2**
BBC	0.25**	0.30***	4.1***
IOB	-0.61***	0.13	8.2***
BOC	0.11	0.64***	7.4***
LR	-0.16*	0.13	1.9
BR	-0.05	0.45***	4.1***
LD	-0.03	0.45***	4.5***
LIF	-0.07	0.13	0.7
BIF	-0.18*	0.04	2.7**
PPL	0.13	0.33***	2.4*
LBP	-0.01	0.54***	6.5***
BM1s	-0.21**	0.48***	5.8***
PPB	0.20**	0.43***	3.7***
DAB	0.68***	-0.17*	7.1***
BZP	-0.05	0.11	1.6
LM1–3	-0.15	0.35***	2.5*
WM1	-0.04	0.45***	4.4***
Eigenvalue	2.18	1.30	
% Variation	45.5	27.2	

* = $P \leq 0.05$; ** = $P \leq 0.01$; *** = $P \leq 0.001$.

As so defined, the *E. tanala* species group is narrower than the arrangement proposed by Carleton and Goodman (2007), who also included *E. webbi*. Although some authors have viewed *E. tanala* and *E. webbi* as closely related, perhaps sister species (Carleton, 1994; Jansa et al., 1999), other molecular studies have suggested that *E. webbi* is distantly related to the *E. tanala* assemblage (Rakotoarisoa et al., 2010, 2013; this study). Three other species groups, sensu Carleton and Goodman (2007), are represented among the species we considered—*E. antsingy* and *E. carletoni*, *E. majori*, *E. myoxinus*, and *E. minor*; all are distantly related to the *E. tanala* assemblage based on our gene trees (figs. 3, 4, 6). Although our results reinforce certain sister-group patterns disclosed in past studies (e.g., Jansa et al., 1999; Goodman et al., 2009), no study to date has included a sufficiently broad sampling of taxa or traits to resolve evolutionary relationships at the deeper nodes within the phylogenesis of *Eliurus* species. The improved understanding of species limits and diversity afforded by this study sets the stage for a more rigorous phylogenetic study of *Eliurus*, an investigation that must simultane-

ously address the relationships and generic validity of *Voalavo*.

The three species of the *E. tanala* group share the cardinal generic traits that are now well understood to differentiate *Eliurus* from other genera of nesomyine rodents (Ellerman, 1949; Carleton, 1994, 2003). Members of this species group can be distinuished from most other *Eliurus* species through a combination of qualitative differences in pelage and quantitative and qualitative differences in the cranium, mandible, and dentition (see Carleton and Goodman 2007, and comparisons below). However, members of the *E. tanala* species group are remarkably similar morphologically to members of the *E. antsingy* group (*E. antsingy*, *E. carletoni*), despite their relatively distant phylogenetic relationship as revealed by molecular data (figs. 3, 4, 6). Therefore, to clarify differences between these two species groups and reduce repetition in the species descriptions below, we first contrast traits shared by members of the *E. tanala* group with those of the *E. antsingy* group.

Eliurus antsingy Group vis-à-vis *E. tanala* Group

The five species belonging to these two species groups are among the largest forms within *Eliurus*, e.g., as indexed by the size of body (HBL ≈ 145–155 mm), skull (ONL ≈ 38–42 mm), or molars (LM1–3 > 5.5 mm); their univariate ranges overlap considerably, such that most individual variables offer little utility when used alone as key characters for species identification. Crania of members of the *E. tanala* group generally display relatively longer rostra (LR ≈ 36% of ONL) than do species of the *E. antsingy* group (LR ≈ 33% of ONL); however, certain other proportional features of the diastema and palate are more readily discernable (table 6).

Carleton and Goodman (2007: 15) emphasized the relatively long and wide incisive foramina possessed by *E. antsingy* in isolating the species in its own group. Accordingly, these variables (BIF, LIF), and their proportions relative to the upper diastema (LD) and bony palate (LBP), figured prominently in multivariate discrimination of crania of the two species groups, whether in the western or northern sectors of their distributions (figs. 7, 8; table 4). Thus, when identifying specimens from western *tsingy*-associated habitats, *E. antsingy* and the new species described below can be readily segregated by inspecting the size of the incisive foramina (LIF) relative to the bony palate (LBP), shorter in the latter species and longer in the former (fig. 10A); these proportional contrasts are also obtained between examples of *E. carletoni* and *E. ellermani* in northern Madagascar. Similarly, members of the *E. tanala* species group possess noticeably shorter incisive foramina (LIF) compared with diastemal length (LD) than do specimens of *E. antsingy* and *E. carletoni* (fig. 10B). Other cranial variables were less informative for consistently contrasting members of the two species groups, whether used in univariate comparisons (compare tables 7 and 8) or multivariate analyses (see table 4).

Carleton and Goodman (2007) also highlighted the length of the lower incisor alveolus and its terminal expression on the ascending ramus as another trait for separating species of the *tanala* and *antsingy* groups. In examples of the former, the alveolar tract of the lower incisor is longer, usually forming a knobby capsular projection that passes just beyond the base of the coronoid process and terminates immediately below the ventral rim of the sigmoid notch (fig. 11A; also see Carleton, 1994: fig. 20). In members of the *antsingy* group, the lower incisor is shorter, ending at the level of the coronoid process, appreciably below the sigmoid notch and forming an indistinct mound (fig. 11B). Other cranial characteristics of the species groups are here expressed as population tendencies, although we expect that careful scoring of character states would reveal quantitatively significant trait-frequency differences. Noteworthy are the degree of fenestration of the bony palate and the patency of the subsquamosal fenestra and correlative definition of a hamular process (table 6).

TABLE 6

Qualitative characters useful for identifying members of the *Eliurus antsingy* and *E. tanala* species groups

	E. antsingy group		*E. tanala* group		
Character	*E. antsingy*	*E. carletoni*	*E. ellermani*	*E. tanala*	*E. tsingimbato*
Incisive foramina[1]	moderately long & wide LIF/LD ≈ 50–58%		relatively short & narrow LIF/LD ≈ 38–46%		
Palatal fenestration[2]	minimal	minimal	extensive	extensive	moderate
Subsquamosal fenestra[3]	present, small	present, small	absent or tiny	absent or tiny	present, small
Incisor capsule[4]	indistinct	indistinct	protuberant	protuberant	protuberant
Tail tuft color[5]	dark tip (100%)	dark tip (93%)	white tip (76%)	white tip (93%)	dark tip (100%)
Length tail tuft/TL[6]	long ≈ 55%	medium ≈ 45%	short ≈ 35%	short ≈ 35%	medium ≈ 40%
Ventral pelage[7]	Gray or White	White (89%)	White (100%)	Gray (80%)	White (100%)

[1] Character states based on size of incisive foramen (LIF) relative to diastemal length (LD), × 100, as measured on adult specimens with intact skulls; see figure 10 and text for additional description. Sample sizes: *E. antsingy*, *N* = 11; *E. carletoni*, *N* = 72; *E. ellermani*, *N* = 34; *E. tanala*, *N* = 128; *E. tsingimbato* n. s., *N* = 26.

[2] Development of palatal vacuities: "minimal" = palatal perforations limited to the posterior palatine foramina, located in the palatine-maxillary suture at the level of the anterior M2; "moderate" = supernumerary openings occasionally present posterior to the posterior palatine foramina, but not forming elongate vacuities; "extensive" = supernumerary openings commonly present posterior to the posterior palatine foramina, often forming elongate vacuities.

[3] Development of subsquamosal fenestra: "present, small" = subsquamosal fenestra open, exposing periotic bone and defining a short, broad hamular process; "absent or tiny" = subsquamosal fenestra absent or weakly expressed as a minute opening, without clear definition of a hamular process.

[4] Terminus of lower incisor alveolus on mandibular ascending ramus (see fig. 11): "indistinct" = incisor alveolus relatively short, terminating at the level of the coronoid process, appreciably below the sigmoid notch and forming a low mound; "protruberant" = alveolus long, extending below the rim of the sigmoid notch and forming a raised capsular projection.

[5] Predominant tuft color based on examinations of skins with fully intact tails; see fig 12 and species accounts for additional description of variation. Sample sizes for percentages: *E. antsingy*, *N* = 6/6; *E. carletoni*, *N* = 37/40; *E. ellermani*, *N* = 13/17; *E. tanala*, *N* = 53/57; *E. tsingimbato* n. s., *N* = 22/22.

[6] Based on measurements of skins with fully intact tails; see fig. 12 and species accounts for descriptions. Sample sizes: *E. antsingy*, *N* = 5; *E. carletoni*, *N* = 39; *E. ellermani*, *N* = 15; *E. tanala*, *N* = 54; *E. tsingimbato* n. s., *N* = 20.

[7] Typical ventral pelage color based on examination of prepared skins. Sample sizes: *E. antsingy*, *N* = 7; *E. carletoni*, *N* = 44; *E. ellermani*, *N* = 18; *E. tanala*, *N* = 64; *E. tsingimbato* n. s., *N* = 24; see fig. 14 and species accounts for discussion of variation.

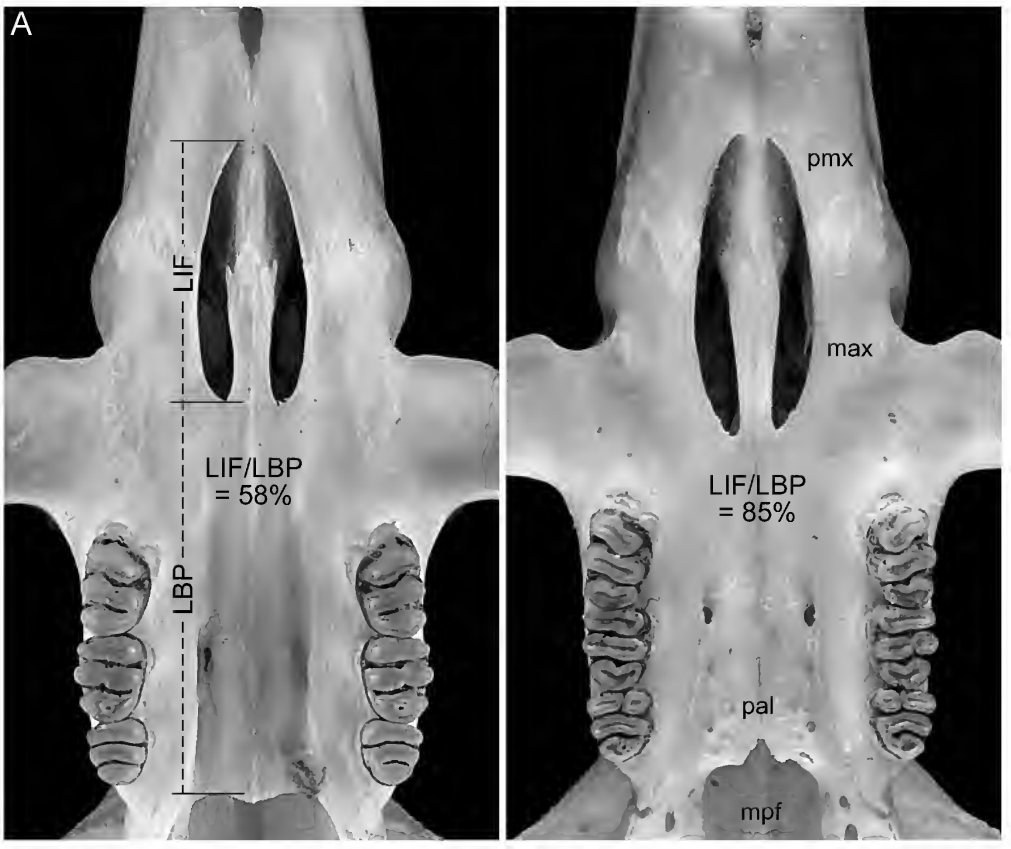

FIG. 10. Proportional differences between the palatal regions in members of the *Eliurus antsingy* and *E. tanala* groups. **A.** (*above*) Ventral view of the bony palate and diastema: left, *Eliurus tsingimbato* n. s. (FMNH 172723, holotype; LM1–3 = 5.94 mm), an adult male from 3.5 km E Bekopaka, PN de Bemaraha; right, *E. antsingy* (FMNH 172721; LM1–3 = 6.09 mm), an adult male from 3.5 km E Bekopaka, PN de Bemaraha. The left photograph displays the landmarks defined for our LBP and LIF measurements, whose proportions offer distinctive ratios for separating the two species. Abbreviations: **LBP,** length of bony palate; **LIF,** length of incisive foramen; **mpf,** mesopterygoid fossa; **mx,** maxillary; **pa,** palatine; pmx, premaxillary. **B.** (*opposite page*) Dice-Leraas diagrams comparing expanse of the incisive foramen (LIF) relative to the diastema (LD) in species representing the *E. antsingy* (*E. antsingy*, *E. carletoni*) and *E. tanala* (*E. ellermani*, *E. tanala*, *E. tsingimbato*) groups. Symbols: horizontal line = sample mean; vertical line = observed range; open rectangle = ± one standard deviation; closed rectangle = ± two standard errors of the mean.

Members of the *E. antsingy* group possess bushier, more visually prominent tail tufts compared with those of the *E. tanala* group, a contrast resulting both from elaboration of a tuft over a greater length of the tail and from the longer caudal hairs that compose the terminal tuft (fig. 12). The longer tuft in species of the *E. antsingy* group comprises about 45%–55% of tail length versus about 35%–40% in species of the *E. tanala* group (table 6). The tuft is monocolored, dusky brown to blackish, over its full length in nearly all specimens of *E. antsingy* (fig. 12E) and *E. carletoni*, but bright white hairs accentuate the terminal tuft in most examples of *E. ellermani* and *E. tanala* (table 6; fig. 12D). The new species is exceptional among species of the *E. tanala* group in typically having a tail tuft with a brown tip (fig. 12B, C; see species accounts for description of variation).

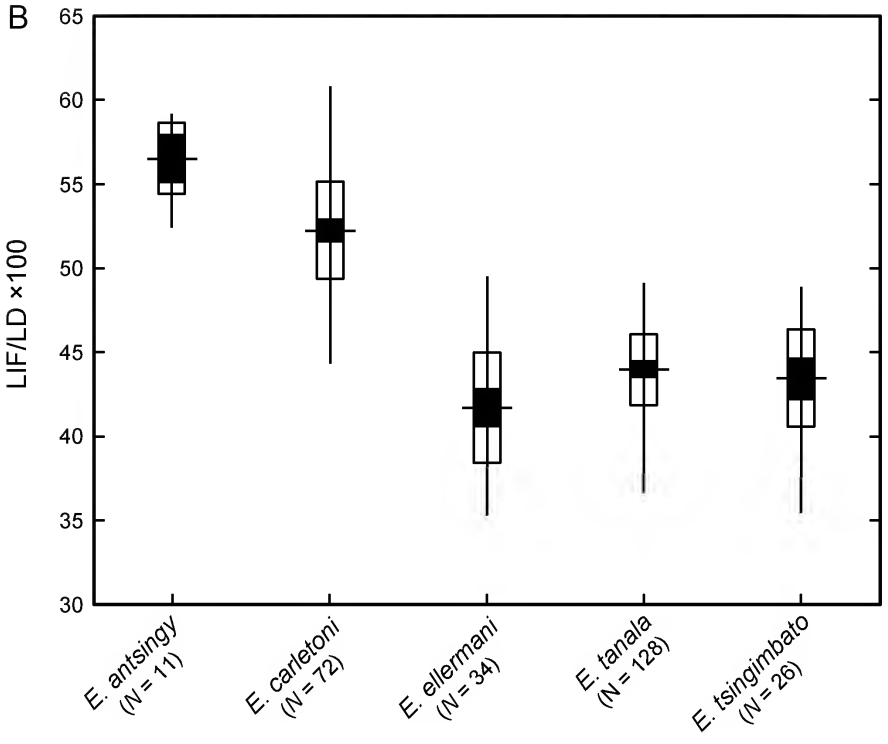

Species of the *E. tanala* Group

***Eliurus tsingimbato*, new species**

Figures 10–16; table 7

Eliurus cf. *E. ellermani* and *E. tanala*; Carleton et al., 2001: 980 (part; description of *E. antsingy* and morphological comparisons).

Eliurus aff. *E. tanala* Group; Carleton and Goodman, 2007: 20 (part; taxonomic commentary on species group associations).

Eliurus antsingy; Goodman et al., 2009: 149 (part; species description of *E. carletoni* and misidentification of comparative specimens).

Eliurus tanala-A; this study.

Holotype: Field Museum of Natural History number 172723, an adult male prepared as skin, skull, partial skeleton, and tissue; collected 30 November 2001 by Steven M. Goodman (original number SMG 12518; fig. 13).

The round skin and skull are in fine condition. The skull's basisphenoid suture is completely fused and its third molar is slightly worn. The animal was noted as having slightly scrotal testes, measuring 12 × 5 mm, with convoluted epididymides. See table 7 for external and cranial measurements of the holotype.

Type Locality: Madagascar, Province de Mahajanga, Région de Melaky, Parc National de Bemaraha, south bank of Manambolo River, 3.5 km E Bekopaka, near Tombeau Vazimba, 100 m; geographic coordinates 19°08.4′S, 44°49.7′E, based on GPS reading.

Diagnosis: A species of *Eliurus* that forms a clade with *E. tanala* and *E. ellermani* (figs. 3, 4, 6). Morphologically defined by a combination of entirely white ventral pelage (fig. 14D), sharply demarcated from the dorsum (ventral pelage usually pale gray in *E. tanala*, dorsal-ventral countershading less conspicuous); tip of tail tuft dark brown, tuft entirely brown in most specimens (caudal tuft typically white in *E. tanala* and

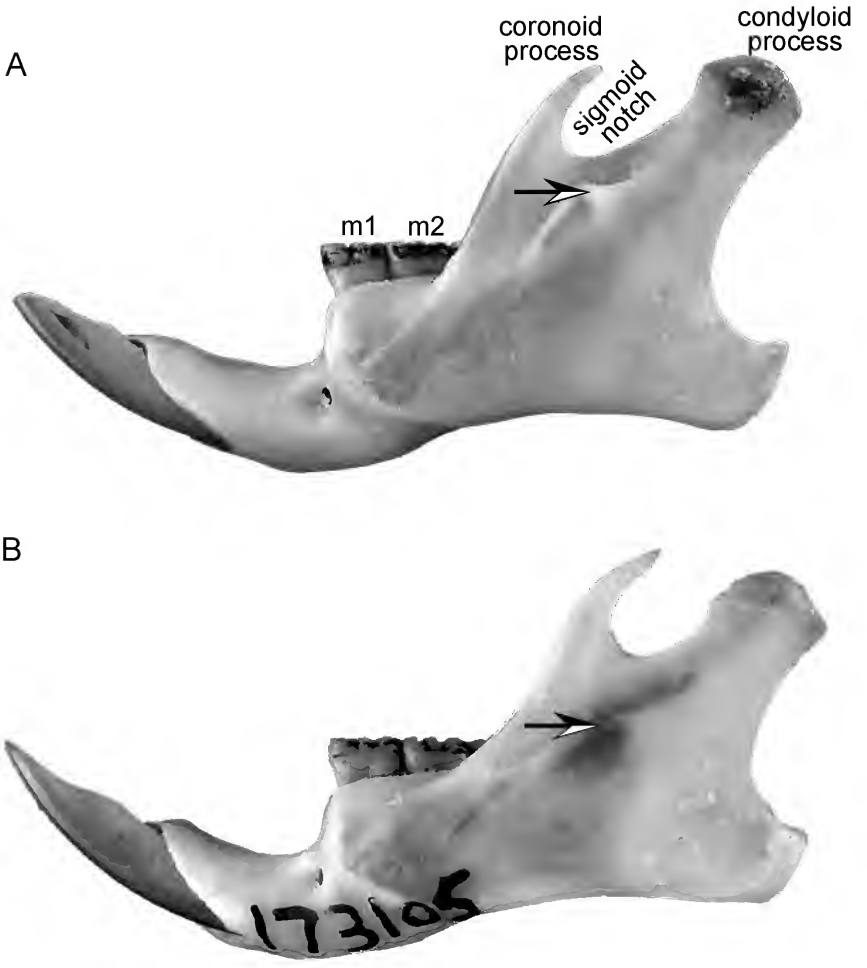

FIG. 11. Lateral view (ca. 4 ×) of left mandible in adult representatives of two *Eliurus* species groups. **A,** *E. tanala* species group as represented by *E. tsingimbato* (FMNH 172723, holotype), a male from 3.5 km E Bekopaka, PN de Bemaraha; **B,** *E. antsingy* species group as represented by *E. carletoni* (FMNH 173105, holotype), a female from 7.5 km NW Mahamasina, RS d'Ankarana. Arrows indicate the posterior terminus of the lower incisor's alveolus within the ascending ramus of the mandible. Members of the *E. tanala* group (A) possess longer incisors, their posterior extension producing a protuberant capsule below the ventral rim of the sigmoid notch; in species of the *E. antsingy* group (B), the incisor's alveolus forms an indistinct mound set appreciably below the sigmoid notch.

E. ellermani; fig. 12); skull (fig. 15) with relatively narrow interorbital constriction (wider in *E. tanala* and *E. ellermani*) and larger auditory bullae (smaller in *E. tanala* and *E. ellermani*); subsquamosal fenestra small but consistently present, hamular process short (subsquamosal fenestra tiny or absent, hamular process weakly defined in *E. tanala* and *E. ellermani*); and supernumerary vacuities posterior to post palatine foramina uncommon (elongate palatal vacuities typically present in *E. tanala* and *E. ellermani*).

DISTRIBUTION: Karst landscapes of western Madagascar (fig. 16) dominated by *tsingy* formations (Veress et al., 2008, 2009), Province de Mahajanga, from the Namoroka Massif (ca. 16°S), including the eastern portion of the Kel-

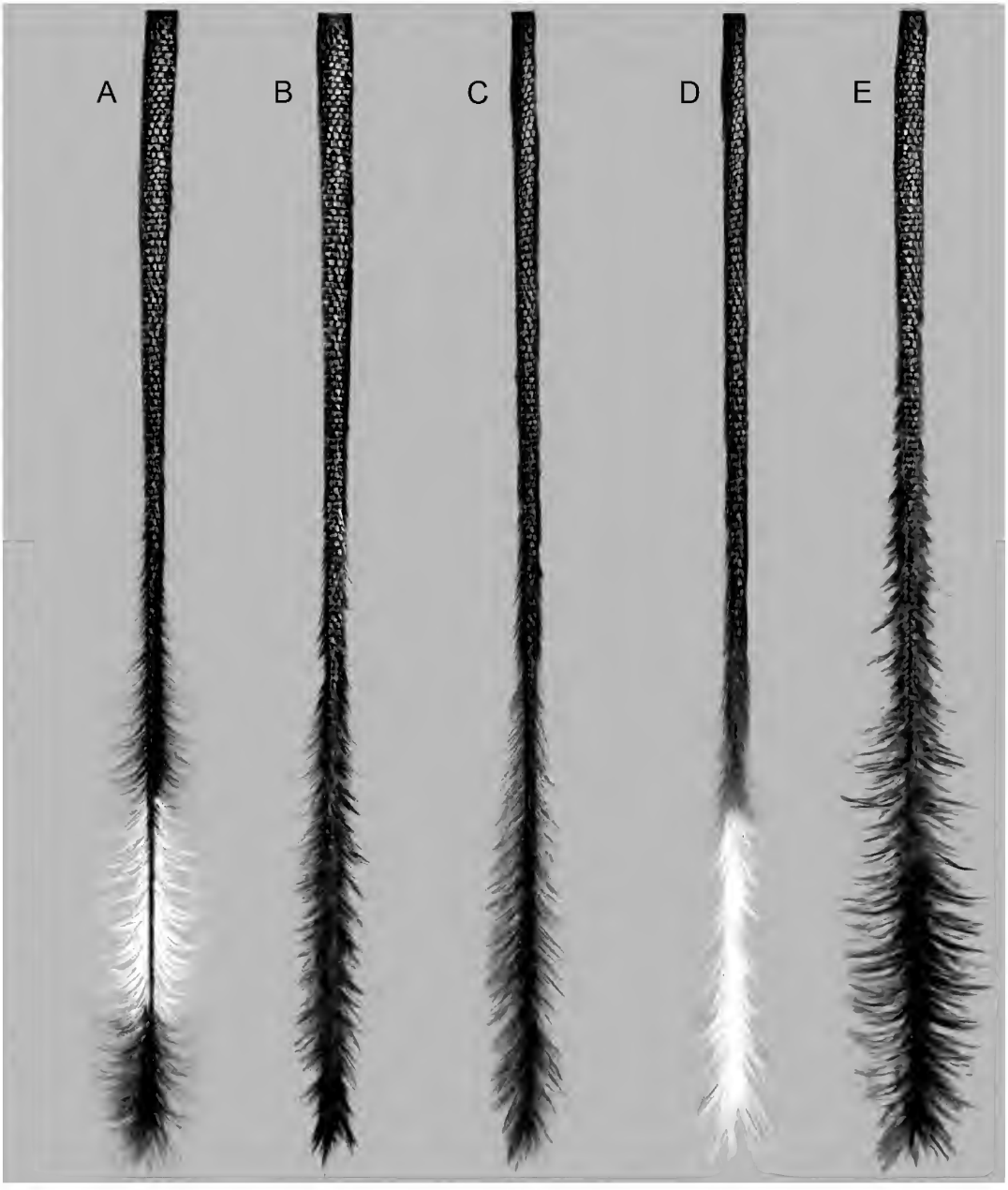

FIG. 12. Variation in tail-tuft development and color pattern in gene-sequenced adult specimens of three *Eliurus* species covered herein: **A,** *E. tsingimbato* (FMNH 172723, holotype, TL = 192 mm), a male from 3.5 km E Bekopaka, PN de Bemaraha; **B,** *E. tsingimbato* (FMNH 209224), a female from 4.9 km S Ambinda, Forêt de Beanka; **C,** *E. tsingimbato* (FMNH 175911, TL = 171 mm), a male from Forêt d'Ambovonomby, RNI de Namoroka; **D,** *E. tanala* (FMNH 170836, TL = 172 mm), a male from 15.5 km SE Vohitrafeno, Forêt de Vinanitelo; **E,** *E. antsingy* (FMNH 175913, TL = 169 mm), a female from Forêt de Mahabo, RNI de Namoroka. Specimens figured in B and C illustrate typical development of the tail tuft observed in *E. tsingimbato*; however, a few specimens, including the holotype shown in A, possess a subterminal band of white hairs, although the tip itself is dark brown. Drawings by Velizar Simeonovski.

FIG. 13. Color image of the *Eliurus tsingimbato* holotype (FMNH 172723; TOTL = 355 mm; WT = 118 g), taken soon after its capture on limestone *tsingy* in the PN de Bemaraha. The slight reflective coloration of the dorsum, tail and hindfoot is associated with the camera flash. Photograph by Harald Schütz.

ifely Plateau, southward to the vicinity of Bekopaka, Bemaraha Massif (ca. 19°S); documented elevational range 100–320 m (fig. 17).

Referred Specimens: $N = 38$, as follows.

Province de Mahajanga: 2 km SE Namoroka (village), Site Andriabe, RNI de Namoroka, 110 m (FMNH 178587, 178591–178593); Forêt d'Ambovonomby, 26 km NW Andranomavo, RNI de Namoroka, 200 m (FMNH 175911); Forêt d'Analamavo, 27 km N Kandreho, Ankara Plateau, 220 m (FMNH 194554–194557, 194564–194567); Forêt d'Analanomby, 21 km NNW Kandreho, Kelifely Plateau, District de Kandreho, 280 m (FMNH 194558–194562, 194568); 1.1 km E Ambinda village, Beanka Forest, site 1, District de Maintirano, 220 m (FMNH 209221, 209222; UADBA 48103–48108, 48801); 4.9 km S Ambinda village, Beanka Forest, site 2, District de Maintirano, 320 m (FMNH 209223–209226; UADBA 48806); Forêt d'Antsahalaza, along Antsoa River, RNI de Bemaraha (UADBA 16341); near Bekopaka, "forêt de l'antsingy" (MNHN 1966.2221); Ankidrodroa, 2.5 km NE Bekopaka, District d'Antsalova, 100 m (FMNH 172722); 3.5 km E Bekopaka, near Tombeau Vazimba, PN de Bemaraha, 100 m (FMNH 172724, 172725).

Morphological Description and Comparisons: The following information emphasizes the new species *E. tsingimbato* and those features that provide differentiation from its nearest relatives, *E. tanala* and *E. ellermani*.

Texture of body fur of *E. tsingimbato* is generally soft and relatively fine. Dorsal cover hairs are 6–7 mm long at the nape, lengthening to

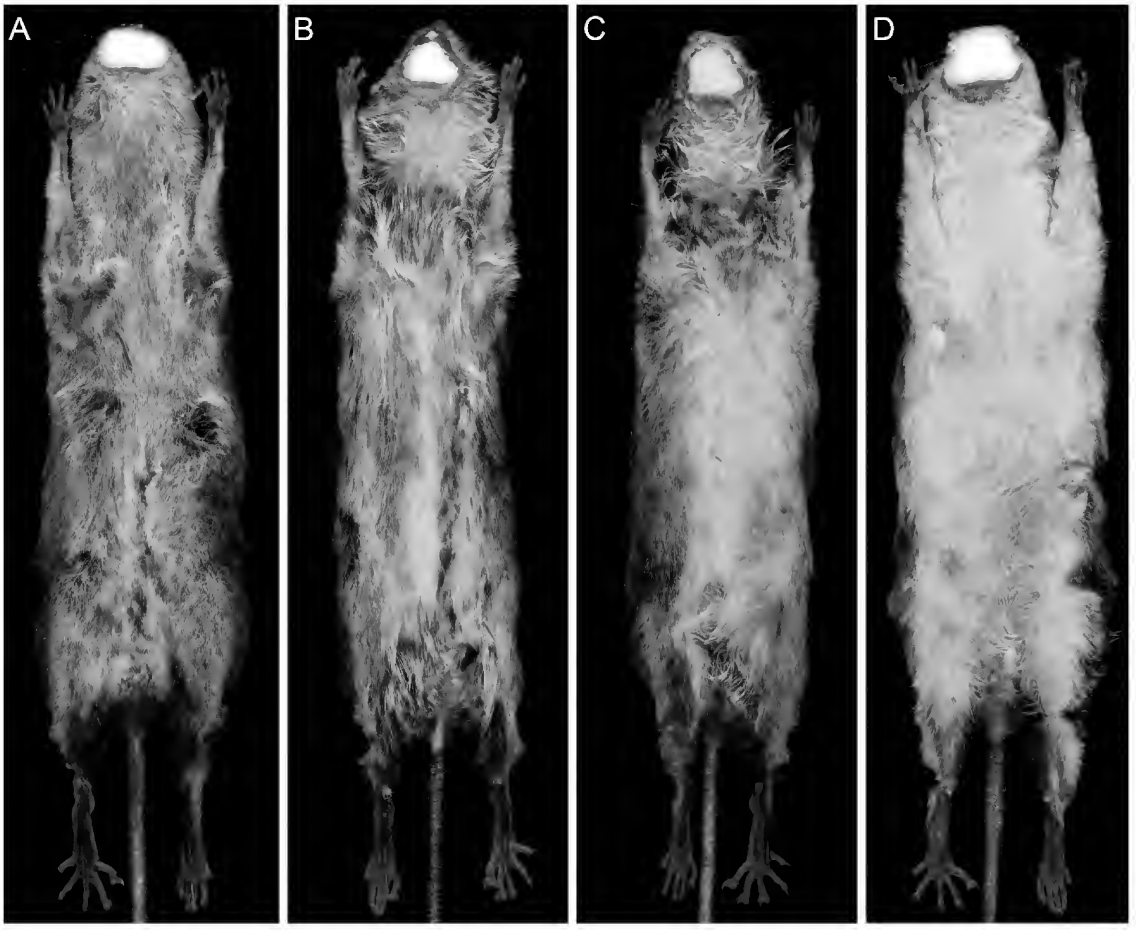

FIG. 14. Variation in ventral pelage color observed among adult examples of the *Eliurus tanala* group (about 0.7×). **A,** *E. tanala*, a female from Vatoharanana, PN de Ranomafana (FMNH 170827; HBL = 157 mm); **B,** *E. tanala*, a male from 8 km NE Ivohibe (FMNH 162086; HBL = 145 mm); **C,** *E. tanala*, a female from 6.5 km ESE Ivohibe, RS d'Ivohibe (FMNH 162082; HBL = 145 mm); **D,** *E. tsingimbato*, a female from 4.9 km S Ambinda, Forêt de Beanka (FMNH 209224; HBL = 160 mm).

9–11 mm over middle rump. In adults, most cover hairs of dorsum are bicolored with proximal two-thirds medium brown and distal one-third medium buff; some dorsal hairs tricolored, tipped with faint dusky brown or light buff. Dorsal pelage overall appears dark brown to brownish gray over middle back, grading to bright tawny along the central flank and pale tawny over the hips (fig. 13). Hairs of ventral pelage are self-colored, entirely white from base to tip in all specimens examined with well-prepared round skins ($N = 20$). Ventral pelage thus appears creamy white from the chin to inguinal region, including underparts of the arms and legs (fig. 14D); dorsal-ventral countershading is correspondingly pronounced, especially along the chest and abdomen. Tops of the hind feet are light tan to pale brown proximally, becoming creamy or bright white on the metatarsals and phalanges.

As in examples of *E. tsingimbato*, ventral pelage color in *E. ellermani* is some shade of white, ranging from creamy to bright white and sharply contrasting with the drab brown or grayish

FIG. 15. Dorsal, ventral, and lateral views of the skull and lateral view of the left mandible of the holotype of *E. tsingimbato* (FMNH 172723, ONL = 41.7 mm), an adult male from 3.5 km E Bekopaka, PN de Bemaraha, 100 m.

brown of the dorsum. The predominant pelage color of the underparts in samples of *E. tanala* is a pale or buffy gray (fig. 14A), although some population samples exhibit variably sized patches of entirely white hairs (fig. 14B, C). Ventral pelage color varies geographically in *E. antsingy*: pale gray in the south, PN de Bemaraha ($N = 3$), and uniformly buffy white in the north, PN de Namoroka ($N = 4$). The small sample sizes for both regions temper conclusions about the stability or taxonomic significance of this geographic difference, but all sequenced specimens from these two regions comprise a single, well-supported clade that is sister group to examples of *E. carletoni* (figs. 3, 4).

In *E. tsingimbato*, caudal hairs over the proximal two-thirds of tail length are short, sparsely distributed, and exposing the rectangular caudal scales. The caudal epidermis appears dusky brown dorsally and indistinctly paler on the ventral surface (fig. 13). Visible penicillation invests the distal 40% of tail length, terminating with caudal hairs about 10–13 mm long and forming a distinct tuft (fig. 12A–C). Among those specimens of *E. tsingimbato* with an unbroken tail, the majority (17 of 20) bear an entirely dark brown tuft (fig. 12B, C). In three specimens (FMNH 172723, 209225; MNHN 1966.2221), including the holotype (fig, 12A), a subterminal band (10–32 mm long) of white hairs interrupts the otherwise brown distal tuft; nonetheless, all three retain a distal segment (8–17 mm long) of brown hairs at the tip of their tuft.

A gossamer white tail tuft characterizes most examples of *E. tanala* (fig. 12D) and *E. ellermani*; furthermore, the length of conspicuous caudal pilosity appears shorter (ca. 35% of TL) in these species, but longer in examples of *E. tsingimbato* (ca. 40% of TL). Tail length averages longer in our samples of *E. tanala* and *E. ellermani*, somewhat shorter in *E. tsingimbato* (table 7), but range overlap is substantial in this large external variable and age effect is considerable. The terminal tail tuft is distinctly bushier and longer in *E. antsingy* (fig. 12E) compared with *E. tsingimbato* (fig. 12A–C), a useful trait for distinguishing the two species where their distributions overlap.

Specimens of *E. tsingimbato* possess a large, sturdy skull, approximating the cranial size and proportions observed in samples of *E. ellermani* and *E. tanala* (fig. 15; table 7). Among the 18 cranial dimensions quantified, only two—width of the interorbital region (IOB) and inflation of the ectotympanic bullae (DAB)—significantly contributed to morphometric separation of *E. tsingimbato* from the two eastern humid-forest montane species (see table 5). Thus, the interorbital constriction is absolutely and relatively narrower in *E. tsingimbato* compared with the eastern species; whereas, its ectotympanic bulla is absolutely and relatively larger (table 7). In terms of practical anatomical landmarks, these slight mensural differences are visualized as the area of the orbital floor exposed when inspecting skulls in dorsal view—more in *E. tsingimbato*, less in *E. ellermani* and *E. tanala*—and the area of the posteromedial petromastoid observed when sorting skulls in ventral view—a narrow, short wedge in *E. tsingimbato* versus an elongate, broad wedge in *E. ellermani* and *E. tanala*. However, these differences are subtle and neither alone serves to provide unambiguous discrimination of *E. tsingimbato* from the other species, advising their use in combination with pelage and qualitative cranial traits.

The three members of the *E. tanala* group are similarly difficult to tease apart using qualitative cranial features (table 6). The posterior palatine foramina in *E. tsingimbato* appear as small ovals, situated within the maxillary-palatine suture at the level of the anterior lamina of M2. Supernumerary palatal foramina uncommonly occur behind the posterior palatine foramina and, if present, are seldom conjoined with the posterior palatine foramina or with one another to form elongate palatal vacuities (fig. 10A). In contrast, extensive palatal fenestration is commonplace within series of *E. ellermani* and *E. tanala* (see Carleton, 1994: fig. 19). A subsquamosal fenestra is consistently present, albeit small, in specimens of *E. tsingimbato* and defines a short, stout hamu-

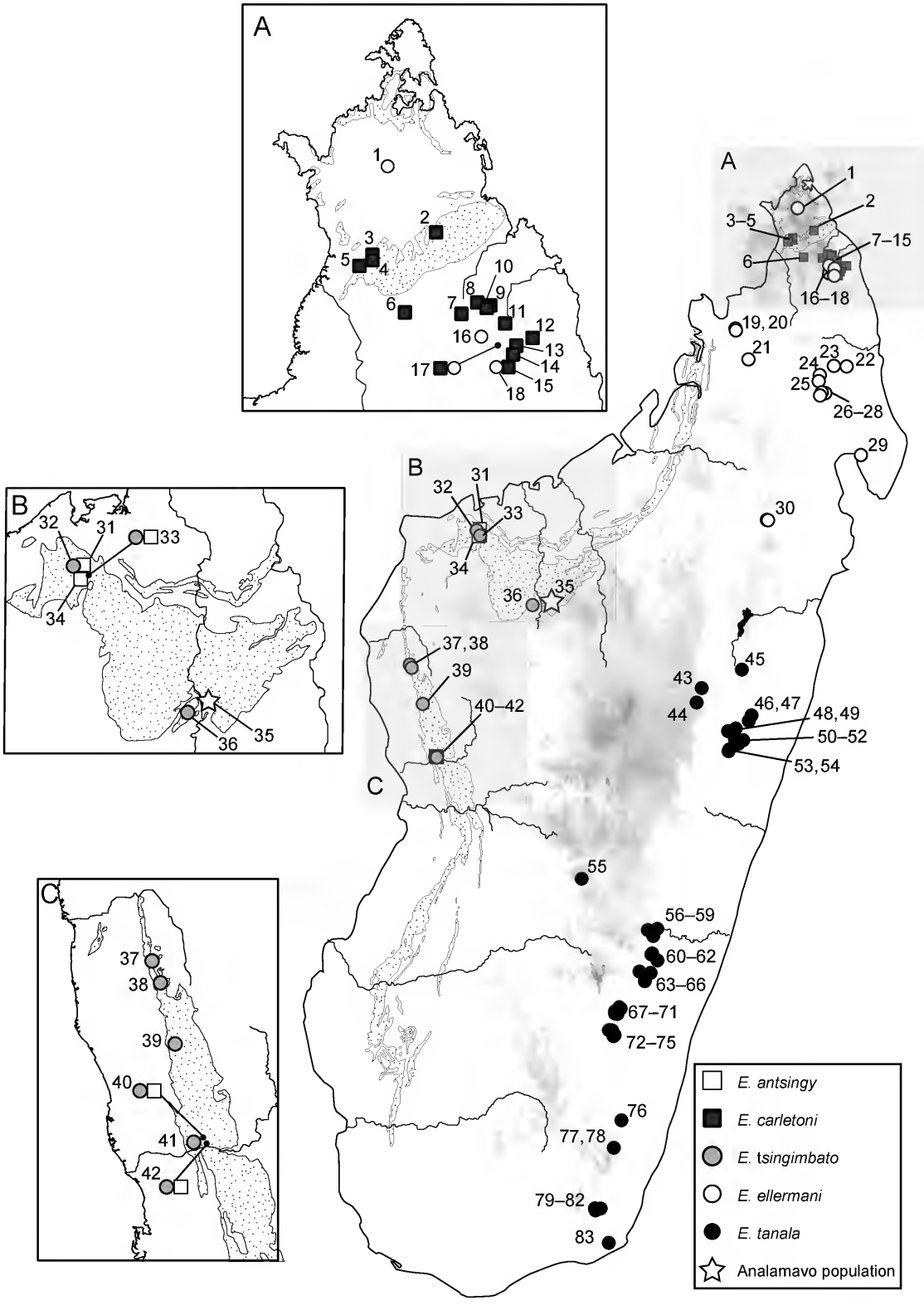
A
1
2
3
5
4
6
7
8
9
10
11
12
13
14
15
16
17
18
A
1
2
3–5
6
7–15
16–18
19, 20
21
22
23
24
25
26–28
29
30
B
32
31
33
34
35
36
37, 38
39
40–42
43
44
45
46, 47
48, 49
50–52
53, 54
B
32
31
33
34
36
35
C
55
56–59
60–62
63–66
67–71
72–75
76
77, 78
79–82
83
C
37
38
39
40
41
42
E. antsingy
E. carletoni
E. tsingimbato
E. ellermani
E. tanala
Analamavo population

lar process; in lateral view, the fenestra's small size provides a view of the periotic, but not the interior braincase. The subsquamosal fenestra may be nearly occluded or absent in examples of *E. tanala* and *E. ellermani*, the hamular process indistinct to weakly defined (see Carleton 1994: fig. 18).

NATURAL HISTORY NOTES: Populations of *E. tsingimbato* are known to inhabit two different forest types, both of them considered dry forest. Animals from the PN de Bemaraha, Beanka Forest and PN de Namoroka were trapped in forested zones dominated by limestone pinnacles (*tsingy*), varying from 2–4 m high, to those interspersed with limestone outcrops less than 0.5 m high (fig. 18). The natural vegetation at such sites is dry deciduous forest, which experiences annual periods of nearly six months without measurable precipitation, rendering the forest nearly leafless. In intact or relatively intact forest, canopy height reaches about 10–20 m, the understory is dense and a profusion of lianas and vines spans the vertical distance from just above the ground to at least the middle canopy. Certain localized conditions may support an evergreen forest throughout much of the year within these sites, e.g., where groundwater occurs close to the surface or deep canyons shelter the vegetation from solar radiation. The second forest type occupied by *E. tsingimbato* is also considered dry deciduous, often resting on limestone bedrock, but without the distinct *tsingy* formations (e.g., the Ankara Plateau and Kelifely Plateau). At these places, the canopy height may attain 12–15 m, the understory is notably dense, but vertical lianas and vines are uncommon.

The series of *E. tsingimbato* from the PN de Bemaraha includes genetically closely related specimens collected from both sides of the Manambolo River. One specimen was taken at Ankidrodroa (FMNH 172722), just to the north of river; three animals, including the holotype, were trapped close to the Tombeau Vazimba (FMNH 172723–172725), on the south bank of the same river.

Eliurus tsingimbato has been documented in sympatry with three other species of nesomyine rodents. In certain *tsingy* areas with forested habitat, it is found with the similarly sized *E. antsingy*; the two species have been trapped in sympatry in the Forêt d'Ambovonomby, PN de Namoroka (fig. 16: locality 36), and at 3.5 km E Bekopaka, PN de Bemaraha (fig. 16: locality 42). At most sites where *E. tsingimbato* is know, it can be captured in the same trap line with *E. myoxinus* and the introduced murid rodent *Rattus rattus*; within the PN de Bemaraha, it cooccurs with the large terrestrial nesomyine *Nesomys lambertoni*.

Animals collected during the end of the dry season (i.e., the last four months of the calendar year in western Madagascar) displayed signs of oncoming reproductive activity, namely, adult females in estrous and adult males with large scrotal testicles and enlarged epididymides. During this inventory period, no female was found carrying embryos or lactating, and the subadults captured were presumed to be no more than 3–4 months old and probably born in the previous breeding season. Taken together, these observations imply that *E. tsingimbato* mates during the rainy season, generally late December to March, giving birth and raising young during the subsequent period of presumably maximum fruit and seed abundance.

ETYMOLOGY: The name *tsingimbato* is framed as a noun in apposition, a derived combination of the Malagasy words *tsingy*, meaning in this context limestone pinnacle formations, and *vato*, meaning rock or stone. The epithet evokes the *tsingy* rock formations where examples of this species have been found.

FIG. 16. Map illustrating the distributions of the three species of the *Eliurus tanala* group recognized as valid (*E. ellermani*, *E. tanala*, *E. tsingimbato*), together with distributions of the *E. antsingy* group (*E. antsingy*, *E. carletoni*). Numbered collecting localities (see appendix 1) represent all specimens used in our morphological examinations, morphometric comparisons and/or molecular analyses; inset maps A–C illustrate regions where species occur in sympatry or close allopatry. Outlined stippled areas indicate major Mesozoic limestone regions (after Bésairie, 1964); elevations above 800 m are shown in shades of grey, grading to darker gray at higher elevations.

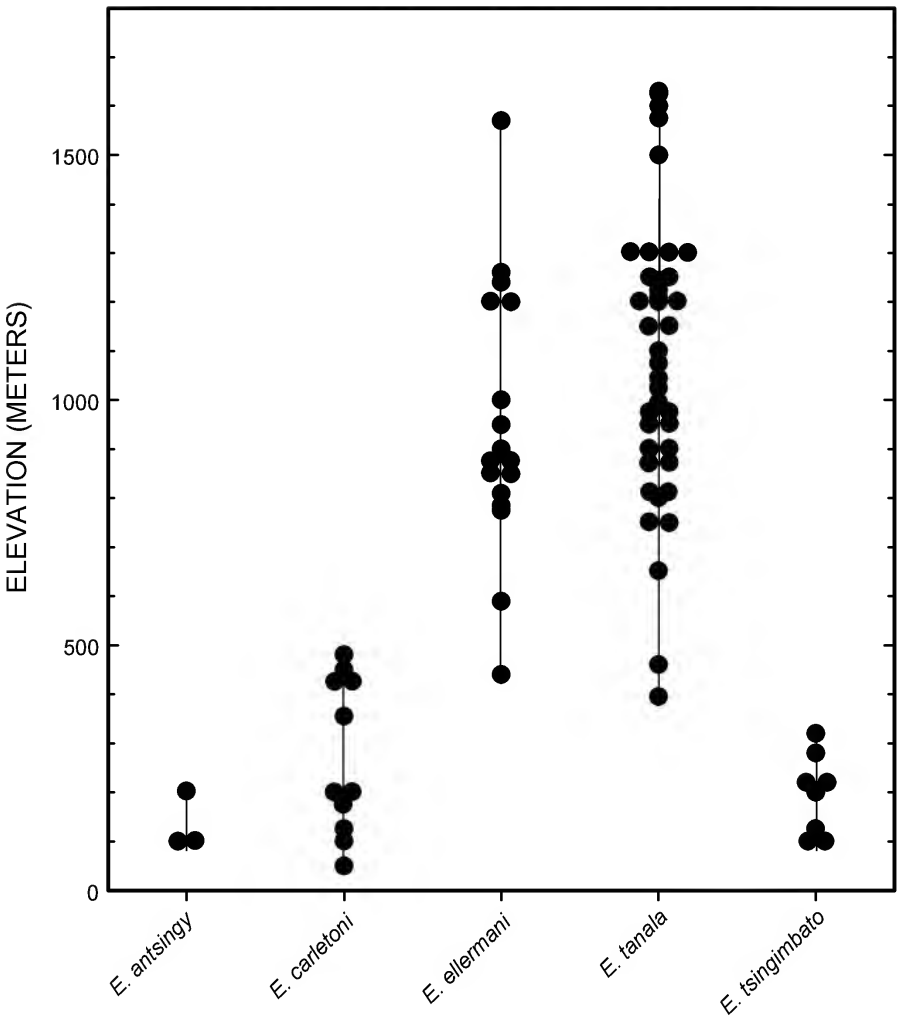

FIG. 17. Plot of elevational ranges (in m above sea level) of taxa representing the *Eliurus antsingy* (*E. antsingy*, *E. carletoni*) and *E. tanala* (*E. ellermani*, *E. tanala*, *E. tsingimbato*) species groups. Vertical line embraces the elevational range of each species and filled circles indicate elevations of individual collecting localities, including any duplicate sites recorded for the same elevation (see Specimens Examined within species accounts and appendix 3).

FIG. 18. Two views of western dry deciduous forest habitat in the Forêt de Beanka (near sites 37 and 38, appendix 1), where individuals of *Eliurus tsingimbato* were collected. **A,** General view of the lower portion of the forest, in close vicinity to a large exposed outcrop of sculpted karst limestone, a formation known as *tsingy*. The red ribbon in the lower left is a trail marker. **B,** A view of the understory of *tsingy*-associated forest with the characteristic vegetation, often composed of spiny plants belonging to the genus *Pandanus*, and shallow soils as witnessed by the exposed bedrock limestone. Photographs by Laurent Gautier.

TABLE 7

Descriptive statistics for selected OTUs of the *Eliurus tanala* species group

Statistics include the sample mean, ± one standard deviation, the observed range and sample size (in parentheses); measurements from the holotype for each species are presented under the specimen number. See Materials and Methods for variable abbreviations and geographic coverage of OTUs.

Variable	*E. tanala*		*E. ellermani*		*E. tsingimbato*	
	BMNH 97.9.1.154	PN de Ranomafana & vicinity	MNHN 1981.871	RS d'Anjanaharibe-Sud & vicinity	FMNH 172723	All localities
TOTL	–	340.7 ± 16.4	–	342.1 ± 33	355	326.9 ± 26
		310–362 (19)		283–381 (10)		265–364 (12)
HBL	–	155.1 ± 9.1	152	157.1 ± 14.3	150	148.7 ± 5.5
		144–175 (22)		126–174 (11)		140–160 (10)
TL	–	186.4 ± 12.4	177	180.3 ± 21.2	192	174 ± 15.9
		163–210 (19)		150–204 (10)		140–195 (12)
HFL	–	33.6 ± 1.0	35	33.3 ± 2.0	34	29.9 ± 1.6
		31–37 (22)		30–38 (11)		28–34 (13)
DHFL	32.5	32.6 ± 1.0	34	32.8 ± 1.2	33.5	31.6 ± 1.1
		31–34.5 (19)		31.2–34.7 (10)		30–33.7 (12)
EL	–	24.0 ± 1.3	20	22.2 ± 2.7	25	24.8 ± 0.9
		21–26 (22)		15–24 (10)		23–26 (13)
WT	–	88.7 ± 11.9	–	99.3 ± 22	118	94.9 ± 22.3
		66–115 (22)		55–120 (11)		45.5–125 (12)
ONL	41.6	40.9 ± 1.5	43.8	42.6 ± 2.1	41.7	41.8 ± 1.9
		36.8–43.8 (25)		36.2–45.7 (18)		37.2–44.3 (19)
ZB	19.3	19.4 ± 0.8	21.7	20.6 ± 1.2	20.3	19.9 ± 1.2
		16.9–20.6 (25)		17.2–21.9 (18)		16.7–21.6 (19)
BBC	14.6	14.7 ± 0.4	15.2	15.2 ± 0.5	15.7	15.2 ± 0.5
		13.5–15.5 (25)		14.0–16.0 (18)		14.2–16.2 (19)
IOB	6.0	6.0 ± 0.3	6.3	6.0 ± 0.2	5.6	5.6 ± 0.2
		5.6–6.8 (25)		5.5–6.3 (18)		5.3–6.0 (19)
BOC	8.6	8.6 ± 0.3	9.3	9.1 ± 0.3	9.2	8.8 ± 0.3
		8.0–9.4 (25)		8.6–9.8 (18)		8.3–9.2 (19)
LR	14.9	14.7 ± 0.7	15.1	15.1 ± 0.9	15.4	14.6 ± 1.0
		13.1–15.9 (25)		12.9–16.6 (18)		12.3–16.3 (19)
BR	7.2	7.1 ± 0.4	8.1	7.6 ± 0.5	7.5	7.3 ± 0.5
		6.2–7.8 (25)		6.3–8.2 (18)		6.1–8.0 (19)
LD	12.4	12.3 ± 0.6	13.4	13.3 ± 0.9	12.4	12.5 ± 0.8
		10.7–13.6 (25)		10.8–14.5 (18)		10.6–13.6 (19)
LIF	5.6	5.4 ± 0.4	5.8	5.4 ± 0.6	6.1	5.5 ± 0.5
		4.5–6.1 (25)		3.9–6.6 (18)		4.4–6.6 (19)

Variable	*E. tanala*		*E. ellermani*		*E. tsingimbato*	
	BMNH 97.9.1.154	PN de Ranomafana & vicinity	MNHN 1981.871	RS d'Anjanaharibe-Sud & vicinity	FMNH 172723	All localities
BIF	1.9	2.3 ± 0.1	2.3	2.3 ± 0.1	2.5	2.3 ± 0.2
		2.1–2.6 (25)		2.0–2.6 (18)		2.0–2.5 (19)
LBP	9.4	9.2 ± 0.4	9.2	9.9 ± 0.7	9.3	9.3 ± 0.4
		8.2–10.1 (25)		9.0–11.4 (18)		8.7–10.1 (19)
PPL	13.9	14.2 ± 0.7	15.5	14.8 ± 0.9	15.0	14.7 ± 0.9
		12.2–15.5 (25)		12.4–15.5 (18)		11.9–15.6 (19)
BM1s	8.0	7.9 ± 0.3	8.4	8.2 ± 0.3	8.0	7.8 ± 0.4
		7.3–8.6 (25)		7.7–8.7 (18)		6.8–8.3 (19)
PPB	5.2	5.4 ± 0.2	5.5	5.5 ± 0.3	5.6	5.6 ± 0.3
		4.8–6.0 (25)		4.9–6.2 (18)		5.1–6.5 (19)
DAB	5.3	5.2 ± 0.2	5.1	5.3 ± 0.2	5.6	5.6 ± 0.2
		4.9–5.5 (25)		4.9–5.5 (18)		5.3–6.0 (19)
BZP	3.7	3.9 ± 0.3	4.0	4.1 ± 0.4	3.7	3.9 ± 0.3
		3.2–4.7 (25)		3.2–4.9 (18)		3.4–4.5 (19)
LM1–3	5.85	5.73 ± 0.14	5.82	5.81 ± 0.22	5.94	5.72 ± 0.24
		5.46–5.95 (25)		5.39–6.22 (18)		5.27–6.13 (19)
WM1	1.57	1.54 ± 0.06	1.61	1.60 ± 0.08	1.59	1.56 ± 0.08
		1.42–1.69 (25)		1.46–1.75 (18)		1.35–1.68 (19)

Eliurus tanala Major, 1896

Figures 12, 14, 16; table 7

Eliurus tanala Major, 1896a: 462 (original description).

Eliurus myoxinus tanala; Ellerman, 1949: 166 (name combination, generic review and retention as valid subspecies).

Holotype: BMNH 97.9.1.154, an adult female, skin and skull preparation, collected 27 May 1896 by C.I. Forsyth Major.

Major (1896a: 463) originally used his field number (M1358) to designate the type of his new species, a common practice for the era, and a museum catalog number was later assigned in 1897. Both skin and skull are intact and in good condition for their age.

Type Locality: "Forest of the Independent Tanala of Ikongo, neighbourhood of Vinanitelo, 30 miles south of Fianarantsoa" (Major, 1896a: 463).

In Malagasy, the word *vinanitelo* means "three rivers," ostensibly referring to a region where different river tributaries converge. The Vinanitelo visited by Major in the late 19th century is consistently located in period maps and was well known to contemporary travelers (see Jenkins and Carleton, 2005: locality 19). The coordinates supplied by the National Geospatial-Intelligence Agency actually place Vinanitelo to the southeast of Fianarantsoa; we amend the type locality as Madagascar, Fianarantsoa Province, region of Vinanitelo, ca. 35 km SE Fianarantsoa, ca. 1100 m, coordinates ca. 21°43′S, 47°16′E. The terrain around this site is now largely denuded of original forest, but continuous stands of montane forest remain 10 km farther to the southeast. The latter forest tract was visited in October 2000, at a site 15.5 km SE Vohitrafeno and along a trail leading to the Tanala village of Ikongo (see appendix 1: locality 65). The area was locally called "Vinanitelo" and almost

certainly lies nearby or within the vicinity visited by Major in 1896.

PARATYPES: BMNH 1958.2.28.7, a female, skull and partial postcranial skeleton preparation, collected June 1896 by C.I. Forsyth Major; FMNH 5631, an adult male, skin and skull preparation, collected 4 June 1896 by C.I. Forsyth Major.

In his species description, Major (1896a: 463) specifically indicated two other specimens by their field numbers, and these become de facto paratypes of *E. tanala* (International Commission on Zoological Nomenclature, 1999: articles 72.4.5, 73D): M1510 (now = FMNH 5631), subsequently exchanged with the FMNH; and M1515 (now = BMNH 1958.2.28.7), rediscovered later in the BMNH collection and cataloged in 1958.

EMENDED DIAGNOSIS: A species of *Eliurus* that forms a clade with *E. ellermani* and *E. tsingimbato* (figs. 3, 4, 6). Morphologically defined by a combination of gray or grayish white ventral pelage (fig. 14), weakly delineated from the dorsum (ventral pelage entirely creamy white, dorsal-ventral countershading pronounced in *E. ellermani* and *E. tsingimbato*); terminal tail tuft usually white (caudal tuft typically dusky brown in *E. tsingimbato*; fig. 12); skull having a comparatively broad interorbital constriction (narrower in *E. tsingimbato*) and small auditory bullae (larger in *E. tsingimbato*); subsquamosal fenestra little expressed, hamular process weakly defined or indistinct (subsquamosal fenestra open, short hamular process apparent in *E. tsingimbato*); and palatal fenestration extensive (supernumerary vacuities uncommon in *E. tsingimbato*).

DISTRIBUTION: Humid-forest habitats of eastern Madagascar (fig. 16), from the mountain ridges east of Lac Alaotra (ca. 18°S), southward through the Central Highlands, to the southernmost terminus of the Southern Highlands (ca. 25°S); known elevational range 395–1630 m, most locality records documented between 800 and 1300 m (fig. 17).

MORPHOLOGICAL DESCRIPTION AND COMPARISONS: Specimens composing the large clade that represents the Central and Southern highlands (fig. 3) are certainly identifiable as *E. tanala* and conform to the morphological descriptions offered by previous authors (Carleton, 1994, 2003; Goodman and Carleton, 1996; Goodman et al., 1999; Soarimalala et al., 2001, 2007). The following observations amplify patterns of pelage variation.

Ventral pelage is commonly a uniform pale gray or grayish white among locality series of *E. tanala* (fig. 14A), a condition observed in 51 of 64 (80%) round skins examined. Ventral hairs in these specimens are bicolored, their basal half a pale gray and distal half dull white or buff; the combination of gray bases and especially the hue of the white to buffy tips yields the general impressions of a gray belly or "under surface yellowish white" as characterized by Major (1896a: 463). Invasive patches of self-colored, creamy white hairs are occasionally observed on the ventral surfaces of some specimens within a locality series (eight of 64 skins = 12%); such patches may be localized, e.g., expressed as a midventral streak (fig. 14B), or more broadly extend across the chest and abdomen as a grayish-white mottling (fig. 14C). Such variable extensions of creamy white hairs appear transitional to the all white underparts characteristic of *E. ellermani* and *E. tsingimbato* (fig. 14D). Some specimens of *E. tanala* have a bright, wholly white ventral pelage (5 of 64 = 8%), including the three from the Forêt d'Ianasana (Itremo Massif), a population isolated at the westernmost distribution of the species (fig. 16: locality 55). Nonetheless, *Cytb* sequences nested all three within the *E. tanala* clade (fig. 3), and their crania unambiguously clustered with OTUs of *E. tanala* when entered as unknowns in discriminant function analysis (see above).

The caudal tuft in a majority of specimens that retain their complete tail length, 56 of 60 (93%), consists of bright white hairs (fig. 12D), this terminal segment measuring 6–95 mm long (x = 34, N = 56). A minority of *E. tanala* surveyed possesses either an entirely dark tail tuft (FMNH 156640, 162084) or a dark tip with white subterminal band (FMNH 178700, 178701), a

chromatic variant also observed in a few *E. tsingimbato* (fig. 12A).

Remarks: Major's (1896a: 462–463) description of *E. tanala* is brief: "More closely related to *E. majori*, Thos., than to the other two species [*E. myoxinus*, *E. minor*], but distinguished from the first [*E. majori*] by a somewhat larger size, by a slight difference in coloration—the centre of the back being of a darker grey and the under surface yellowish white—as well as by a longer snout and smaller molars." Curiously, Major neglected to mention the white tail tuft of his new species, a trait that is conspicuous on the round skin of the holotype (BMNH 97.9.1.154) and the one paratype with skin (FMNH 5631). As further documented above, a white caudal plume is a characteristic trait of Major's species.

Specimens Examined: $N = 192$, as follows.

Province d'Antananarivo: 17 km NE Anjozorobe, Anorana, District d'Anjozorobe, 1250 m (UADBA 49953); 18 km NE Anjozorobe, Anorana, District d'Anjozorobe, 1150 m (UADBA 49978); 13 km SE Anjozorobe, 1300 m (FMNH 159474).

Province de Toamasina: Sihanaka Forest (BMNH 35.10.12.2, 36.11.2.1, 36.11.2.2; MCZ 29249); 13 mi N Rogez, near Lohariandava, 1300 ft (BMNH 47.1623); 10 mi NW Lohariandava, 1500 ft (BMNH 47.1573); PN de Mantadia, 900 m (FMNH 166065); 10 km E Ambohimanarivo, Ambatovy-Analamay, Site 5, District de Moramanga, 1045 m (UADBA 30665); Périnet, near Moramanga, 3000 ft (BMNH 47.1557–47.1572); Périnet (MNHN 1961.176; USNM 588734); 1 km E Périnet (USNM 341826); 2 km E Périnet (USNM 328828–328830); 13 km E Périnet (USNM 341827); Forêt de Maromizaha, 8.3 km SE d'Andasibe (Périnet), 980 m (FMNH 209157); 14.5 km SW Andasibe (Périnet) village, Ampasimpotsy-Anivonimaro, Lakato, Ambalafary Forest, 995 m (UADBA 31568); Sahambaky, along tributary of Sahatandra River, 31.5 km NNW Lakato, Alaotra Mangoro Region, 980 m (FMNH 204448).

Province de Fianarantsoa: Forêt d'Ianasana, 7 km W Itremo, 1630 m (FMNH 166053–166055); Forêt d'Antetezana, along Ranomena River, PN de Ranomafana, 970 m (FMNH 169249); 3 km (by road) NNW Vohiparara, Prefecture de Fianarantsoa, 1225 m (USNM 449251–449255, 449383–449385); Ambodiamontana, ca. 7 km (by road) W Ranomafana, 950 m (USNM 448906–448910, 448981–448990, 448997, 449250); near Vatoharanana River Camp, PN de Ranomafana, 950 m (FMNH 151605); Vatoharanana, 4 km SW Ranomafana (ville), PN de Ranomafana, 1025 m (FMNH 170824–170832); 1 km NW Andrambovato, 875 m (USNM 449256, 449386); 2 km W Andrambovato, along Tatamaly River, 1075 m (FMNH 170833–170835); Mandriandry, 4.4 km SW Tolongoina, 750 m (FMNH 169246); 9 km WNW Ambatofotsy, along Maroangira River, 750 m (FMNH 169247); Vinanitelo, 30 km S Fianarantsoa (BMNH 97.9.1.154, 1958.2.28.7; FMNH 5631); Forêt de Vinanitelo, 15.5 km SE Vohitrafeno, foot of Mt Ambodivohitra, 1100 m (FMNH 170836–170841); Forêt d'Ambatomainty, along Sandranta River, 11.6 km WNW Ikongo, 645 m (FMNH 169248); Forêt de Manambolo, Ambavafatra, along Andohabatotany River, 1300 m (FMNH 167638, 167639); 7 km SW Andohabatotany Forest, Ambalamanenjana, District d'Ambalavao, 1300 m (FMNH 194696–194698); 19.5 km SE Sendrisoa, Forêt de Manambolo, W slope Mt Vohipia, 1600 m (FMNH 167580, 167640–167644); 38 km S Ambalavao, Andringitra Reserve, 1625 m (FMNH 151691, 151692, 151744, 151878–151883); 40 km S Ambalavao, Andringitra Reserve, 1210 m (FMNH 151690, 151743, 151872–151877, 151897); 43 km S Ambalavao, Andringitra Reserve, 810 m (FMNH 151687–151689, 151869–151871, 177330, 177364); 8 km NE Ivohibe, 5.5 km SE Angodongodona, 1200 m (FMNH 162086); 9 km NE Ivohibe, 6.5 km ESE Angodongodona, 900 m (FMNH 161898–161900, 162087–162090); 8 km E Ivohibe, RS d'Ivohibe, 1200 m (FMNH 161895, 162080); 6.5 km ESE Ivohibe, at source of Andranomainty River, RS d'Ivohibe, 1575 m (FMNH 161896, 161897, 162081–162085); 1.2 km ENE Ampatramary, W slope Mt Ambatobe, 9.5 km NE Midongy-Sud, 650 m (FMNH 178702); 2.5 km

TABLE 8

Descriptive statistics for selected OTUs of the *Eliurus antsingy* species group

Statistics include the sample mean, ± one standard deviation, the observed range and sample size (in parentheses); measurements from the holotype for each species are presented under the specimen number. See Materials and Methods for variable abbreviations and geographic coverage of OTUs.

	E. antsingy		*E. carletoni*		
Variable	MNHN 1966.2220	All localities	FMNH 173105	RS d'Ankarana & vicinity	PHP de Loky-Manambato
TOTL	–	327.2 ± 18.0	335	323.6 ± 29.0	331.8 ± 18.1
		305–354 (5)		282–378 (10)	282–369 (34)
HBL	–	149.4 ± 7.4	143	141.3 ± 8.6	148.9 ± 6.6
		142–160 (5)		130–153 (10)	135–160 (37)
TL	–	168.4 ± 11.9	183	169.2 ± 13.1	176.4 ± 14.1
		153–186 (5)		145–190 (10)	145–209 (34)
HFL	–	29.4 ± 2.4	29	28.7 ± 1.5	30.6 ± 0.8
		26–32 (5)		25–31 (12)	29–32 (37)
DHFL	30.0	30.3 ± 1.4	30.5	29.6 ± 1.1	29.9 ± 0.8
		29.0–32.5 (5)		27.5–30.9 (9)	28.0–31.6 (37)
EL	–	25.0 ± 0.7	25	23.8 ± 1.2	23.3 ± 1.1
		24–26 (5)		22–26 (12)	21–26 (37)
WT	–	100.4 ± 18.0	99	90.5 ± 9.2	89.8 ± 11.7
		87–131 (5)		72–103 (12)	57–110 (37)
ONL	41.9	41.2 ± 1.6	40.5	39.9 ± 1.2	40.0 ± 1.4
		39.2–44.1 (11)		37.8–41.9 (14)	36.8–42.9 (58)
ZB	20.8	19.7 ± 1.1	20.1	19.4 ± 0.8	19.4 ± 0.9
		18.5–21.8 (11)		18.2–20.9 (14)	17.4–21.1 (58)
BBC	16.3	15.4 ± 0.5	14.9	15.0 ± 0.5	15.1 ± 0.4
		14.9–16.3 (11)		13.9–15.8 (14)	14.1–15.8 (58)
IOB	5.9	5.9 ± 0.2	5.6	5.7 ± 0.2	5.7 ± 0.2
		5.6–6.3 (11)		5.3–6.0 (14)	5.2–6.3 (58)
BOC	9.5	9.1 ± 0.3	8.7	8.8 ± 0.3	8.9 ± 0.3
		8.7–9.7 (11)		8.2–9.3 (14)	8.3–9.8 (58)
LR	14.8	13.8 ± 0.8	13.9	13.5 ± 0.5	13.3 ± 0.6
		12.6–15.1 (11)		12.7–14.4 (14)	11.9–14.4 (58)
BR	7.4	7.1 ± 0.3	7.4	7.0 ± 0.4	7.1 ± 0.4
		6.5–7.5 (11)		6.2–7.7 (14)	6.2–7.8 (58)
LD	11.7	11.4 ± 0.5	11.4	11.3 ± 0.6	11.1 ± 0.6
		10.8–12.4 (11)		10.2–12.3 (14)	9.8–12.3 (58)
LIF	6.7	6.4 ± 0.2	6.0	5.8 ± 0.4	5.9 ± 0.4
		6.0–6.8 (11)		5.3–6.7 (14)	4.9–6.9 (58)
BIF	3.1	2.7 ± 0.2	2.9	2.6 ± 0.1	2.7 ± 0.2

Variable	*E. antsingy*		*E. carletoni*		
	MNHN 1966.2220	All localities	FMNH 173105	RS d'Ankarana & vicinity	PHP de Loky-Manambato
		2.4–3.1 (11)		2.4–2.9 (14)	2.3–3.2 (58)
LBP	7.8	7.5 ± 0.3	7.9	7.8 ± 0.5	7.6 ± 0.5
		7.1–7.9 (11)		7.1–8.8 (14)	6.6–8.8 (58)
PPL	14.7	14.8 ± 0.7	14.9	14.4 ± 0.6	14.4 ± 0.7
		14.1–16.4 (11)		13.4–15.4 (14)	13.1–15.7 (58)
BM1s	8.0	7.7 ± 0.3	7.8	7.5 ± 0.3	7.5 ± 0.3
		7.3–8.3 (11)		6.9–8.1 (14)	6.8–8.1 (58)
PPB	6.1	5.7 ± 0.3	5.5	5.5 ± 0.2	5.6 ± 0.3
		5.3–6.1 (11)		5.3–5.8 (14)	4.8–6.4 (58)
DAB	6.0	5.7 ± 0.2	5.3	5.5 ± 0.2	5.4 ± 0.1
		5.5–6.4 (11)		5.2–5.7 (14)	5.0–5.8 (58)
BZP	3.5	3.8 ± 0.2	4.1	3.7 ± 0.4	3.7 ± 0.3
		3.4–4.3 (11)		3.1–4.3 (14)	3.1–4.3 (58)
LM1–3	6.00	5.77 ± 0.20	5.90	5.67 ± 0.19	5.61 ± 0.19
		5.42–6.08 (12)		5.24–6.00 (14)	5.11–6.15 (58)
WM1	1.65	1.53 ± 0.06	1.65	1.55 ± 0.09	1.52 ± 0.06
		1.45–1.65 (12)		1.41–1.70 (14)	1.41–1.66 (58)

SW Befotaka, Mt Papango, along Andranomena River, PN de Midongy-Sud, 875 m (FMNH 178692–178696); 3.5 km SW Befotaka, NE slope Mt Papango, PN de Midongy du Sud, 1250 m (FMNH 178644, 178645, 178697–178701).

Province de Toliara: Marosohy Forest, 16 km WNW Ranomafana[-Sud], Fivondronana de Tolagnaro, 800 m (USNM 578688–578691, 578797, 578798); 15 km NW Eminiminy, RNI d'Andohahela, parcel 1, 1500 m (FMNH 156515–156521, 156531, 156532, 156639, 156640); 13.5 km NW Eminiminy, RNI d'Andohahela, parcel 1, 1200 m (FMNH 156637, 156638); 12.5 km NW Eminiminy, RNI d'Andohahela, parcel 1, 810 m (FMNH 156514, 156528, 156631–156636, 156641); Manantantely, 8–12 km WNW Tolagnaro, Fivondronana de Tolagnaro (USNM 577222–577225).

Eliurus ellermani Carleton, 1994
Figure 16; table 7

Eliurus ellermani Carleton, 1994: 39 (original description).

Eliurus tanala; Carleton and Goodman, 1998: 178 (part; faunal report, amendment of type

locality and discussion of taxonomic status of *E. ellermani*).

Eliurus sp. B; Jansa et al., 1999: 267 (part; indeterminate specific assignment of specimens clustered in molecular tree).

Eliurus aff. *E. tanala* Group; Carleton and Goodman, 2007: 20 (part; taxonomic commentary on species group associations).

Eliurus tanala-B; this study.

HOLOTYPE: MNHN 1981.871, an adult male prepared as skin and skull, collected January 1968 by R. Albignac.

TYPE LOCALITY: "Hiaraka, near Maroantsetra, 850 m," corrected by Carleton and Goodman (1998: 181) to read "Toamasina Province, near Hiaraka, about 18 km ESE Maroantsetra, 850 m, coordinates about 15°30′S, 49°56′E."

The "Hiaraka" to the northwest of Maroantsetra, as mistakenly located by MacPhee (1987) and Carleton (1994), was corrected by Carleton and Goodman (1998) to identify a Hiaraka on the Masoala Peninsula, to the east of Maroantsetra (fig. 16: locality 29). The latter Hiaraka, also as Iharaka, is situated near the northwestern boundary of the PN de Masoala, approximate to undisturbed transitional lowland–montane forest (600–1000 m) where samples of "*E. tanala*" have been documented (Andrianjakarivelo et al., 2005).

EMENDED DIAGNOSIS: A species of *Eliurus* that forms a clade with *E. tanala* and *E. tsingimbato* (figs. 3, 4, 6). Morphologically defined by a combination of entirely white ventral pelage, sharply demarcated from the drab, grayish-brown dorsum (ventral pelage usually pale gray in *E. tanala*, dorsal-ventral countershading not so conspicuous); tail tuft white in most specimens (caudal tuft typically dusky brown *E. tsingimbato*); skull with broad interorbital constriction (narrower in *E. tsingimbato*) and small auditory bullae (larger in *E. tsingimbato*); subsquamosal fenestra little expressed, hamular process weakly defined or indistinct (subsquamosal fenestra open, short hamular process apparent in *E. tsingimbato*); and palatal fenestration extensive (supernumerary vacuities uncommon in *E. tsingimbato*).

DISTRIBUTION: Humid-forest associations of the Northern Highlands (fig. 16), from the northernmost isolate Montagne d'Ambre (ca. 12.5°S), throughout the core Northern Highlands, to southern outliers in the central mountains of the Masoala Peninsula and the northernmost reaches of the Central Highlands (ca. 16°S); known elevational range 440–1570 m, most locality records documented between 800 and 1200 m (fig. 17).

MORPHOLOGICAL DESCRIPTION AND COMPARISONS: Gene-sequenced specimens of *E. ellermani* (*E. tanala*-B) describe an external morphology characterized by large size (table 7), a wholly white venter that accentuates the dorsal-ventral pelage contrast, and typically a white terminal tail tuft (table 6). Ventral cover hairs are monocolored, imparting a dingy creamy white to creamy buff color to the underparts from the chin to groin; the uniformly white ventrum is sharply delineated along the flanks from the dark grayish brown of the dorsal pelage. In most specimens, the terminal tail tuft is wholly white, 14–50 mm long ($x = 33$, $N = 13$), but some individual variation is evident. The tuft of one specimen (FMNH 159696) possesses a white subterminal band and a dark tip, a condition observed in a few examples of *E. tsingimbato* (e.g., fig. 12A); two specimens (FMNH 195865, 195868) bear an entirely dark, pale brown to dusky brown tuft. Carleton (1994) and Carleton and Goodman (1998; reported as *E. tanala*) provided additional pelage description and interspecific comparisons of *E. ellermani*.

Examples of *E. ellermani*, like those of *E. tanala*, possess a large, stoutly constructed skull with heavy incisors. Although samples of *E. ellermani* average larger than *E. tanala* in most cranial dimensions, these values overlap substantially (table 7). Morphometric analyses fail to wholly segregate crania of the two species in multivariate space; in particular, the sample of *E. ellermani* from the Northern Highlands is phenetically indistinguishable from the OTU of *E. tanala* in the northern Central Highlands (t1—PN d'Analamazaotra and vicinity). In addition to skull

size and proportions, series of *E. ellermani* and *E. tanala* also agree in many qualitative cranial traits, such as the presence of supernumerary palatal perforations, a nearly occluded subsquamosal fenestra and correspondingly short or indistinct hamular process, and lower incisors terminating as a capsular protruberance set high on the ascending mandibular ramus (fig. 11).

Remarks: Carleton (1994: 39) typified the new species *E. ellermani* as "a robust version of *E. tanala* except with the tail brush completely dark to the tip." Possession of an entirely dark tail tuft was a crucial element in his diagnosis. At the time, only two specimens of *E. ellermani* were available; no series of large *tanala*-like animals were then available from the Northern Highlands, a circumstance that changed dramatically with the renewal of directed biotic surveys in the 1990s (see fig. 1). In reporting results of one of those surveys, undertaken in the RS d'Anjanaharibe-Sud, Carleton and Goodman (1998: 175–182) reviewed the status of *E. ellermani*, narrowed the diagnosis of *E. ellermani* to possession of a dark tail tuft, and provisionally assigned the Anjanaharibe-Sud specimens to *E. tanala*. The gene-sequence data presented herein repeatedly recovered a well-supported clade, *E. tanala*-B, that represents population samples from the Northern Highlands (figs. 3, 4) and that includes the holotype of *E. ellermani* (MNHN 1981.871). Color of the tail tuft evident within series from those Northern Highland localities is typically white, infrequently entirely dark. Our emended diagnosis reflects this expanded appreciation of population variation.

We here reallocate the paratype (BMNH 47.1623) of *E. ellermani* to the species *E. tanala*. The specimen was collected near Lohariandava, 21 km N Andekaleka (appendix 1: locality 46), nearby other series confidently identified as *E. tanala* and far south of the currently understood distribution of *E. ellermani* (fig. 16). Some ventral hairs of this specimen were noted as having their bases gray, a variation atypical of *E. ellermani* but documented within series of *E. tanala*. Similarly, the paratype's wholly dark tail tuft cannot be now construed as typical of *E. ellermani* based on the larger series of the species at present available from the Northern Highlands.

Nearly all specimens here vouchered as *E. ellermani* issue from sites in the Northern Highlands, except those collected from the vicinity of Marotandrano (appendix 1: locality 30), situated south of the Mandritsara Basin that isolates the Northern from the Central highlands. We have not examined the Marotandrano specimens, held in UADBA, to verify whether they conform to the chromatic traits and physical size characteristic of *E. ellermani*.

Specimens Examined: $N = 54$, as follows.

Province d'Antsiranana: 5.5 km SW Joffreville, PN de la Montagne d'Ambre, 1000 m (FMNH 154621–154623, 154625); Forêt d'Antsahabe, 12 km W Daraina, 850–950 m (FMNH 195901, 195903, 195904, 195906); Forêt de Binara, 7.5 km SW Daraina, 325–550 m (FMNH 172666–172675, 172693); Forêt d'Ambohibe, 16.0 km SW Daraina, 490–680 m (FMNH 195865, 195868, 195967, 195970, 195972); 12.8 km Antanambao, RS de Manongarivo, 785 m (FMNH 166248–166250); 14.5 km Antanambao, RS de Manongarivo, 1240 m (FMNH 166251); Bemanevika Forest, Peregrine Fund Camp, Région Sofia, 1570 m (FMNH 226019); 10 km NW Manantenina, along tributary of Manantenina River, RNI de Marojejy, 775 m (FMNH 159696, 159697); 11.5 km SE Doany, PN de Marojejy, 810 m (FMNH 172615, 172616, 172637, 172640, 173628); 8.5 km NW Ambodiangezoka, Forêt de Betaolana, along Ambolokopatrika River, 875 m (FMNH 167515, 167516); 11 km NW Ambodiangezoka, Forêt de Betaolana, 1200 m (FMNH 167517–167519); 6.5 km SSW Befingotra, RS d'Anjanaharibe-Sud, 875 m (FMNH 154049); 9.2 km WSW Befingotra, RS d'Anjanaharibe-Sud, 1260 m (FMNH 154050, 154051, 154249, 154250).

Province de Mahajanga: 13.5 km SW Befingotra, western slope of Anjanaharibe-Sud, 1200 m (FMNH 167467, 167468); 12 km SSE Marotandrano, Anjiambolo, District de Mandritsara, 950 m (UADBA 47002); 12.5 km SSE Marotandrano, along Riamalandy waterfall, District de Mandritsara, 850 m (UADBA 47003–47005, 47052).

FIG. 19. Two views of montane eastern humid forest where individuals of *Eliurus ellermani* were collected, in close vicinity to Ambohitsitondroina, PN de Masoala, 1078 m, a site situated in close proximity to Hiaraka (fig. 16: locality 29), the type locality of this species. **A,** Panoramic view from a neighboring ridge of the dense canopy of montane forest and the topographic features of the Masoala Peninsula. **B,** The understory of montane forest showing characteristic vegetation, often composed of plants belonging to the genera *Cyathea* and *Pandanus*, and epiphytic vegetation on tree trunks and limbs. Photographs by Voahangy Soarimalala.

Province de Toamasina: near Hiaraka, ca. 18 km ESE Maroantsetra, 850 m (MNHN 1981.871).

Natural History Notes: Like its sister species *E. tanala*, populations of *E. ellermani* have been documented from evergreen humid forest in montane settings (figs. 16, 19). Such floristically diverse plant communities on eastern mountains are generally classified as moist montane or sclerophyllous montane forest depending upon elevation (e.g., Messmer et al., 2000: table 3-4). As exemplified by the forest understory in the PN de Masoala, lianas are commonplace, epiphytes are abundant, and tree trunks and branches are densely covered by moss and lichen (fig. 19B).

DISCUSSION

Taxonomic Issues and Species Delimitation

Genetic, morphological, morphometric and distributional evidence provided concordant evidence that three species exist within the *Eliurus tanala* group, one described as new to science (*E. tsingimbato*) and two whose distribution and definition were substantially revised (*E. ellermani*, *E. tanala*). Analyses of both mitochondrial (figs. 3, 4) and nuclear (fig. 6, table 2) DNA sequences united samples of western *E. tsingimbato* in a clade isolated from those of the two eastern species *E. ellermani* and *E. tanala*. Morphological traits and morphometric analyses consolidated samples of *E. tsingimbato* apart from those of *E. ellermani* and *E. tanala* (figs. 9, 12). Moreover, morphometric (Mahalanobis D^2) and genetic (uncorrected pairwise) distance measures are strongly correlated among six selected *Eliurus* species we evaluated, including those of the *E. tanala* group (fig. 20; table 9). Distributional records of *E. tsingimbato* uniformly document the species in low elevation, dry forests of western Madagascar, an environmental setting that sharply contrasts with the middle to high elevation occurrence of *E. ellermani* and *E. tanala* in eastern humid forests (figs. 16, 17, 19). These independent lines of evidence offer pluralistic and robust justification for the description of *E. tsingimbato* as a new species, consistent with an integrated taxonomic approach (e.g., Padial et al., 2010; Galimberti et al., 2012; Dávalos and Russell, 2014; Pante et al., 2015).

Notwithstanding the usual reciprocal illumination supplied by molecular and morphometric data, two areas of apparent conflict require discussion. One issue involved contradictory evidence for recognition of *E. ellermani* as a species distinct from *E. tanala*. A second dilemma concerned the species allocation of the population sample from Forêt d'Analamavo, in western Madagascar (fig. 16: locality 35), as inferred from mitochondrial genes (= *E. tanala*) or from nuclear genes and morphological similarity (= *E. tsingimbato*).

Evidence for recognizing *E. ellermani* as distinct from *E. tanala* is strongly supported by molecular data (including multilocus, coalescent-aware analyses of species limits), which unambiguously delineate populations in the Northern Highlands (*E. ellermani*) from those distributed across the Central and Southern highlands (*E. tanala*). Based on mitochondrial *Cytb* sequences, the holotype of *E. ellermani* definitively clustered within the large clade that represents localities in the Northern Highlands (fig. 3). On the other hand, our morphometric comparisons, like those of Carleton and Goodman (1998), offered inconclusive results that could be interpreted as a latitudinal size cline, with larger animals in the north and smaller ones in the south. In fact, the two northernmost samples—one genetically identifiable as *E. ellermani* (fig. 16: localities 22–29) and the other as *E. tanala* (fig. 16: localities 43, 49, 53)—are indistinguishable in morphometric space based on discriminant function analysis (fig. 9). Having eliminated a dark tail tuft as strictly diagnostic of *E. ellermani*, the most perceptible external contrast between the taxa involves their ventral pelage color, bicolored ventral hairs and overall grayish appearance in examples of *E. tanala* versus monocolored ventral hairs and creamy white underparts in *E. eller-*

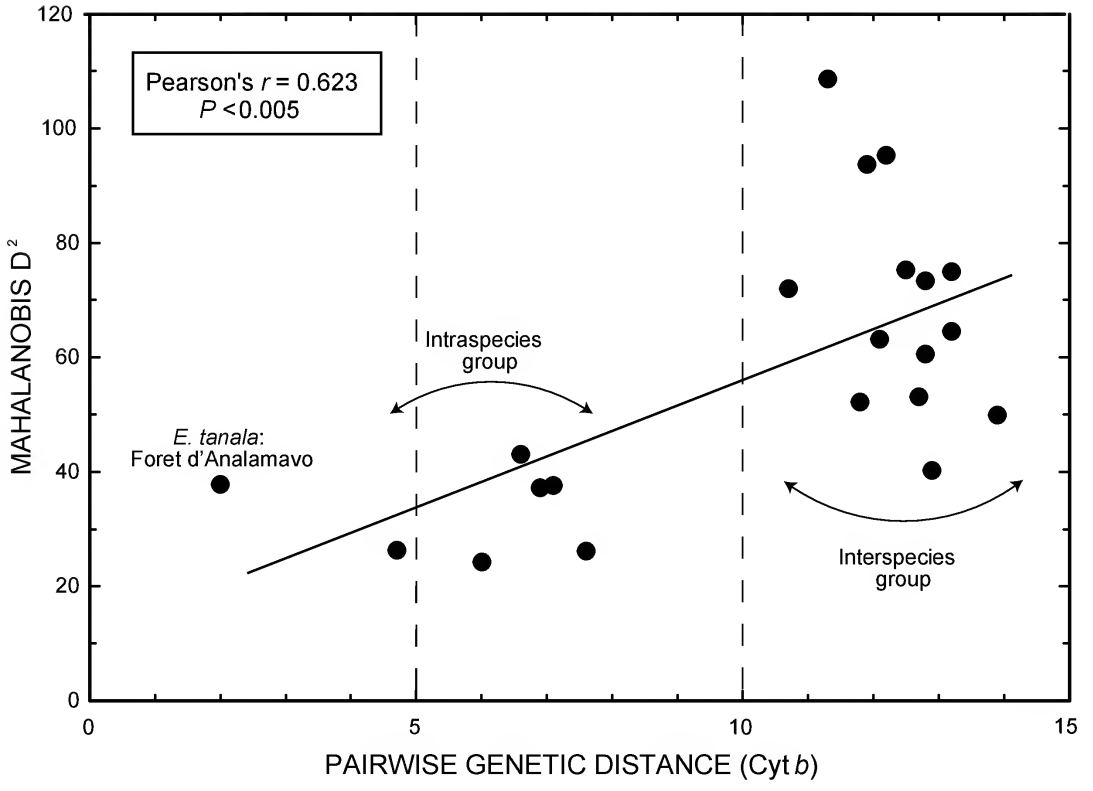

FIG. 20. Scatterplot of distance values derived from *Cytb* sequences (uncorrected pairwise distances) and discriminant function analysis (Mahalanobis D^2) of six species of *Eliurus* plus the Forêt d'Analamavo sample (see table 9). "Intraspecies group" denotes values derived between species within the same species group (*E. antsingy* and *E. tanala* groups), including sister species; "Interspecies group" denotes values derived between species assigned to different species groups (*E. antsingy*, *E. myoxinus* and *E. tanala* groups).

mani. We underscore that the taxonomic status of *E. ellermani* vis-à-vis *E. tanala* is amenable to clarification based on additional collecting in remaining forests intermediate to the southernmost locality of *E. ellermani*, near Marotandrano (fig. 16: locality 30), and the northernmost site recorded for *E. tanala*, around the Sihanaka Forest (fig. 16: locality 45), a hiatus of some 200 km. Pending new analyses of such potentially transitional samples, we accept *E. ellermani* as a distinct species based principally on its singular genetic integrity.

Mitochondrial gene sequences (figs. 3, 4) surprisingly grouped the six individuals from the Forêt d'Analamavo, a dry-forest site in western Madagascar (fig. 16: locality 35), with samples of *E. tanala*, a species broadly distributed across eastern montane forests in the Central and Southern highlands (fig. 16). In contrast to the genetic affinity conveyed by mitochondrial loci, however, the X-linked gene affiliates the Forêt d'Analamavo specimens with examples of *E. tsingimbato* (*E. tanala*-A in fig. 5; PP = 1.00). Independent analyses of the three autosomal loci did not yield a comprehensible picture of species membership (fig. 5), but coalescent-aware, species-tree analysis of all four nuclear genes (fig. 6; PP = 0.99), as well as species-delimitation analysis based on these data (table 1), affirms the close relationship of the Forêt d'Analamavo series with *E. tsingimbato* (*E. tanala*-A). With their creamy white ventral pel-

TABLE 9

Matrix of morphometric and genetic distances between species of *Eliurus* (see fig. 20), including the sample from the Forêt d'Analamavo

Above diagonal: uncorrected pairwise distances (x 100) based on *Cytb* sequences. Below diagonal: Mahalanobis D^2 values based on seven-group* discriminant functional analysis.

	ant.	*car.*	*ell.*	*myo.*	Anal.	*tan.*	*tsi.*
E. antsingy	–	4.7	11.3	12.5	12.8	11.9	12.1
E. carletoni	26.3	–	13.2	12.7	13.9	13.2	12.9
E. ellermani	108.7	75.0	–	12.2	6.6	6.0	6.9
E. myoxinus	75.3	53.1	95.3	–	11.8	10.7	12.8
F. d'Analamavo	73.4	49.9	43.1	52.2	–	2.0	7.6
E. tanala	93.7	64.5	24.2	72.0	37.8	–	7.1
E. tsingimbato	63.2	40.2	37.2	60.6	26.1	37.6	–

*Species OTUs, as defined per Materials and Methods: *E. antsingy* (N = 11; all localities); *E. carletoni* (N = 14; RS d'Ankarana and vicinity); *E. ellermani* (N = 18; RS d'Anjanaharibe-Sud and vicinity); *E. myoxinus* (N = 14, southern Toliara Province—see Appendix 3); Forêt d'Analamavo (N = 8; locality 35); *E. tanala* (N = 37; t2—PN de Ranomafana and vicinity and t3—Forêt de Vinanitelo and vicinity); *E. tsingimbato* (N = 19; Namoroka and Bemaraha formations).

age and dusky brown tail tuft, the morphological appearance of the Forêt d'Analamavo animals does not evoke an image of *E. tanala*. Nor are qualitative cranial traits and cranial morphometry equivocal: the Forêt d'Analamavo sample decidedly resembles other specimens of *E. tsingimbato* (figs. 7C, 9). In summary, these several independent lines of evidence persuasively explain the conflicting signal from mitochondrial DNA as an instance of incomplete lineage sorting (e.g., Avise et al., 1983; Pamilo and Nei, 1988; Hudson and Turelli, 2003). As in the case of *E. ellermani* and *E. tanala*, directed collecting may illuminate the stability and/or geographic scope of this *tanala* haplotype within *E. tsingimbato*. The Forêt d'Analamavo is situated only 14 km from the Forêt d'Analanomby (fig. 16: locality 36), where genetically and morphologically typical specimens of *E. tsingimbato* were obtained.

Although the evidence in combination is compelling for recognizing three species in the *E. tanala* group, hierarchical relationship among the three is not decisively supported in any phylogenetic analysis of the genetic data. The mitochondrial tree based on *Cytb* (fig. 3) and nuclear-gene species tree (fig. 6) both recovered *E. tsingimbato* and *E. tanala* as sister species, with negligible nodal support. The concatenated mitochondrial gene tree (fig. 4) instead portrays *E. ellermani* as sister to *E. tanala*, again with uninspiring support. Among the discrete morphological characters marshaled by Carleton (1994), *E. tanala* and *E. ellermani* share several derived traits—presence of white tail tuft, greater fenestration of the bony palate, reduction or closure of the subsquamosal fenestra—that suggest their more recent common ancestry compared with *E. tsingimbato*; although not strictly phylogenetic, craniodental morphometry demonstrates the closer phenotypic similarity of *E. ellermani* and *E. tanala* to one another and their equal degree of divergence from *E. tsingimbato* (fig. 9; tables 6, 9).

This weak phylogenetic resolution can be attributed to multiple factors, including a lack of informative sites, conflict among gene partitions, or closely spaced speciation events (Hoelzer and Meinick, 1994; Walsh et al., 1999; Winkler et al., 2015). In this case, the lack of coalescence for individual nuclear genes, along with the relatively short branches describing relationships

among the three species, suggests that speciation was both recent and rapid (Hudson and Turelli, 2003; Rosenberg, 2003; Degnan and Rosenberg, 2009). A scenario of rapid speciation is consistent with the nature of our morphological diagnoses, which are polythetic formulations (or "cluster classes," as used by Zachos, 2016). That is, traits cited as diagnostic are exhibited by the majority of specimens within locality samples, but not one is necessarily fixed within the species (class); their diagnostic value is operationally realized when used in combination with one another to effect a unique taxonomic definition.

A case in point, as exemplified by our experience with the *E. tanala* group, involves the color of the distal tail tuft, the presence of a terminal brush of elongated hairs being a cardinal trait of the genus (fig. 12). Based on two specimens, Major (1896a) had overlooked the significance of a white terminal tuft in his description of *E. tanala*; based on two specimens, Carleton (1994) emphasized possession of a fully dark tuft as central to his diagnosis of *E. ellermani*. The accumulation of vastly improved species samples (see fig. 1), in number and in geographic coverage, has revealed that a white caudal pencil is common within both species, each strongly supported by inclusive molecular clades that represent many localities over broad geographies. In retrospect, the underappreciation of population variation or stability in terminal tuft color is partially attributable to the encumbrance of taxonomic history. In the early descriptive era of Malagasy biodiversity, Oldfield Thomas and C.I. Forsyth Major had meager museum series at hand to forge their new species discoveries. Even by 1994, Carleton documented about 200 specimens in his generic revision of all species of *Eliurus*. Our current study utilized some 370 vouchered specimens to clarify the systematics of three species, representing one of five species groups within the genus. As integrated with genetic data, qualitative cranial traits and ventral pelage color, possession of a white caudal tuft has emerged as an informative feature for identification of two of those species, *E. ellermani* and *E. tanala*.

Biogeography

Several hypotheses have been advanced to explain the patterns and processes of diversification of species endemic to Madagascar, as synthetically reviewed by Vences et al. (2009). A refined taxonomic foundation, derived from a well-documented understanding of species limits and their distributions, is integral to testing these hypotheses. Fortunately, the taxonomic framework is much improved for Madagascar's native rodent fauna (Nesomyinae), in particular *Eliurus*, thanks to the last two decades of directed biological exploration (e.g., Goodman and Rasolonandrasana, 1999; Goodman et al., 2007, 2013b), revisionary work (e.g., Carleton, 1994; Carleton et al., 2001; Carleton and Goodman, 2007), and phylogenetic study (Jansa et al., 1999; Jansa and Carleton, 2003; Goodman et al., 2009). These synergistic efforts have substantively enhanced our knowledge of how many nesomyine species exist, where they occur among the island's habitats, and how this diversity may have arisen.

Species of *Eliurus* are scansorial or semiarboreal rodents and with few exceptions inhabit native forests, a behavioral habit and ecological reliance that make the genus an excellent model to examine phylogeographic structure and speciation patterns associated with Madagascar's complex geology, topography, and climate (Wilmé et al., 2006; Muldoon and Goodman, 2010; Rakotomalala and Goodman, 2010; Shi et al., 2013). Although discovery of the genus *Eliurus* and its type species, *E. myoxinus*, emanated from a western environment (Milne Edwards, 1885), descriptive activity over the next 120 years would concentrate on eastern humid forests, where 10 new species were eventually recognized. Not until 2001 was a second species of *Eliurus*, *E. antsingy* (Carleton et al., 2001), described from western dry forest, followed shortly thereafter by documentation of *E. carletoni* (Goodman et al., 2009). Both taxa are largely confined to dry forests that overlie areas of Mesozoic limestone, a geological stratum that is intermittently exposed along the island's western lowlands and extends to the far

north and northeast (figs. 2, 16). At certain areas across this zone, the limestone formations are eroded to form unusual karst pinnacles, also known as *tsingy* (Bésairie, 1964; Du Puy and Moat, 1996; Veress et al., 2008).

Dry forests associated with *tsingy* formations contain a highly endemic biota whose diversity is only beginning to be appreciated (Rajeriarison et al., 2000; Cardiff and Befourouack, 2003; Bora et al., 2009; Glaw et al., 2009; Goodman et al., 2011, 2013b). *Eliurus tsingimbato*, the new species documented herein, represents another member of this unique biota, the fourth nesomyine rodent known to be endemic to *tsingy* environments, joining *E. antsingy*, *E. carletoni*, and *Nesomys lambertoni*.

Description of the new species *E. tsingimbato* from the island's dry forests brings the number of *Eliurus* known from western landscapes to three, including *E. antsingy* and *E. myoxinus*. Two of these, *E. antsingy* and *E. tsingimbato*, have been documented only in dry forests associated with *tsingy* (fig. 16); one, *E. myoxinus*, is more broadly distributed in western Madagascar, inhabiting not only *tsingy*-associated dry forest but also spiny-bush forest in the south, dry deciduous forest in the west and humid forest with an extended dry season in the north (Goodman et al., 1999, 2009; Carleton et al., 2001; Soarimalala and Goodman, 2003; Shi et al., 2013). Each of the three western *Eliurus* has been provisionally allocated to different species groups (Carleton and Goodman, 2007); none of the three was recovered as sister species in phylogenetic analyses of molecular data (figs. 3, 4, 6). These phylogenetic results indicate at least two independent origins of *tsingy*-forest denizens among *Eliurus* species, once in the *E. tsingimbato* lineage and once in the ancestor of the *E. antsingy* species group, *E. antsingy* and *E. carletoni*. The latter two species are allopatric, latitudinally isolated in *tsingy*-associated forests of the west (Bemaraha and Namoroka formations) and north (Ankarana formation).

Distributional records of sympatry between members of different species groups within *Eliurus* are commonplace: for instance, the cooccurrence of *E. tsingimbato* with *E. antsingy* and *E. myoxinus* in western Madagascar; of *E. ellermani* with *E. carletoni* or *E. majori* in northern Madagascar; of *E. tanala* with *E. majori* and *E. minor* in the Central Highlands. To date, there are few records of strict syntopy between species within the same species group, such as that recorded for *E. minor* and *E. myoxinus* along the northwestern slopes of the PN de Marojejy (Soarimalala and Goodman, 2003); in most species groups, member species geographically replace one another (Goodman et al., 2013a). Demonstration of sympatry usefully presupposes isolated gene pools and removes ambiguity about species status. Within *Eliurus*, genetic distances calculated between species of different groups exceed by twofold those derived between species within a particular group (table 9; fig. 20).

Finally, patterns of phylogeographic structure within species groups of *Eliurus*, as so far understood, conform to three of the species-diversification patterns distilled by Vences et al. (2009). All three invoke a process of geographic isolation instigated by bioclimatic oscillations, ultimately culminating in vicariant speciation (their ecogeographic constraint model also considers parapatric speciation across a steep east-west environmental gradient).

(1) According to the ecogeographic constraint model of Vences et al. (2009), a phylogenetic division separates sister species or clades in western and eastern Madagascar, respectively corresponding to dry- versus humid-forest associations. Isolation of *E. tsingimbato* in western dry forest, wholly allopatric to the eastern humid-forest clade *E. tanala* and *E. ellermani* (fig. 16), is consistent with their east-west phylogeographic pattern, which suggests origination from a formerly widespread, habitat-generalist species, subsequent adaptation to locally arid (western) or mesic (eastern) conditions, and finally divergence into two species clades. Preliminary gene-sequence evidence indicates that *E. myoxinus*, broadly distributed in western dry forest, and *E. minor*, equally broadly distributed

in eastern humid forest, may also comprise an east-west kinship group (figs. 3, 4; also see Jansa et al., 1999: fig. 1; Rakotoarisoa et al., 2010: fig. 2); although this relationship requires additional investigation with a broad geographic and taxonomic sampling of nuclear genes.

(2) Vences et al. (2009) applied their montane refugia model to north-south divisions within the eastern humid forest, whereby widespread populations restricted to high elevations become isolated in neighboring mountain systems during geological periods of drier climate. Within the *E. tanala* group, differentiation of the eastern clade, *E. ellermani* and *E. tanala*, plausibly transpired within such montane refugia, centered in the Northern versus Central highlands and separated by the lowlands forming the Mandritsara Basin (fig. 1). According to this view, the record of *E. ellermani* in the northernmost Central Highlands, to the south of the Mandritsara Basin (fig. 16: locality 30), would represent an instance of secondary population expansion. Because divergence among *E. tanala*, *E. ellermani*, and *E. tsingimbato* appears to be coeval (fig. 6), their initial isolation may be attributable to a single, recent episode of climatic drying; however, a rigorous test of this hypothesis will require a more comprehensive, time-scaled phylogeny.

(3) Vences et al. (2009) identified a second east-west diversification mechanism, involving the formation of western rainforest refugia. In this model, a widespread, humid-forest species becomes isolated in relictual pockets of western humid forest during cool, dry climatic periods, eventually differentiating from sister taxa in the continuous block of eastern humid forest. Speciation among members of the *E. majori* species group (*E. danieli*, *E. majori*, *E. penicillatus*) merits consideration in this context. Available molecular data have allied *E. danieli*, isolated on the Isalo Massif in south-central Madagascar, with *E. majori*, a montane species broadly distributed in eastern humid forest (Jansa et al., 1999: fig. 1, sp. A = *E. danieli*; Goodman et al., 2009: fig. 6). Here again, taxon and geographic sampling must be augmented, in particular to include examples of *E. penicillatus*, a species localized along the eastern flank of the Central Highlands (also see Carleton and Goodman, 2007: 13).

With respect to conservation issues, *Eliurus tsingimbato* is fortuitously restricted to forest habitats that occur on limestone base rock, several of which are now incorporated within Madagascar's system of protected areas. This official protection, and the general lack of agricultural productivity on *tsingy* karst, should minimize human despoliation of these western dry forests, factors that bode well for the conservation of this distinctive species into the near future. However, none of Madagascar's pristine forests, including those within protected areas, is proving exempt from the recent wave of hardwood exploitation; such overharvesting would impinge on the limited range of this species, as well as many other *tsingy*-dependent taxa, and impact survival of local populations.

ACKNOWLEDGMENTS

Many museum staff, by means of loans and visits arranged over many years, have enabled our access to specimens documented herein, including P. Jenkins (BMNH); L. Heaney, J. Phelps, and W. Stanley (FMNH); M. Rutzmoser (MCZ); C. Callou, C. Denys, and M. Tranier (MNHN); and D. Rakotondravony and M. Raheriarisena (UADBA). We especially thank Cécile Callou (MNHN), who facilitated the sampling of the holotype of *Eliurus ellermani* used in our molecular analyses. Effective illustration of our results depended upon the creative talents of John Weinstein (FMNH) for the cranial photography, Harald Schütz for the color image of the holotype, and Velizar Simeonovski (FMNH) for the tail drawings. We thank Robert Voss and an anonymous reviewer for suggestions that improved the manuscript.

Field surveys in limestone areas of western and northern Madagascar were financed by grants from the Volkswagen Foundation, the Vontobel Foundation, the National Geographic

Society (6637-99 and 7402-03) and the National Science Foundation (DEB-0516313). Permission to conduct fieldwork on Madagascar was granted by the Direction du Système des Aires Protégées, Direction Générale de l'Environnement et des Forêts and Madagascar National Parks. Molecular work was funded by National Science Foundation grant DEB-1119918 to S.A.J. For help in the field and for trapping some of the rodents used in this study, we are grateful to Martin Raheriarisena and Haridas H. Zafindranoro. For help with molecular work in S.A.J.'s lab, we thank Carmen Martin and Jordan Tysdal.

REFERENCES

Andrianjakarivelo, V., E. Razafimahatratra, Y. Razafindrakoto, and S.M. Goodman. 2005. The terrestrial small mammals of the Parc National de Masoala, northeastern Madagascar. Acta Theriologica 50: 537–549.

Avise, J.C., J.F. Shapira, S.W. Daniel, C.F. Aquadro, and R.A. Lansman. 1983. Mitochondrial DNA differentiation during the speciation process in *Peromyscus*. Molecular Biology and Evolution 1: 38–56.

Bésairie, H. 1964. Carte géologique de Madagascar, au 1:1,000,000e, trois feuilles en couleur. Antananarivo: Service Géologique.

Bora, P., et al. 2009. Amphibians and reptiles of the Tsingy de Bemaraha Plateau, western Madagascar: checklist, biogeography and conservation. Herpetological Conservation and Biology 5: 111–125.

Brown, J.D. 2009. Choosing the right type of rotation in PCA and EFA. Shiken: JALT Testing and Evaluation SIG Newsletter 13 (3): 20–25.

Cardiff, S.G., and J. Befourouack. 2003. The Réserve Spéciale d'Ankarana. *In* S.M. Goodman and J.P. Benstead (editors), The natural history of Madagascar: 1501–1507. Chicago: University of Chicago Press.

Carleton, M.D. 1994. Systematic studies of Madagascar's endemic rodents (Muroidea: Nesomyinae): Revision of the genus *Eliurus*. American Museum Novitates 3087: 1–55.

Carleton, M.D. 2003. *Eliurus*, tufted-tailed rats. *In* S.M. Goodman and J.P Benstead (editors), The natural history of Madagascar: 1373–1380. Chicago: University of Chicago Press.

Carleton, M.D., and S.M. Goodman. 1998. New taxa of nesomyine rodents (Muroidea: Muridae) from Madagascar's northern highlands, with taxonomic comments on previously described forms. Fieldiana: Zoology (new series) 90: 163–200.

Carleton, M.D., and S.M. Goodman. 2007. A new species of the *Eliurus majori* complex (Rodentia: Muroidea: Nesomyidae) from south-central Madagascar, with remarks on emergent species groupings in the genus *Eliurus*. American Museum Novitates 3547: 1–21.

Carleton, M.D., and D.F. Schmidt. 1990. Systematic studies of Madagascar's endemic rodents (Muroidea: Nesomyinae): an annotated gazetteer of collecting localities of known forms. American Museum Novitates 2987: 1–36.

Carleton, M.D., and W.T. Stanley. 2012. Species limits within the *Praomys delectorum* group (Rodentia: Muridae: Murinae) of East Africa: a morphometric reassessment and biogeographic implications. Zoological Journal of the Linnean Society 165: 420–469.

Carleton, M.D., R.D. Fisher, and A.L. Gardner. 1999. Identification and distribution of cotton rats, genus *Sigmodon* (Muridae: Sigmodontinae), of Nayarit, México. Proceedings of the Biological Society of Washington 112: 813–856.

Carleton, M.D., S.M. Goodman, and D. Rakotondravony. 2001. A new species of tufted-tailed rat, genus *Eliurus* (Muridae: Nesomyinae), from western Madagascar, with notes on the distribution of *E. myoxinus*. Proceedings of the Biological Society of Washington 114: 972–987.

Dávalos, L.M., and A.L. Russell. 2014. Sex-biased dispersal produces high error rates in mitochondrial distance-based and tree-based species delimitation. Journal of Mammalogy 95: 781–791.

Degnan, J.H., and N.A. Rosenberg. 2009. Gene tree discordance, phylogenetic inference and the multispecies coalescent. Trends in Ecology and Evolution 24: 332–340.

Drummond, A.J., and A. Rambaut. 2007. BEAST: Bayesian evolutionary analysis by sampling trees. BMC Evolutionary Biology 7: 214.

Du Puy, D., and J. Moat. 1996. A refined classification of the primary vegetation of Madagascar based on the underlying geology. *In* W.R. Lourenço (editor), Biogéographie de Madagascar: 205–218. Paris: Editions de l'Orstom.

Edgar, R.C. 2004. MUSCLE: multiple sequence alignment with high accuracy and high throughput. Nucleic Acids Research 32 (5): 1792–1797.

Ellerman, J.A. 1949. The families and genera of living rodents. Vol. 3, appendix 2 [Notes on the rodents from Madagascar in the British Museum, and on a

collection from the island obtained by Mr. C.S. Webb]. London: British Museum (Natural History), v + 210 pp.

Galimberti, A., et al. 2012. Integrated operational taxonomic units (IOTUs) in ecolocating bats: a bridge between molecular and traditional taxonomy. PLoS ONE 7 (6): e40122.

Gautier, L., and S.M Goodman. 2002. Histoire de la prospection biologique dans le massif de Manongarivo, Madagascar. Boissiera 59: 13–20.

Glaw, F., J. Köhler, and M. Vences. 2009. A new species of cryptically coloured day gecko (*Phelsuma*) from the Tsingy de Bemaraha National Park in western Madagascar. Zootaxa 2195: 61–68.

Goodman, S.M. 1996. Description of the 1993 biological inventory of the Réserve Naturelle Intégrale d'Andringitra, Madagascar. Fieldiana: Zoology (new series) 85: 1–19.

Goodman, S.M. 1998. Description of the 1994 biological inventory of the Réserve Spéciale d'Anjanaharibe-Sud, Madagascar. Fieldiana: Zoology (new series) 90: 1–16.

Goodman, S.M. 1999. Description of the Réserve Naturelle Intégrale d'Andohahela, Madagascar, and the 1995 biological inventory of the reserve. Fieldiana: Zoology (new series) 94: 1–9.

Goodman, S.M. 2000. Description of the Parc National de Marojejy, Madagascar, and the 1996 biological inventory of the reserve. Fieldiana: Zoology (new series) 97: 1–18.

Goodman, S.M., and M.D. Carleton. 1996. The rodents of the Réserve Naturelle Intégrale d'Andringitra, Madagascar. Fieldiana: Zoology (new series) 85: 257–283.

Goodman, S.M., and V. Mass. 2010. Biodiversity, exploration, and conservation of the natural habitats associated with the Ambatovy project. Malagasy Nature 3: 1–222.

Goodman, S.M., and B.P.N. Rasolonandrasana. 1999. Inventaire biologique de la Réserve Spéciale de Pic d'Ivohibe et du couloir forestier qui la relie au Parc National d'Andringitra. Recherches pour le Développement, Série Sciences Biologiques 15: 1–180.

Goodman, S.M., and V.R. Razafindratsita. 2001. Inventaire biologique du Parc National de Ranomafana et du couloir forestier qui la relie au Parc National d'Andringitra. Recherches pour le Développement, Série Sciences Biologiques 17: 1–243.

Goodman, S.M., and L. Wilmé. 2003. Nouveaux résultats d'inventaires biologiques faisant référence à l'altitude dans la région des massifs montagneux de Marojejy et Anjanaharibe-Sud. Recherches pour le Développement, Série Sciences Biologiques 19: 1–302.

Goodman, S.M., and L. Wilmé. 2006. Inventaires de la faune et de la flore du nord de Madagascar dans la région Loky-Manambato, Analamerana et Andavakoera. Recherches pour le Développement, Série Sciences Biologiques 23: 1–238.

Goodman, S.M., M.D. Carleton, and M. Pidgeon. 1999. The rodents of the Réserve Naturelle Intégrale d'Andohahela, Madagascar. Fieldiana: Zoology (new series) 94: 217–249.

Goodman, S.M., A.P. Raselimanana, and L. Wilmé. 2007. Inventaires de la faune et de la flore d'Anjozorobe-Angavo. Recherches pour le Développement, Série Sciences Biologiques 24: 1–217.

Goodman, S.M., M. Raheriarisena, and S.A. Jansa. 2009. A new species of *Eliurus* Milne Edwards, 1885 (Rodentia: Nesomyinae) from the Réserve Spéciale d'Ankarana, northern Madagascar. Bonner Zoologische Beiträge 56: 133–149.

Goodman, S.M., M.J. Raherilalao, and N.L. Block. 2011. Patterns of morphological and genetic variation in the *Mentocrex kioloides* complex (Aves: Gruiformes: Rallidae) from Madagascar, with the description of a new species. Zootaxa 2776: 49–60.

Goodman, S.M., V. Soarimalala, M. Raheriarisena, and D. Rakotondravony. 2013a. Small mammals or tenrecs (Tenrecidae) and rodents (Nesomyinae). *In* S.M. Goodman and M.J. Raherilalao (editors), Atlas of selected land vertebrates of Madagascar: 211–269. Antananarivo: Association Vahatra.

Goodman, S.M., L. Gautier, and M.J. Raherilalao. 2013b. The Beanka Forest, Région Melaky, western Madagascar. Malagasy Nature 7: 1–291.

Hammer Ø., D.A.T. Harper, and P.D. Ryan. 2001. PAST: paleontological statistics software package for education and data analysis. Paleontologia Electronica 4: 1–9.

Heled, J., and A.J. Drummond. 2009. Bayesian inference of species trees from multilocus data. Molecular Biology and Evolution 27: 570–580.

Hoelzer, G.A., and D.J. Meinick. 1994. Patterns of speciation and limits to phylogenetic resolution. Trends in Ecology and Evolution 9: 104–107.

Hudson, R., and M. Turelli. 2003. Stochasticity overrules the 'three-times rule': genetic drift, genetic draft, and coalescence times for nuclear loci versus mitochondrial DNA. Evolution 57: 182–190.

International Commission on Zoological Nomenclature. 1999. International code of zoological nomen-

clature, 4th ed. London: International Trust for Zoological Nomenclature.

Jansa, S.A., and M.D. Carleton. 2003. Systematics and phylogenetics of Madagascar's native rodents. *In* S.M. Goodman and J.P. Benstead (editors), The natural history of Madagascar: 1257–1265. Chicago: University of Chicago Press.

Jansa, S.A., and M. Weksler. 2004. Phylogeny of muroid rodents: relationships within and among major lineages as determined by IRBP gene sequences. Molecular Phylogenetics and Evolution 31: 256–276.

Jansa, S.A., S.M. Goodman, and P.K.Tucker. 1999. Molecular phylogeny and biogeography of the native rodents of Madagascar (Muridae: Nesomyinae): a test of the single-origin hypothesis. Cladistics 15: 253–270.

Jenkins, P.D., and M.D. Carleton. 2005. Charles Immanuel Forsyth Major's expedition to Madagascar, 1894 to 1896: beginnings of modern systematic study of the island's mammalian fauna. Journal of Natural History 39 (20): 1779–1818.

Kearse, M., et al. 2012. Geneious Basic: an integrated and extendable desktop software platform for the organization and analysis of sequence data. Bioinformatics 28 (12): 1647–1649.

Lanfear, R., B. Calcott, S.Y.W. Ho, and S. Guindon. 2012. PartitionFinder: combined selection of partitioning schemes and substitution models for phylogenetic analyses. Molecular Biology and Evolution 29: 1695–1701.

MacPhee, R.D.E. 1987. The shrew tenrecs of Madagascar: systematic revision and Holocene distribution of *Microgale* (Tenrecidae, Insectivora). American Museum Novitates 2889: 1–45.

Major, C.I.F. 1896a. Descriptions of four additional new mammals from Madagascar. Annals and Magazine of Natural History (ser. 6) 18: 461–463.

Major, C.I.F. 1896b. Diagnoses of new mammals from Madagascar. Annals and Magazine of Natural History (ser. 6) 18: 318–325.

Messmer, N., P.J. Rakotomalaza, and L. Gautier. 2000. Structure and floristic composition of the vegetation of the Parc National de Marojejy, Madagascar. Fieldiana: Zoology, new series 97: 41–104.

Milne Edwards, A. 1885. Description d'une nouvelle espèce de rongeur provenant de Madagascar. Annales des Sciences naturelles, Zoologie et Paléontologie (Paris) 4: Article 1 bis.

Muldoon, K.M., and S.M. Goodman. 2010. Ecological biogeography of Malagasy non-volant mammals: community structure is correlated with habitat. Journal of Biogeography 37: 1144–1159.

Musser, G.G., and M.D. Carleton. 2005. Superfamily Muroidea. *In* D.E. Wilson and D.E. Reeder (editors), Mammal species of the world: a taxonomic and geographical reference, 3rd ed., vol. 2: 894–1531. Baltimore: Johns Hopkins University Press.

Padial, J.M., A. Miralles, I. De la Riva, and M. Vences M. 2010. The integrative future of taxonomy. Frontiers in Zoology 7: 16.

Pamilo, P., and M. Nei. 1988. Relationships between gene trees and species trees. Molecular Biology and Evolution 5: 568–583.

Pante, E., C. Schoelinck, and N. Puillandre. 2015. From integrative taxonomy to species description: one step beyond. Systematic Biology 64: 152–160.

Posada, D. 2008. jModelTest: Phylogenetic model averaging. Molecular Biology and Evolution 25: 1253–1256.

Rajeriarison, C., E. Roger, and H. Rabarison. 2000. Diversité et endémisme dans le Bemaraha. *In* W.R. Lourenço and S.M. Goodman (editors), Diversité et endémisme à Madagascar: 37–44. Paris: Mémoires de la Société de Biogéographie.

Rakotoarisoa, J.E., M. Raheriarisena, and S.M. Goodman. 2010. Phylogeny and species boundaries of the endemic species complex, *Eliurus antsingy* and *E. carletoni* (Rodentia: Muroidea: Nesomyidae), in Madagascar using mitochondrial and nuclear DNA sequence data. Molecular Phylogenetics and Evolution 57: 11–22.

Rakotoarisoa, J.E., S.M. Goodman, and M. Raheriarisena. 2012. A phylogeographic study of the endemic rodent *Eliurus carletoni* (Rodentia: Nesomyinae) in an ecological transition zone of northern Madagascar. Journal of Heredity 104: 23–35.

Rakotoarisoa, J.E., M. Raheriarisena, and S.M. Goodman. 2013. Late Quaternary climatic vegetational shifts in an ecological transition zone of northern Madagascar: insights from genetic analyses of two endemic rodent species. Journal of Evolutionary Biology 26 (5): 1019–1034.

Rakotomalala, Z., and S.M. Goodman. 2010. Diversité et remplacement longitudinal des espèces de petits mammifères dans les forêts des basins versants des fleuves de l'ouest de Madagascar. Revue d'Ecologie (la Terre et la Vie) 65: 343–358.

Rambaut, A., M.A. Suchard , D. Xie, and A.J. Drummond. 2014. Tracer v1.6. Online resource (http://beast.bio.ed.ac.uk/Tracer).

Rannala, B., and Z. Yang. 2013. Improved reversible jump algorithms for Bayesian species delimitation. Genetics 194: 245–253.

Rosenberg, N.A. 2003. The shapes of neutral gene genealogies in two species: Probabilities of monophyly, paraphyly, and polyphyly in a coalescent model. Evolution 57: 1465–1477.

Shi, J.J., et al. 2013. Latitude drives diversification in Madagascar's endemic dry forest rodent, *Eliurus myoxinus* (subfamily Nesomyinae). Biological Journal of the Linnean Society 110: 500–517.

Soarimalala V., and S.M. Goodman. 2003. Diversité biologique des micromammifères non volants (Liptotyphla et Rodentia) dans le complexe Marojejy-Anjanaharibe-Sud. Recherches pour le Développement, Série Sciences Biologiques 19: 231–278.

Soarimalala, V., and S.M. Goodman. 2011. Les petits mammifères de Madagascar. Antananarivo: Association Vahatra.

Soarimalala, V., S.M. Goodman, H. Ramiarinjanahary, L.L. Fenohery, and W. Rakotonirina. 2001. Les micro-mammifères non-volants du Parc National de Ranomafana et du couloir forestier qui relie au Parc National d'Andringitra. Recherches pour le Développement, Série Sciences Biologiques 17: 197–229.

Soarimalala, V., L.T. Ramanana, J.M. Ralison, and S.M. Goodman. 2007. Les petits mammifères non-volants du «Couloir forestier d'Anjozorobe-Angavo». Recherches pour le Développement, Série Sciences Biologiques 24: 141–182.

Stamatakis, A. 2006. RAxML-VI-HPC: maximum likelihood-based phylogenetic analyses with thousands of taxa and mixed models. Bioinformatics 22: 2688–2690.

Stephens, M., and P. Donnelly. 2003. A comparison of Bayesian methods for haplotype reconstruction. American Journal of Human Genetics 73: 1162–1169.

Stephens, M., N.J. Smith, and P. Donnelly. 2001. A new statistical method for haplotype reconstruction from population data. American Journal of Human Genetics 68: 978–989.

Systat Software, Inc. 2004. Systat for Windows. Version 11.0.

Thomas, O. 1895. On a new species of *Eliurus*. Annals and Magazine of Natural History (ser. 6) 26: 164–165.

Vences, M., K.C. Wollenberg, D.R. Vieites, and D.C. Lees. 2009. Madagascar as a model region of species diversification. Trends in Ecology and Evolution 24: 456–465.

Veress, M., D. Lóczy, Z. Zentai, G. Tóth, and R. Schläffer. 2008. The origin of the Bemaraha tsingy (Madagascar). International Journal of Speleology 37 (2): 131–142.

Veress, M., G. Tóth, Z. Zentai, and R. Schläffer R. 2009. The Ankarana tsingy and its development. Carpathian Journal of Earth and Environmental Sciences 4: 95–108.

Voss, R.S., and L.F. Marcus. 1992. Morphological evolution in muroid rodents. II. Craniometric factor divergence in seven Neotropical genera, with experimental results from *Zygodontomys*. Evolution 46: 1918–1934.

Voss, R.S., L.F. Marcus, and P. Escalante. 1990. Morphological evolution in muroid rodents. I. Conservative patterns of craniometric covariance and their ontogenetic basis in the Neotropical genus *Zygodontomys*. Evolution 44: 1568–1587.

Walsh, H.E., M.G. Kidd, T. Moum, and V.L Friesen. 1999. Polytomies and the power of phylogenetic inference. Evolution 53: 932–937.

Wilmé, L., S.M. Goodman, and J.U. Ganzhorn. 2006. Biogeographic evolution of Madagascar's microendemic biota. Science 312: 1063–1065.

Winkler, I.S., et al. 2015. Explosive radiation or uninformative genes? Origin and early diversification of tachinid flies (Diptera: Tachinidae). Molecular Phylogenetics and Evolution 88: 38–54.

Yang, Z., and B. Rannala. 2010. Bayesian species delimitation using multilocus sequence data. Proceedings of the National Academy of Sciences of the United States of America 107: 9264–9269.

Zachos, F.E. 2016. Species concepts in biology. Historical development, theoretical foundations and practical relevance. Switzerland: Springer International Publishing, xii + 220 pp.

Appendix 1

Gazetteer of Collecting Localities

The 372 specimens utilized in our study represent the following 83 principal collecting localities, which were used to prepare distributional maps and to define analytical samples. Localities are numbered from north to south (see fig. 16). Longitude and latitude are given in decimal degrees and correspond to the bold-faced portion of the locality to the left of the semicolon; other locality modifiers and elevation in meters (m) are provided in regular font to the right of the semicolon, along with year of collection and institutional repositories. The species here recognized as valid are also indicated for each collecting site, together with a parenthetical abbreviation that indicates the information source, whether morphological (M) or gene-sequence (G) data. Coordinates and their sources are either those given by the collector or collectors (C), whether determined from fine-scale topographic maps or global positioning devices; or the National Geospatal-Intelligence Agency (NGA), which provides online access to the U.S. Board on Geographic Names database; or various faunal publications and gazetteers that address Malagasy taxa. The skin tags of most specimens reported herein bear a provincial designation as the first-order geopolitical division, a system replaced in 2009 by the 22 regions. Several localities listed below have been subsequently incorporated into Madagascar's system of protected areas, or in certain cases, the statute or delimitation of protected areas has changed.

1. **Joffreville, 5.5 km SW**; PN de la Montagne d'Ambre, 1000 m; 12.5272°S, 49.1717°E (C); Mar 1995, FMNH—*E. ellermani* (G).
2. **Forêt d'Ankavanana**; 15.8 km SE Anivorano-Nord, RS d'Analamerana, 200 m; 12.795°S, 49.3683°E (C; also see Goodman and Wilmé, 2006); Jan 2004, FMNH—*E. carletoni* (G, M).
3. **Mahamasina, 10 km NW**; RS d'Ankarana, 100 m; 12.8867°S, 49.11°E (C); Apr 2002, FMNH—*E. carletoni* (G, M).
4. **Mahamasina, 7.5 km NW**; Encampment des Anglais (Anilotra), RS d'Ankarana, 125 m; 12.9083°S, 49.11°E (C); Apr 2002, FMNH—*E. carletoni* (G, M). Type locality of *E. carletoni* Goodman, Raheriarisena and Jansa (2009).
5. **Andrafiabe, 2.6 km E**; near Andrafiabe Cave, RS d'Ankarana, 50 m; 12.9317°S, 49.0567°E (C); Jan 2001, FMNH—*E. carletoni* (G, M).
6. **Forêt d'Andavakoera**; 4.5 km N Betsiaka, 480 m; 13.12°S, 49.2417°E (C; also see Goodman and Wilmé, 2006); Feb 2004, FMNH—*E. carletoni* (G, M).
7. **Forêt d'Ambohitsitondroina**; 23 km NW Daraina; 13.1268°S, 49.4707°E (C; also see Goodman and Wilmé, 2006); Dec 2006, FMNH—*E. carletoni* (M).
8. **Forêt d'Ambohibory**; 20 km NW Daraina; 13.0794°S, 49.5352°E (C; also see Goodman and Wilmé, 2006); Nov 2006, FMNH—*E. carletoni* (M).
9. **Forêt de Solaniampilana**; 15.2 km NNW Daraina; 13.0914°S, 49.5882°E (C; also see Goodman and Wilmé, 2006); Nov 2006, FMNH—*E. carletoni* (M).
10. **Forêt d'Ampasibe-Maroadabo**; 15.2 km NW Daraina, 130–220 m; 13.1017°S, 49.57.36°E (C; also see Goodman and Wilmé, 2006); Nov 2006, FMNH—*E. carletoni* (M).
11. **Forêt d'Ambilondambo**; 5 km N Daraina, 300–550 m; 13.165°S, 49.6483°E (C; also see Goodman and Wilmé, 2006); Jan 2002, UADBA—*E. carletoni* (M).
12. **Forêt de Bobankora**; 11 km ESE Daraina, 350–550 m; 13.2233°S, 49.76°E (C; also see Goodman and Wilmé, 2006); Feb 2003, UADBA—*E. carletoni* (M).
13. **Forêt d'Ankazomasina**; 6.3 km SE Daraina, 160–240 m; 13.255°S, 49.6934°E (C; also see Goodman and Wilmé, 2006); Oct 2006, FMNH—*E. carletoni* (M).
14. **Forêt d'Ankaramianabo**; 9.6 km S Daraina, 320–390 m; 13.2912°S, 49.6801°E (C; also

see Goodman and Wilmé, 2006); Oct 2006, FMNH—*E. carletoni* (M).

15. **Forêt d'Antsahasolika**; 15 km SSW Daraina, 350–500 m; 13.34.15°S, 49.6620°E (C; also see Goodman and Wilmé, 2006); Nov 2006, FMNH—*E. carletoni* (G, M).
16. **Forêt d'Antsahabe**; 12 km W Daraina, 850–950 m; 13.2184°S, 49.5520°E (C; also see Goodman and Wilmé, 2006); Dec 2006, FMNH—*E. ellermani* (M).
17. **Forêt de Binara**; 7.5 km SW Daraina, 325–550 m; 13.255°S, 49.6167°E (C; also see Goodman and Wilmé, 2006); Nov 2001, FMNH—*E. carletoni* (G, M) and *E. ellermani* (G, M).
18. **Forêt d'Ambohibe**, 16 km SW Daraina, 490–680 m; 13.3417°S, 49.6126°E (C; also see Goodman and Wilmé, 2006); Nov 2006, FMNH—*E. carletoni* (G, M).
19. **Antanambao, 12.8 km SW**; RS de Manongarivo, 785 m; 13.9767°S, 48.4233°E (C; also see Gautier and Goodman, 2002); Mar 1999, FMNH—*E. ellermani* (G).
20. **Antanambao, 14.5 km SW**; RS de Manongarivo, 1240 m; 14.0°S, 48.4243°E (C; also see Gautier and Goodman, 2002); Mar 1999, FMNH—*E. ellermani* (G).
21. **Bemanivika Forest**; Peregrine Fund Camp, Région Sofia, 1570 m; 14.3484°S, 48.5798°E (C); Oct 2013, FMNH—*E. ellermani* (M).
22. **Manantenina, 10 km NW**; along tributary of Manantenina River, RNI de Marojejy, 775 m; 14.4333°S, 49.7617°E (C; also see Goodman, 2000; Goodman and Wilmé, 2003); Oct 1996, FMNH—*E. ellermani* (G, M).
23. **Doany, 11.5 km SE**; PN de Marojejy, 810 m; 14.4267°S, 49.6083°E (C; also see Goodman and Wilmé, 2003); Oct 2001, FMNH—*E. ellermani* (G, M).
24. **Ambodiangezoka, 8.5 km NW**; Forêt de Betaolana, along Ambolokopatrika River, 875 m 14.5383°S, 49.4383°E (C; also see Goodman and Wilmé, 2003); Oct 1999, FMNH—*E. ellermani* (G, M).
25. **Ambodiangezoka, 11 km NW**; Forêt de Betaolana, 1200 m; 14.61°S, 49.425°E (C; also see Goodman and Wilmé, 2003); Oct 1999, FMNH—*E. ellermani* (G, M).
26. **Befingotra, 9.2 km WSW**; RS d'Anjanaharibe-Sud, 1260 m; 14.745°S, 49.4617°E (C; also see Goodman, 1998; Goodman and Wilmé, 2003); Nov 1994, FMNH—*E. ellermani* (M).
27. **Befingotra, 6.5 km SSW**; RS d'Anjanaharibe-Sud, 785 m; 14.755°S, 49.505°E (C; also see Goodman, 1998; Goodman and Wilmé, 2003); Oct 1994, FMNH—*E. ellermani* (M).
28. **Befingotra, 13.5 km SW**; western slope of Anjanaharibe-Sud, 1200 m; 14.7833°S, 49.4417°E (C; also see Goodman and Wilmé, 2003); Oct 1999, FMNH—*E. ellermani* (G, M).
29. **Hiaraka, near**; ca. 18 km ESE Maroantsetra, 850 m; ca. 15.5°S, 49.9333°E (Carleton and Goodman, 1998); Jan 1968, MNHN—*E. ellermani* (G, M). Type locality of *E. ellermani* Carleton (1994), as amended by Carleton and Goodman (1998: 181).
30. **Marotandrano, 12.5 km SSE**; along Riamalandy waterfall, District de Mandritsara, 850 m; 16.285°S, 48.815°E (C); Nov 2004, UADBA—*E. ellermani* (G). Including 12 km SSE Marotandrano, 900 m.
31. **Forêt de Mahabo**; 31 km NW Andranomavo, RNI de Namoroka, 100 m; 16.39°S, 45.3483°E (C); Oct 2002, FMNH—*E. antsingy* (G, M).
32. **Namoroka village, 2 km SE**; Site Andriabe, RNI de Namoroka, 110 m; 16.4067°S, 45.3067°E (C); Sep 2003, FMNH—*E. tsingimbato* (G, M).
33. **Forêt d'Ambovonomby**; 26 km NW Andranomavo, RNI de Namoroka, 200 m; 16.47°S, 45.3483°E (C); Oct 2002, FMNH—*E. antsingy* (G, M) and *E. tsingimbato* (G, M).
34. **RNI de Namoroka**; 16.48°S, 45.33°E (C); Jun 1999, FMNH and UADBA—*E. antsingy* (M).
35. **Forêt d'Analamavo**; 27 km N Kandreho, Ankara Plateau, District de Kandreho, 220

m; 17.2408°S, 46.0936°E (C); Oct 2006, FMNH—*E. tsingimbato* (G, M).

36. **Forêt d'Analanomby**; 21 km NNW Kandreho, Kelifely Plateau, District de Kandreho, 280 m; 17.3161°S, 46.0036°E (C); Oct 2006, FMNH—*E. tsingimbato* (G, M).
37. **Ambinda, 1.1 km E**; Forêt de Beanka, District de Maintirano, 220 m; 18.0236°S, 44.5022°E (C; also see Goodman et al., 2013b); Oct 2009, FMNH and UADBA—*E. tsingimbato* (G, M).
38. **Ambinda, 4.9 km S**; Forêt de Beanka, District de Maintirano, 320 m; 18.0617°S, 44.525°E (C; also see Goodman et al., 2013b); Oct 2009 and Jan 2010, FMNH and UADBA—*E. tsingimbato* (G, M).
39. **Forêt d'Antsahalaza**; along Antsoa River, RNI de Bemaraha; 18.497°S, 44.658°E (C); Jun 2001, UADBA—*E. tsingimbato* (G).
40. **Bekopaka, near**; forêt de l'antsingy; ca. 19.125°S, 44.8167°E (Carleton et al., 2001: 975); Jul and Sep 1964, MNHN—*E. antsingy* (M) and *E. tsingimbato* (M). Type locality of *E. antsingy* Carleton, Goodman, and Rakotondravony (2001); see their discussion for its probable location to the northeast of the village, in *tsingy* forest near the former Bekopaka airfield and along the Bekopaka-Andriandriambe trail. The recently collected specimen of *E. antsingy* from locality 42, below, is reasonably regarded as almost topotypic.
41. **Bekopaka, 2.5 km NE**; Ankidrodroa, PN de Bemaraha, 100 m; 19.1317°S, 44.8083°E (C); Nov 2001, FMNH—*E. tsingimbato* (G, M).
42. **Bekopaka, 3.5 km E**; PN de Bemaraha, 100 m; 19.14°S, 44.8283°E (C); Nov–Dec 2001, FMNH—*E. antsingy* (G, M) and *E. tsingimbato* (G, M).
43. **Anjozorobe, 17 km NE**; Anorana, District d'Anjozorobe, 1250 m; 18.3083°S, 48.0151°E (C; also see Goodman, Raselimanana and Wilmé, 2007; Soariamalala et al., 2007); Oct 2009, UADBA—*E. tanala* (G). Including 18 km NE Anjozorobe, 1150 m; Mar 2010, UADBA.
44. **Anjozorobe, 13 km SE**; 1300 m; 18.48°S, 47.955°E (C; also see Goodman et al., 2007; Soariamalala et al., 2007); Dec 1996, FMNH—*E. tanala* (M).
45. **Sihanaka Forest**; 18.0833°S, 48.5°E (Carleton and Schmidt, 1990); 1932–1936, BMNH and MCZ—*E. tanala* (M).
46. **Rogez [Andekaleka], 21 km N**; near Lohariandava, 395 m; 18.6333°S, 48.6167°E (Carleton and Schmidt, 1990); 1939, BMNH—*E. tanala* (M).
47. **Lohariandava, 16 km NW**; 460 m; 18.7°S, 48.5833°E (Carleton and Schmidt, 1990); 1939, BMNH—*E. tanala* (M).
48. **PN de Mantadia**; 900 m; 18.7917°S, 48.4267°E (C); Nov 1998, FMNH—*E. tanala* (M).
49. **Ambohimanarivo, 10 km E**; Ambatovy-Analamay, Site 5, District de Moramanga; 18.8239°S, 48.3338°E (C; see also Goodman and Mass, 2010); Feb 2009, UADBA—*E. tanala* (G).
50. **Andasibe** [Périnet]; near Moramanga, 915 m; 18.9252°S, 48.4187°E (NGA); 1939, BMNH—*E. tanala* (M). Including 1 km E and 2 km E Périnet, 1300 m; Oct 1958, USNM.
51. **Andasibe [Périnet], 13 km E**; 18.9333°S, 48.5167°E (Carleton and Schmidt, 1990); Apr 1959, USNM—*E. tanala* (M).
52. **Forêt de Maromizaha**; 8.3 km SE Andasibe (Périnet), 980 m; 18.9756°S, 48.4583°E (C); Oct 2008, FMNH—*E. tanala* (M).
53. **Andasibe (Périnet) village, 14.5 km SW**; Ampasimpotsy-Anivonimaro, Lakato, Ambalafary Forest, 995 m; 19.0439°S, 48.3486°E (C); Mar 2011, FMNH—*E. tanala* (G).
54. **Sahambaky**; along tributary of Sahatandra River, 31.5 km NNW Lakato, Alaotra Mangoro Region, 980 m; 19.065°S, 48.34°E (C); Oct 2007, FMNH—*E. tanala* (M).
55. **Forêt d'Ianasana**; 7 km W Itremo, 1630 m; 20.6017°S, 46.5717°E (C); Feb 1999, FMNH—*E. tanala* (G, M).
56. **Forêt d'Antetezana**; along Ranomena River, PN de Ranomafana, 970 m; 21.2019°S,

47.4822°E (C; also see Goodman and Razafindratsita, 2001); Nov 2000, FMNH—*E. tanala* (G, M).

57. **Vohiparara, 3 km (by road) NNW**; Prefecture de Fianarantsoa, 1225 m; 21.2167°S, 47.3667°S (C); Jul 1988, USNM—*E. tanala* (M).
58. **Ambodiamontana**; ca. 7 km (by road) W Ranomafana, 950 m; 21.27°S, 47.43°E (C); Jul–Aug 1987, USNM—*E. tanala* (G, M).
59. **Vatoharanana**; 4 km SW Ranomafana (ville), PN de Ranomafana, 1025 m; 21.29°S, 47.4333°E (C; also see Goodman and Razafindratsita, 2001); Oct 2000, FMNH—*E. tanala* (G, M). Including Vatoharanana River Camp, 950 m; Dec 1991, FMNH.
60. **Andrambovato, 1 km NW**; 875 m; 21.5°S, 47.42°E (C; also see Goodman and Razafindratsita, 2001); Aug 1988, USNM—*E. tanala* (M).
61. **Andrambovato, 2 km W**; along Tatamaly River, 1075 m; 21.5117°S, 47.41°E (C; also see Goodman and Razafindratsita, 2001); Oct 2000, FMNH—*E. tanala* (G, M).
62. **Mandriandry**; 4.4 km SW Tolongoina, 750 m; 21.5842°S, 47.4836°E (C; also see Goodman and Razafindratsita, 2001); Oct 2000, FMNH—*E. tanala* (G, M).
63. **Ambatofotsy, 9 km WNW**; along Maroangira River, 750 m; 21.7339°S, 47.4014°E (C; also see Goodman and Razafindratsita, 2001); Oct 2000—*E. tanala* (G, M).
64. **Vinanitelo**; 1300 m; 21.7167°S, 47.2667°E (NGA; also see Goodman and Razafindratsita, 2001; Jenkins and Carleton, 2005); May–Jun 1896, BMNH, FMNH and MCZ—*E. tanala* (M). Type locality of *E. tanala* Major (1896a). Major (1896b: 320) earlier gave an expanded version of this locality—"the forest of the Independent Tanala of Ikongo, in the neighbourhood of Vinanitelo, one day's journey south of Fianarantsoa"—a placement suggesting that specimens from the next locality originated from the same forest block where Major had collected in 1896.
65. **Forêt de Vinanitelo**; foot of Mt Ambodivohitra, 15.5 km SE Vohitrafeno, 1100 m; 21.7767°S, 47.3467°E (C; also see Goodman and Razafindratsita, 2001); Oct 2000, FMNH—*E. tanala* (G, M).
66. **Forêt d'Ambatomainty**; 11.6 km WNW Ikongo, along Sandranta River, 645 m; 21.8339°S, 47.3322°E (C; also see Goodman and Razafindratsita, 2001); Nov 2000, FMNH—*E. tanala* (G, M).
67. **Ambavafatra**; Forêt de Manambolo, along Andohabatotany River, 1300 m; 22.1494°S, 47.0236°E (C; also see Goodman and Razafindratsita, 2001); Nov 1999, FMNH—*E. tanala* (G, M). Including Andohabatotany Forest, 7 km SW Ambalamanenjana, District d'Ambalavao, 1300 m; Mar 2007, FMNH.
68. **Sendrisoa, 19.5 km SE**; Forêt de Manambolo, W slope Mt Vohipia, 1600 m; 22.1633°S, 47.0417°E (C; also see Goodman and Razafindratsita, 2001); Dec 1999, FMNH—*E. tanala* (G, M).
69. **Ambalavao, 38 km S**; Andringitra Reserve, 1625 m; 22.1942°S, 46.9711°E (C; also see Goodman, 1996); Dec 1993, FMNH—*E. tanala* (G, M).
70. **Ambalavao, 40 km S**; Andringitra Reserve, 1210 m; 22.2228°S, 46.9717°E (C; also see Goodman, 1996); Dec 1993, FMNH—*E. tanala* (G, M).
71. **Ambalavao, 43 km S**; Andringitra Reserve, 810 m; 22.2278°S, 47.0036°E (C; also see Goodman, 1996); Dec 1993, FMNH—*E. tanala* (G, M).
72. **Ivohibe, 8 km NE**; 5.5 km SE Angodongodona, 1200 m; 22.4217°S, 46.8893°E (C; see also Goodman and Rasolonandrasana, 1999); Nov 1997, FMNH—*E. tanala* (M).
73. **Ivohibe, 9 km NE**; 6.5 km ESE Angodongodona, 900 m; 22.4267°S, 46.9383°E (C; see also Goodman and Rasolonandrasana, 1999); Nov 1997, FMNH—*E. tanala* (M).
74. **Ivohibe, 8 km E**; RS d'Ivohibe, 1200; 22.4833°S, 46.9683°E (C; see also Goodman and Rasolonandrasana, 1999); Oct 1997, FMNH—*E. tanala* (G, M).

75. **Ivohibe, 6.5 km ESE**; at source of Andranomainty River, RS d'Ivohibe, 1575 m; 22.4967°S, 46.955°E (C; see also Goodman and Rasolonandrasana, 1999); Oct 1997, FMNH—*E. tanala* (G, M).
76. **Ampatramary, 1.2 km ENE**; W slope Mt Ambatobe, 9.5 km NE Midongy-Sud, 650 m; 23.51°S, 47.0517°E (C); Nov 2003, FMNH—*E. tanala* (G, M).
77. **Befotaka, 2.5 km SW**; Mt Papango, along Andranomena River, PN de Midongy-Sud, 875 m; 23.835°S, 46.9633°E (C); Oct 2003, FMNH—*E. tanala* (G, M).
78. **Befotaka, 3.5 km SW**; NE slope Mt Papango, PN de Midongy-Sud, 1250 m; 23.8383°S, 46.9583°E (C); Nov 2003, FMNH—*E. tanala* (G, M).
79. **Marosohy Forest**; 16 km WNW Ranomafana[-Sud], Fivondronana de Tolagnaro, 800 m; 24.57°S, 46.8°E (C); Nov–Dec 1989, USNM—*E. tanala* (M).
80. **Eminiminy, 15 km NW**; RNI d'Andohahela, parcel 1, 1500 m; 24.5692°S, 46.7308°E (C; also see Goodman, 1999); Nov 1995, FMNH—*E. tanala* (M).
81. **Eminiminy, 13.5 km NW**; RNI d'Andohahela, parcel 1, 1200 m; 24.584°S, 46.7347°E (C; also see Goodman, 1999); Nov 1995, FMNH—*E. tanala* (M).
82. **Eminiminy, 12.5 km NW**; RNI d'Andohahela, parcel 1, 810 m; 24.5933°S, 46.7383°E (C; also see Goodman, 1999); Oct–Nov 1995, FMNH—*E. tanala* (G, M).
83. **Manantantely**; 8–12 km WNW Tolagnaro, Fivondronana de Tolagnaro; 24.9833°S, 46.9°E (C); Sep–Oct 1990, USNM—*E. tanala* (M).

APPENDIX 2

Primers Used to Amplify the Six Genetic Loci Sequenced in This Study

Locus	Primer Name	Sequence 5′-3′
Cytb	MVZ05a	5′-GAAAAATCATCGTTGTAATTCAACT
Cytb	Eli_cytb_IntF163	5′-TYTTACAAATYGCCACAGGAC
Cytb	Eli_cytb_IntF430	5′-AYGTACTACCATGRGGCCAAA
Cytb	Eli_cytb_IntR628	5′-CCTGATGGRTTRTTTGATCC
Cytb	Eli_cytb_IntR202	5′-TGRGTGACTGATGARAATGC
Cytb	Eli_cytb_IntR456	5′-TGGCTGARAGWAGGTTTGTR
Cytb	UMMZ04	5′-TCTTCATTTYWGGTTTACAAGAC
Nd2	ND2F1	5′-AAGGTCAGCTAACTAAGCTATCGG
Nd2	ND2R1	5′-TTGTTTTCTAAGGGCTTTGAAGG
Fgb	FGB7F1	5′-ACGGCATGTTCTTCAGCACG
Fgb	FGB7R1	5′-ATCCCTTCCAGTTCATCCACAC
Vwf	vWFA	5′-CTGTGATGGTGTCAACCTCACCTGTGAAGCC
Vwf	vWFNesR1170alt	5′-TCCCTGTGACCATGTAAACCA
Opn1mw	OPNEX3_F2	5′-ATCACAGGCCTCTGGTCCCTGGC
Opn1mw	OPNF1alt	5′-GAATCGTCTTCTCCTGGGTCT
Opn1mw	OPNF623	5′-CCTGGCCACGTTCATTCTTTGGTCAG
Opn1mw	OPN_F554	5′-CCCCCACCACTTTCAGAGGTTTCT
Opn1mw	OPNR972	5′-GAAGGGACATGCACACTGGGTAACC
Opn1mw	OPN_R968	5′-GACTTGAGTCAGAGGGTTTTTATGTTG
Opn1mw	OPNEx4_R3	5′-ATGGCCAGCCACACTTGGAGGTAG
Opn1mw	OPNR1alt	5′-CTGGACCACAGGATGTCTTCA
Rbp3	IRBP-A	5′-ATGGCCAAGGTCCTCTTGGATAACTACTGCTT
Rbp3	IRBP-B	5′-CGCAGGTCCATGATGAGGTGCTCCGTGTCCTG

APPENDIX 3

Comparative Specimens Examined

Listed below are specimens of *Eliurus antsingy*, *E. carletoni* and *E. myoxinus* used in preparing distributional maps, conducting morphological comparisons, and/or generating morphometric and gene-sequence analyses.

Eliurus antsingy: $N = 12$, as follows.

Province de Mahajanga: Forêt de Mahabo, 31 km NW Andranomavo, RNI de Namoroka, 100 m (FMNH 175912, 175913); Forêt d'Ambovonomby, 26 km NW Andranomavo, RNI de Namoroka, 200 m (FMNH 175909, 175910); RNI de Namoroka (FMNH 167563–167566; UADBA 16169); near Bekopaka, forêt de l'antsingy (MNHN 1966.2220, 1966.2222); 3.5 E Bekopaka, PN de Bemaraha, 100 m (FMNH 172721).

Eliurus carletoni: $N = 74$, as follows.

Province d'Antsiranana: Forêt d'Ankavanana, 15.8 km SE Anivorano-Nord, RS d'Analamerana, 200 m (FMNH 178853, 178854, 178872–178874); 10 km NW Mahamasina, RS d'Ankarana, 100 m (FMNH 173107, 173108); 7.5 km NW Mahamasina, Encampment des Anglais (Anilotra), RS d'Ankarana, 125 m (FMNH 173104–173106, 173109); 2.6 km E Andrafiabe, near Andrafiabe Cave, RS d'Ankarana, 50 m (FMNH 169718–169720); Forêt d'Andavakoera, 4.5 km N Betsiaka, 480 m (FMNH 221495); Forêt d'Ambohitsitondroina, 23 km NW Daraina (FMNH 195895, 195897, 195898); Forêt d'Ambohibory, 20 km NW Daraina (FMNH 195888–195880, 195892, 195982, 195984); Forêt de Solaniampilana, 15.2 km NNW Daraina (FMNH 195869–195871); Forêt d'Ampasibe-Maroadabo, 15.2 km NW Daraina, 130–220 m (FMNH 195873, 195874, 194876, 195880–195882, 195884, 195973, 195975, 195976, 195979); Forêt d'Ambilondambo; 5 km N Daraina, 300–550 m (UADBA 46062, 46072, 46073); Forêt de Bobankora, 11 km ESE Daraina, 350–550 m (UADBA 46101); Forêt d'Ankazomasina, 6.3 km SE Daraina, 160–240 m (FMNH 195831, 195833, 195835, 195837, 195839); Forêt d'Ankaramianabo, 9.6 km S Daraina, 320–390 m (FMNH 195840, 195842, 195844–195846, 195850, 195942, 195943, 195945, 195947, 195948, 195951, 191953, 191955, 191958, 191960); Forêt d'Antsahasolika, 15 km SSW de Daraina, 350–500 m (FMNH 195852, 195854, 195855, 195857, 195859, 195862, 195963, 195965, 195966); Forêt de Binara, 7.5 km SW Daraina, 325–550 m (FMNH 172665, 172692).

Eliurus myoxinus: $N = 14$, as follows.

Province de Toliara: 5 mi E Bevilany, Ambovombe-Fort Dauphin road, 245 m (BMNH 47.1601–47.1604, 47.1606, 47.1607); Petriky Forest, 57 km SE Manambaro, 20 m (USNM 578679–578683, 578685, 578686); PN d'Andohahela, Parcel II, 7.5 km ENE Hazofotsy, 120 m (FMNH 156630).

Scientific Publications of the American Museum of Natural History

American Museum Novitates
Bulletin of the American Museum of Natural History
Anthropological Papers of the American Museum of Natural History

Submission procedures can be found at http://research.amnh.org/scipubs

All issues of *Novitates* and *Bulletin* are available on the web (http://digitallibrary.amnh.org/dspace). Order printed copies on the web from:
http://shop.amnh.org/a701/shop-by-category/books/scientific-publications.html

or via standard mail from:
American Museum of Natural History—Scientific Publications
Central Park West at 79th Street
New York, NY 10024

♾ This paper meets the requirements of ANSI/NISO Z39.48-1992 (permanence of paper).

On the cover: The dramatic landscape of Bemaraha, Madagascar, showing the dry-forest habitat where the new species of *Eliurus* is found. The eroded limestone pinnacles are know in Malagasy as *tsingy*, and the new species is named for these unique geological formations (photo by Chien Lee).